Technical and Economic Feasibility of Using Steel Fiber Reinforced Concrete (SFRC) in Slap line of Railroads

Faculty of Civil and Industrial Engineering

Master Degree in Transport System Engineering

Course of Railway Engineering

Candidate:

SEYEDMOHAMMAD FATEMI

Student Number: **1729934**

Advisor:

Prof. Stefano Ricci

A/Y 2018/2019

Acknowledgement

I would like to express my sincere gratitude to my advisor Prof. Stefano Ricci for the continuous support of my Master study and research, for his patience, motivation, enthusiasm, and immense knowledge. His guidance helped me in all the time of research and writing of this thesis. I could not have imagined having a better advisor and mentor for my Master study.

My deep and sincere gratitude to my parents for their continuous and unparalleled love, help and support. I am grateful to my brothers for always being there for me as best friends. I am forever indebted to my parents for giving me the opportunities and experiences that have made me who I am. They selflessly encouraged me to explore new directions in life and seek my own destiny.

Finally, it is a pleasure to thank my love Mozhgan for the wonderful times we shared, and especially for the positive energy that always she sent me.

Abstract

Use of steel fiber in railroad is under consideration in some countries around the world. The purposes of using these materials are, increase of freightage and crack control in the slab line of subway and railroad line and also in developing countries, usage of steel fiber-reinforced cementations composites is widely expanding in structures, due to their high mechanical performance and flexibility (1).

Concrete is one of the world most widely used construction material. However, since the early 1800's, it has been known that concrete is weak in tension (2). Fibers are commercially available and manufactured from steel, plastic, glass and other natural materials. In many situations it is prudent to combine fiber reinforcement with conventional steel reinforcement to improve performance (3). Because of the properties of the material (concrete), computer simulations in the field of reinforced concrete structures are pose a challenge.

There is always a search for concrete with higher strength and durability. In this matter, blended cement concrete with the incorporation of fibers has been introduced to suit the current requirements (4). The model describes three tension phases: achieving elastic tensile concrete strength, material softening, and failure / cracking. The model of concrete can be used for analysis of failure mechanism of reinforced concrete structural elements (5). Although most of the current railway tracks are still of a traditional ballasted type, recent applications tend more and more towards non-ballasted track.

The major advantages of slab track are: low maintenance, high availability, low structure height, and low weight. In addition, recent life cycle studies have shown, that from the cost point of view, slab tracks might be very competitive (6). Slab track designs have significant advantages comparing to ballasted tracks. The most significant are the high stability of the track. Their disadvantages against the ballasted tracks are mainly summarized in their higher construction costs (7).

Keywords: Steel Fiber in concrete, Crack Control, High Performance, High Strength, Durability, Tension, Failure, Non-Ballast Track, Maintenance, Stability, Cost.

Index

Abbreviations

FRC……………………………………………...……*Fiber Reinforced Concrete*

SFRC…………………………………………....*Steel Fiber Reinforced Concrete*

FEM……………………………………………….. …..*Finite Element Method*

EPS………………………………………………...…..*Expanded Poly-Styrene*

FEA………………………………………... ……………*Finite Element Analysis*

SAP……………………………………………*System Application and Products*

MOR……………………………...……………*Mathematic of Operation Research*

SF……………………………...…………………………... …….*Steel Fiber*

SIFCON……………………………………..….*Slurry Infiltrated Fiber Concrete*

SIMCON…………………………………….. …..…*Slurry Infiltrated Mat Concrete*

RC…………………………...…………………………………*Reinforced Concrete*

FRP………………………………………………...……..*Fiber Reinforced Polymer*

TRIS………………………….. …..…*Transportation Research Information Service*

ASTM………………………………….*American Society for Testing and Materials*

EFNARC……..*European Federation of National Associations Representing for Concrete*

FDOT……………………………….. ..…….*Florida Department of Transportation*

ACI…… ……………………………………….……*American Concrete Institute*

LSD………………………………………………..………….*Limit State Design*

LRFD…………………………………..……*Load and Resistance Factor Design*

FIB……………………………………………………………..…*Focused ion Beam*

RILEM…….*Regulation of International Union of Laboratories and Experts in Construction Materials*

CMOD……………………………………………………….*Crack Mouth Opening*

CEP…………………………………………*Committee on Environmental Policy*

CDP…………………………..…………………….*Concrete Damaged Plasticity*

CEB……………………………………...…..*Comte Euro-International du Beton*

SAP…………………………………………….*System Application and Products*

LM…………………………………………..…….*Live Traffic Load Modeling*

AREMA………………..….*American Railway Engineering and Maintenance of Way Association*

UIC……………………………………………….*International Union of Railway*

Chapter 1

Introduction

1.1. Introduction

In the last 40 years, increase in train speed and axle load around the world and other challenges in the conventional ballasted track system gave birth to ballastless railway track system (7).

The purposes of using this materials are, increase of freightage and crack control in the slab of the subway and railroad line. Some practical and experimental works are done regarding the performance of the steel fiber in the pavement, but the specific numerical works that can indicate the influence of fiber on mechanical behavior of slab are not done (1).

Using Non-Ballast railway especially in tunnels and bridges, due to the altitude drop of the railroad line, reduce maintenance and total cost, facilitate higher train speed and increase of lateral resistance are widely increased. A comparison between ballasted and ballastless tracks is essential in order to clearly identify when and where the slab track systems perform better. A simple numerical model is developed to make a comparison between ballasted and ballastless tracks. In many cases slab track systems seem to have the capabilities to serve these high speed routes more efficiently than the ballasted tracks mainly due to their higher structural stability, significantly lower need of maintenance, and longer life cycle. The ballastless systems are divided in two main categories: the discrete rail support and the continuous rail support. These two categories are divided in subcategories, which contain 34 slab track designs that have been used worldwide (7).

One of the issue that can considered, as a disadvantage of this type of pavement, is armature. Discussion in terms of exploitation are cracks caused by passing load and the environment situation. One of the ways to prevent these problems is the utilization of steel fiber in construction of slab lines. In 1970, the use of steel fiber in concrete as regenerator developed for many reasons such as significantly increased flexibility, increasing energy attraction and mechanical properties and disabilities like compressive strength, tensile, bending, incision, impact and resistance against freezing and warming, creep, cavitation and corrosion. Especially steel fiber-reinforced concrete under dynamic load (especially impact) or abrasive load, are effective in pavements and stanchions. Other features of this concrete are work comfortably and high molding speed of fibers (1, 7).

Most developed and many developing countries in the world have high speed lines (~300 km/h) and they are preparing to update their existing lines as well as to create new high speed railway routes (7).

Fiber-reinforced concrete is by adding fibers to the mix. The purpose of the addition of fiber is to increase the tensile strength of concrete, so the concrete can withstand tensile strength due to weather, climate and temperature changes that usually occur in the concrete with a large surface. Types of fiber that used in fiber-reinforced concrete, can be of natural fibers or artificial fibers (8).

Use of continuous reinforcement in concrete (reinforced concrete) increases strength and ductility but requires careful placement and labor skill. The modern development of fiber reinforced concrete (FRC) started in the early sixties. Fibers are produced from different materials in various shapes and sizes. Using fibers in concrete is to improve the characteristics of construction materials (9).

1.2. Research Necessity

In this part, we discuss about damages due to crack of the concrete in the structure of non-ballast lines. Slab Track is a kind of precast concrete structure. Principle of the design of slab track, is no crack design, but some cracks can be found in the slab track due to load action, environmental factor (such as temperature) and creep of concrete. Cracks can appear in the inner side of the slab-track frame and some cracks run through the total depth of it. Some cracks generate form lifting and some generate from steam curing system of slab-track or its structure. Cracks can be finally found in the middle of the slab track and the width of the crack reaches the total width of track (10).

In ballastless lines, there are two risks: first, to decrease the structural durability of line and train safety, second, to unable the insulation system of the isolated points in line. Cracks in the slab track and slab under the structure (roadbed) will become the entryway of the corrosion substances from the surrounding environment with chlorine and CO_2 corroding them. The expansion of corroded materials, causes the extension of crack in concrete and, as a result, it causes the decrease of structural durability (10).

Fig. 1.1. *Crack in track slab*

(a) **Fig. 1.2.** *Crack in the base concrete* (b)

(a) **Fig. 1.3.** *Crack in roadbed slap* (b)

Barros and *Figueiras* searched regarding to mechanical behavior of reinforced slab line with 40 kg steel fiber per square meter (11). They had done their experimentation according to *Teutsch*. They found satisfactory agreement between the load–deflection curves obtained from experiment and those from finite element analysis. And also they predicted the cracking behavior of slab and checked the effect of substrate hardness on them (12).

A number of parametric studies regard mechanical properties of slab lines on ballastless bed. The results show that substrate module contains all parameters including internal forces, tensions and deformations. Moreover, it is indicated that the rail properties, for example moment of inertia, do not have effect on these parameters but it causes the homogenous load distribution on slab lines and several researches regard the effect of fibers on mechanical properties of the slap (11).

Influence of length and volumetric percentage of steel fibers on energy absorption of concrete slabs with various concrete strengths is investigated by *Khaloo*, testing 28 small steel fiber reinforced concrete *(SFRC)* slabs under flexure. The variables include fiber length, volumetric percentage of fibers and concrete strength. Test results indicate that generally longer fibers and higher fiber content provide higher energy absorption, but the size and the amount of fiber do not have significant impact on slab's final bending capacity (13).

In the research by *Madhkhan*, to investigate the spanning behavior of slab tracks, a FEM analysis was representing discrete and continuous systems for cracking behavior. At first, full-size slabs without foundation including solid and hollow-core, specimens (*with 30% weight reduction*) were under test, by extracting centric static (*monotonic*) line loads and load-deflection curves. Then, FEM results for zero foundation stiffness were verified with those of experiments, which were in good agreement. The obtained load from FEM analysis, for slab line reinforced with steel fiber, compared to the results by *Barros* and *Figueiras*, was satisfactory and their results confirmed by experimental models. Final, the real behavior of slab lines on elastic substrate, before and after cracking, is investigated by FEM model with monotonic loads (12).

The use of Expanded Poly-Styrene (*EPS*) under slab tracks in high-speed railways was proposed by the same researcher, in order to reduce the dead weight of the system and, finally, to minimize the cost of stabilizing the foundation soil.

One of the property of this project, compared with previous research, is that, without modeling the steel fiber and their embedment in the concrete, the estimation by applying dynamic loads of the resistance characteristics of fiber. They are due to rail fleet movement and the effect of this kind of load with different speed on the slab, previously investigated only with static loads.

1.3. Investigation Issue Form

According to this issue, we can realize that it is necessary to check, technically and economically, the amount of fiber to use in slab lines. For technical feasibility it is used a numerical analysis of finite components with considering the random distribution of fiber and its deformation loading behavior. Therefore, it is possible to consider the following elements as the project purposes:

- Effect of fiber on flexural and shear capacity on slab lines with service loads;
- Feasibility of using fibers alone in slap line;
- Combination of fibers and armature in case of their simultaneous use;
- Economic analysis of use of armature, fibers and their combination;
- Analysis of lateral resistance against load while using steel fiber;
- Effect of steel fiber concrete on more generally trains performance (speed, acceleration, loads, etc.);
- Effects on maintenance activity and costs.

1.4. Performance Method

At first, concrete with fiber should model with specific property of *ABAQUS* software. Then consider one of the project done by a researcher as a model. After that, according to the results from this model, in comparison with laboratory results, it can arrive to the validation of the model of slab railways, set on the elastic bed and the tolerance of transit load.

Then, it investigates the effect of steel fiber increasing loading behavior of displacement, shear, and bending forces. According to the results, effects of fibers on shear and bending forces, the slap line analysis processes with speeds and reaction coefficient of the bed and various axial loads by *SAP2000* software to compare with available regulations.

The investigation are oriented to the design process of fibered concrete and the possibility of using fiber alone or the combination with armature.

Chapter 2

Review of Technical Literature on Fiber Concrete and Their Utilization in Slabs

2.1. Introduction

Use of fiber in some countries dates back to several thousand years ago. In the past, they used to use short pieces of dried herbs with water and soil as a mixture of clay, to build wall and brick. The fibers are in use for crack control in effect of volumetric changes due to contraction, expansion, thermal stresses, increase of tensile strength, softness, energy absorption capability and provide an integrated system (1, 12). Currently, hundreds types of fibers as herbal, artificial and metal are producing that only some of them are suitable to use in concrete. This chapter gives a brief overview of the types of fibers and a special mention of steel fibers, concrete fibers and their applications.

2.2. History of fibers' utilization

Many years ago, people used different fibers as a building material booster. They used straw to reinforce clay and brick and from horse's hair to reinforce the plaster, and from nineteenth century, they used asbestos to reinforce cement materials. Nowadays, use of steel, polymeric and glassy fibers, etc. seem a suitable alternative for asbestos, since its utilization was out. In 1936, the investigated projects in USA indicate that the tension concentration in crack points decrease, while using steel fiber in the brittle mix. In 1960s, the extensive research confirmed that fibers could compensate the concrete weaknesses points. Usage statistics of steel fiber in concrete indicates in some industrial countries that just over past ten years, over several million square meter of roads pavement, airports, indoor industrial floors, bridges deck, hydraulic structure, etc. performed with reinforced steel fiber (14, 15).

2.3. Different Types of Fiber

There are two methods to categorize fibers according their modulus of elasticity or their origin. In point of elasticity view, the fibers are of two basic categories of fibers that have:

- Higher elastic modulus than concrete mix *(hard intrusion)* and the second;
- Lower elastic modulus than concrete mix *(soft intrusion).*

Steel, carbon and glass have higher elastic modulus than cement mortar matrix and polypropylene and vegetable fibers are low elastic modulus fibers. High elastic modulus fibers simultaneously can improve both flexural and impact resistance, whereas, low elastic modulus fibers can improve the resistance to impact of concrete but do not contribute much to its flexural strength. According to the origin of fibers, they are classified in three categories of Metallic fibers *(such as steel, carbon steel and stainless steel),* Mineral fibers *(such as asbestos and glass fibers)* and Organic fibers (3).

2.3.1. Organic Fibers

Organic fibers can be natural and manufactured. Natural fibers can be vegetable origin or sisal *(such as wood fibers and leaf fibers*) and animal origin *(such as hair fibers and silk)*. Man-made fibers can also be divided into two groups as natural polymer *(such as cellulose and protein fibers)* and synthetic *(such as nylon and polypropylene)* (3).

The ability of the concrete improvement in these fibers depends on their length, appearance and tensile strength. However, their tensile strengths are lower than other fibers, usually cause failure in concrete structure and do not have volumetric stability against humidity.

2.3.2. Mineral Fibers

The mineral fibers were available after the establishment of the petrochemical industry. Some of these fibers are in different industries, like production of textiles and use to resist some parts of car and airplane industry. In addition, they used to refine the material of the paper. Other petrochemical products are chlorine and polypropylene that countries like Canada, Japan and USA use (3). Use of glass fiber in Japan is too practical. Glass brittleness gives specific and precise method for making and mixing concrete.

2.3.3. Steel Fibers

In 1963, the first scientific research on fiber reinforced concrete *(FRC)* was by *Romualdi* and *Baston* in the United States. SFRC is using the conventional hydraulic cements, fine and coarse aggregates, water, and SFs. Steel fiber is more practical than others are. The reasons for this issues are as follow (3):

- Steel fiber creates the highest increasing in resistance and plasticity;
- They are producible to different appearance for improve concrete behavior;
- It is easy to do to mixture of them with other concrete materials.

The behavior of SFRC can be different according to its application, fiber volume percentage and fiber effectiveness (Figure 2.1, 2.2 and Table 2.1). For instance SFRC is classified based on its fiber volume percentage as follows (3):

- Very low volume fraction of SF *(less than 1% per volume of concrete)*, which has been used for many years to control plastic shrinkage and as pavement reinforcement;
- Moderate volume fraction of SFs *(1.5% per volume of concrete)*, which can improve Modulus Of Rupture *(*MOR*)*, flexural toughness, impact resistance and other desirable mechanical properties of concrete;
- High volume fraction of SFs *(more than 2% per volume of concrete)* used to special applications such as impact and blast resistance structure; these include *Slurry Infiltrated Fiber Concrete* (SIFCON) and *Slurry Infiltrated Mat Concrete* (SIMCON).

They have different shapes (smooth, rippling, bent and rounded, oval, rectangle, crescent, and so on) that depend on production and raw materials.

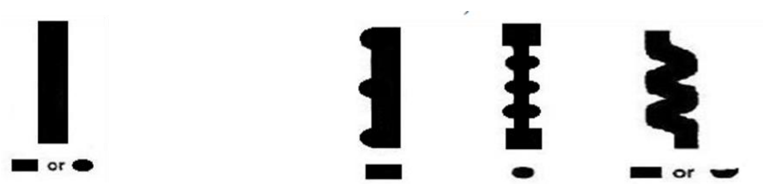

a. Straight slit sheet or wire **b.** Deformed slit sheet or fire

c. Crimped-end wire **d.** Flattened-end slit sheet or wire **e.** Machined chip **f.** Irregular fiber

Fig. 2.1. *Different shapes of steel fibers*

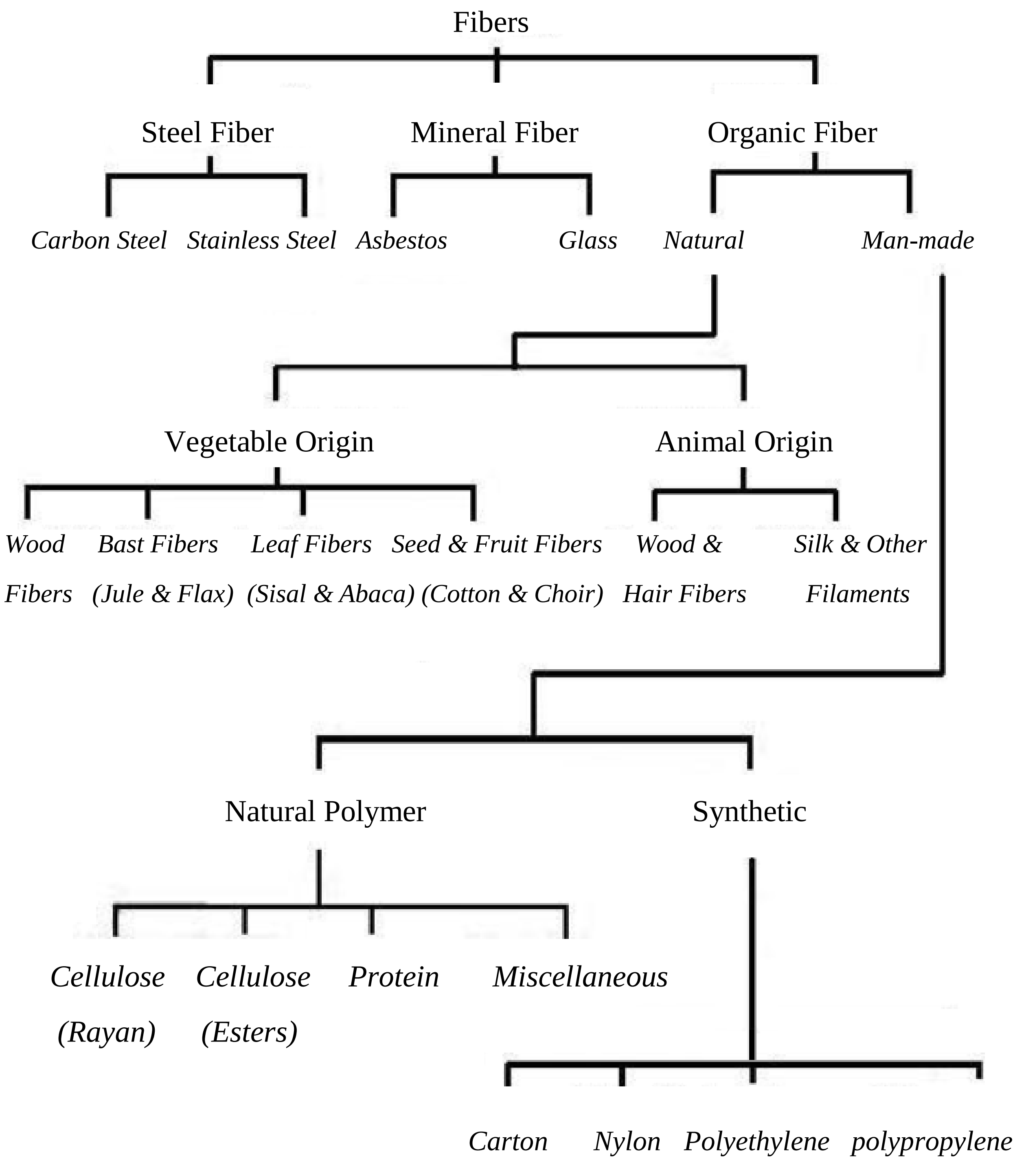

Fig. 2.2. *Fibers Classification*

Fibers	***Diameter (μm)***	***Specific Gravity***	***Modulus of Elasticity (GPa)***	***Tensile Strength (GPa)***	***Elongation To Failure (%)***
Chrysotile Asbestos	*0.02÷20*	*2.55*	*164*	*3.1*	*2÷3*
Crocidolite Asbestos	*0.1÷20*	*2.55*	*196*	*3.5*	*2÷3*
E-Glass	*9÷15*	*2.56*	*77*	*2÷3.5*	*2÷3.5*
AR-Glass	*9÷15*	*2.71*	*80*	*2÷2.8*	*2÷3*
Fibrillated Polypropylene	*20÷200*	*0.91*	*5*	*0.5*	*20*
Steel	*5÷500*	*7.84*	*200*	*1÷3*	*3÷4*
Stainless Steel	*5÷500*	*7.84*	*160*	*2.1*	*3*
Carbon Type I	*3*	*1.90*	*380*	*1.8*	*0.5*
Carbon Type II	*9*	*1.90*	*230*	*2.6*	*1.0*
Aramid (Kevlar)	*10*	*1.45*	*65÷133*	*3.6*	*2.1÷4.0*
Cellulose	*-*	*1.2*	*10*	*0.4*	*-*
Wood	*-*	*1.5*	*71*	*0.9*	*-*
Nylon (Type 242)	*>4*	*1.14*	*4*	*0.9*	*15*

Table 2.1. *General Properties of Fibers*

2.3.4. Fibers Properties

- **Fibers Aspect Ratio**
  The fiber aspect ratio is a measure of the slenderness of individual fibers, computed as fiber length divided by the equivalent fiber diameter for an individual fiber. Fibers for FRC can have an aspect ratio varying from approximately 40 to 1000 but typically less than 300. This parameter is also a measure of fiber stiffness and will affect mixing and placing (16).
- **Equivalent Diameter**
  For fibers that are not circular and prismatic in cross-section, it is useful to determine what would be the diameter of an individual fiber, if actual cross-section is as a prismatic circular cross-section. The equivalent diameter of a

fiber is the diameter of the circle having the same area as that of the average cross-sectional area of an actual fiber. Relatively small equivalent diameter fibers have correspondingly low flexural stiffness and large equivalent diameter fibers have greater flexural stiffness (16).

- **Fiber Geometry**

  Individual fibers are produced in an almost limitless variety of geometric forms including (16):

  - *Prismatic*: rounded or polygon cross-section with smooth surface or deformed throughout or only at the ends.
  - *Irregular cross-section*: variable along the length of the fiber.
  - *Collated*: multifilament or monofilament networks usually designed to separate during FRC production (mixing).

- **Fiber Elasticity Coefficient**

  When the elasticity coefficient of fiber is high, the tension in cemented matrixes and concrete is high. This is an important factor for compression and identify the various fibers benefits (3). If fibers have low elasticity, they indicate some characteristics like creep under load (9).

- **Fiber Matrix Integration**

  One of the important properties of fiber is create resistance in concrete. The methods of fiber cohesion to matrix such as adhesion, friction and mechanical involvement are similar to methods of steel armatures in reinforced concrete (17).

2.4. SFRC Benefits

The beneficial influence of SFs in concrete depends on many factors such as type, shape, length, cross section, strength, fiber content; SFs bond strength, matrix strength, mix design and mixing of concrete. The addition of SFs in the conventional reinforced concrete (RC) members, has several advantages such as (3):

- SFs increase the tensile strength of the matrix, thereby improving the flexural strength of the concrete;
- The crack bridging mechanism of SFs and their tendency to redistribute stresses evenly throughout the matrix contribute to the post-cracking strength and restraining of the cracks in the concrete;
- Increase ductility of the concrete;

- *SFRC is more durable and serviceable than conventional RC.*

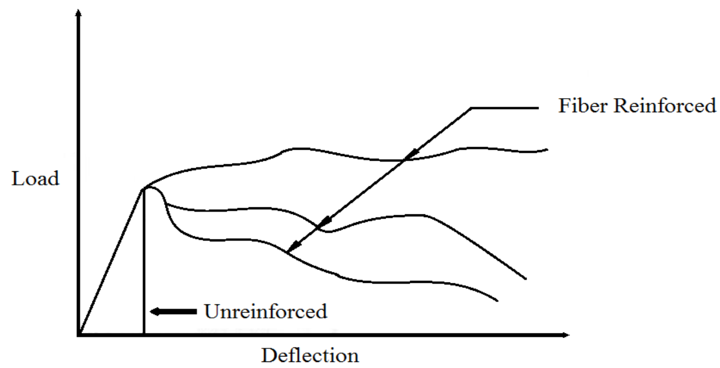

Fig. 2.3. *Load-Deflection Curves for Plain and Fibrous Concrete*

The only disadvantage of SFRC addition would be its decreased workability and accelerated stiffening of fresh concrete, thereby increasing the construction labor and time due to the excessive vibration required to make the SFRC workable. The use of newly developed high range super plasticizers, which not only enhance the workability of SFRC but also maintain the plasticity of the mix for a longer time partially compensate the negative effects.

2.5. SFRC Application

Nowadays, SFRC is in use with an increasing rate in various applications such as the followings.

2.5.1. Fiber Shotcrete

Fiber shotcrete are in use for rock slope stabilization, tunnel lining and bridge repair. Shotcrete applied monolithically on top of the fiber may prevent surface staining due to rusting of SFs and in the protection of steel structures.

2.5.2. Hydraulic Structures

The most important advantage of using SFRC in hydraulic structures is the resistance of SFRC to cavitation or erosion due to the high velocity of water flow compared to conventional RC (3).

2.5.3. Highway and Airport Pavements

A traditional source of published literature on FRP composite for the highway infrastructure is TRB's Transportation Research Information Services (TRIS), which is the official repository of all transportation-related research documentation in the United States (18). SFRC can be used in the construction of new pavements or for the repair of existing pavements by the use of bonded or un-bounded overlays to the beneath slab. It leads to a higher flexural strength causing a decrease in the pavement's thickness. Besides, the resistance to impact and repeated loading will increase. The greater tensile strain capacity of SFRC leads to a drop in the maximum crack widths in comparison with plain concrete (3).

2.5.4. Structural Applications

Steel Fiber Reinforced Concrete has several advantages such as the following:

- Provide an increased impact resistance to conventional reinforced members, enhancing the resistance to local damage and spalling.
- Inhibit crack growth and widening: this may allow the use of high strength steel bars without excessive crack width or deformation under service loads.
- SFs increase the ductility of conventional RC components and enhance their stability and integrity under earthquake and ballast loading.
- SFs increase the shear strength of RC components, as a consequence punching shear strength of slabs will be increased and sudden punching failure can be transformed into a gradual ductile failure (19).

2.6. Mechanical Properties of Steel Fiber

The crack-arrest and crack-control mechanism of SFs has three major effects on the behavior of SFRC structures (20):

- The addition of SFs delays the onset of flexural cracking: the tensile strain at the first crack increases until 100% and the ultimate strain may be 20÷50 times larger than for plain concrete.
- The addition of SFs imparts a well-defined post-cracking behavior to the structure.
- The crack-arrest property and the consequence increase in ductility imparts a greater energy absorption capacity (higher toughness) to the structure prior to failure.

This section presents basic information on the mechanical properties of steel fiber-reinforced, high-strength, lightweight concrete with compressive and flexural strengths up to 85.4 MPa and 11.8 MPa respectively. Test results show that the effect of fiber volume fraction (V_f) and aspect ratio (l_f/d_f) on flexural strength and fracture toughness is extremely prominent. Compressive strength is only slightly improved but the increase of tensile compressive strength ratio is relevant. It is observed that the flexural deflection corresponding to ultimate load increases with the increase of (V_f) and (l_f/d_f) and, due to fiber arresting cracking, the shape of the descending branch of load-deflection tends towards gently (21).

2.6.1. Compressive Strength

Johnston (1974) and Dixon and Mayfield (1971) found that an addition of up to 1.5% of SFs by volume increases the compressive strength until 15% (3). Figure 2.4 shows the relationship between the compressive strength and steel fiber volume fraction and aspect ratio. It clearly demonstrates that the compressive strength increases with increasing fiber volume fraction and aspect ratio (21).

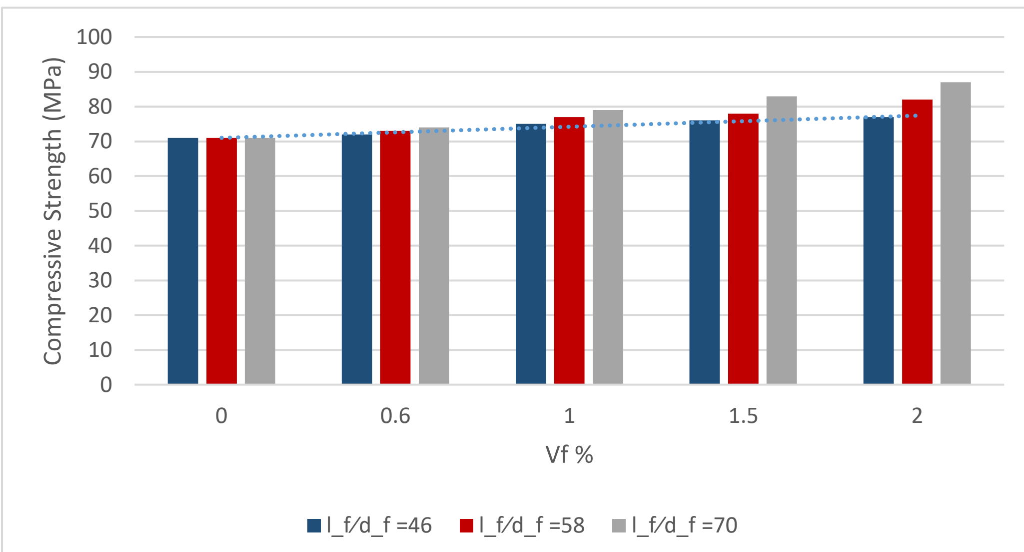

Fig. 2.4. *Effect of V_f and l_f/d_f on compressive strength*

However, it shows a relatively lower rate of increase. Under uniaxial compressive, vertical compressive and transverse tensile strain occurred in concrete compressive strength test specimens and the concrete deformation continuously increased with increasing of load. When the compressive load was increased, cracks that occurred in coarse aggregate extend and propagate into cement paste. When the compressive load reached a certain level of strength, concrete failure occurred. In the test, it was evident that the dispersion of fiber became very difficult, when the fiber volume fraction increased to 2.5%. For this reason, the concrete was not fully compacted. Concrete compressive strength increased with increasing aspect ratio of the fiber. Compressive strength does not benefit very much from a further improvement in matrix strength (21). The improvement of compressive strength of high strength, lightweight concrete with the addition of steel fiber was little. Meanwhile, the tensile/compressive strength ratio was obviously bigger. These were attributed to the effect of the steel fiber arresting cracking (21).

2.6.2. Shear Strength

SFs substantially increases the shear strength of concrete. The ultimate shear strength of SFRC containing 1% by volume of SFs increases up to 170% compared to RC without SFs. The addition of SFs completely replaces the traditional transverse shear. Rather than using a single type of SF, a combination of SFs with various aspect ratios is more effective in improving the mechanical performance of SFRC (3, 22).

2.6.3 Tensile Strength

Addition of 1.5% by volume of SFs can improve the direct tensile strength of concrete up to 40%. Those SFs aligned in the direction of the tensile stress contribute to an appreciable increase in the direct tensile strength of concrete as up to 133% for the addition of 6% by weight of smooth, straight SFs. However, for more or less randomly distributed fibers, the increase in strength is much smaller, ranging to a maximum of 60%, with many investigations indicating intermediate values. Splitting-tension test of SFRC show similar result. Thus, adding fibers merely to increase the direct tensile strength is probably not worthwhile. However, as in compression, steel fibers do lead to major increases in the post-cracking behavior or toughness (3).

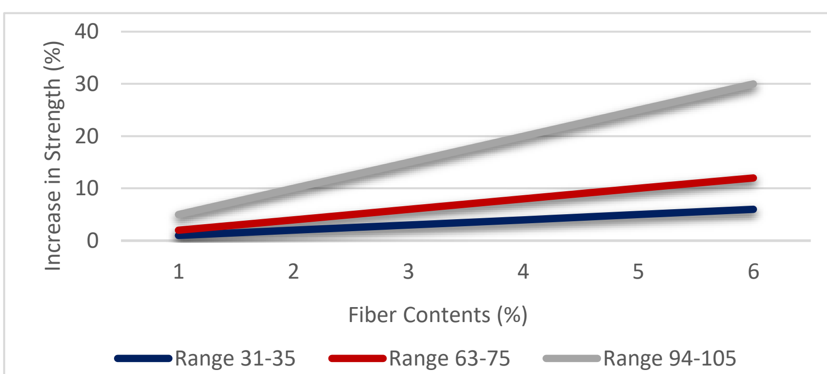

Fig. 2.5. *Influence of Fiber Content on Tensile Strength*

2.6.4. Durability

Corrosion in concrete structures due to the cracks is less severe in the SFRC structures compared to conventional RC ones. In 1985 Schupack found that a well-compacted SFRC has a limited corrosion of fibers close to the surface of the concrete even when concrete is highly saturated with chloride ions. In 2005 Turatsinze, conducted a research to investigate the corrosion of SFRC due to the cracks (3).

Steel fiber increases durability in concrete by reduction in the cement paste content. Durability and other charachteristics of concrete depend upon the properties of its ingredients, the mix properties, the method of compaction and other controls during placing, compaction and curing. Adding fibers in concrete, increase its durability againts chemical attacks (23).

Prismatic SFRC specimens with the dimensions of 100x100x500 mm containing hook-end SFs with the dimensions of 60 mm in length and 0.8 mm in diameter were prepared. Specimens with vertical cracks were exposed to a marine-like environment for 1 year. After 1 year, the prisms were tested in three-point bending setup with the span of 200 mm and load-deflection graphs were plotted and concluded that only SFs crossing the crack within a 2 to 3 mm rim from the external faces of the specimens exhibited extensive corrosion (3). Besides, no SFs corrosion was observed in narrower parts of the cracks (i.e. where crack mouth opening was about 0.1 mm) whilst in the wider parts of the cracks (i.e. where crack mouth opening was equal to 0.5 mm) a light corrosion of the fibers with no reduction in their section was observed. The measurement of concrete electrical resistivity can give an indication of concrete durability.

Figure 2.6. shows the relationship between the concrete electrical resistivity and curing ages and indicates the reduction of concrete electrical resistivity with the increase in the percentage of SFs due to the conductivity of the fibers. However, the gel formation due to the cement hydration and pozzolanic reaction causing a dense microstructure and fills the conductive channel, thereby it decreases the effect of SFs conductivity. In the long run, with the addition of 1% of SFs, the desired concrete electrical resistivity of over 20 kΩ x cm can be reached.

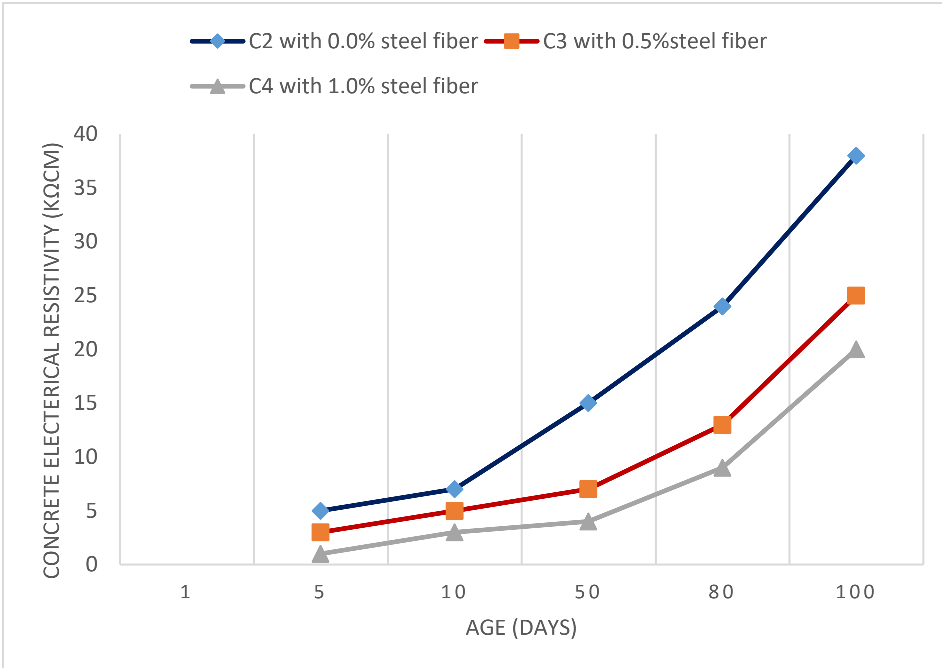

Fig. 2.6. *Effects of Fibre Content on Concrete Electrical Resistivity*

2.7. Method of fiber perch

The method of fiber perch in the crack axis is effective in the power transmission to the crack level. The fibers that are parallel to the crack, do not help the power transmission. But, the fibers indicate the maximum impact from themselves while they are perpendicular to the crack. The amount of matrix reinforcement by fibers depend on the number of distributed cross-section directions:

- Parallel to the tensions;
- Randomly in two dimensions;
- Randomly in three dimensions.

Usually in massive concreting, the fibers are in three-dimensional form and the increase in resistance can happen in all directions. For example in roads and airports pavements, it is necessary to distribute fibers in two dimenions parallel to horizontal or strain tension axis. Finally, the fibers in one dimension, are not effective.

2.8. Important factors in design and selection of fibers

The important factors in the design of fibers are as follow:

- Tensile strength;
- Elasticity coefficient of fibers;
- Separating problems in matrix-fiber;
- Length of fibers;
- Possibility of transformation in concrete;
- Thikness of fibers surface, enlarging or bending their ends;
- Possibility to use multi-string fibers for better adhesion.

The ultimate fiber reinforced concrete depends on (2-1) equation:

$$S_c = AS_m(1 - V_f) + BV_f({}^{L}/{}_{d}) \tag{2-1}$$

Where:

S_c = Final strength of the cement paste;

V_f = Fiber volumetric ratio;

A = Constant Number;

B = Coefficient depending on the consistency resistance and shape of fibers.

2.8.1 Steel Fiber Making Method

One of the main advantage of using steel fibers in concrete is to increase the post-peak load carrying capacity of concrete after initial cracking. Types of steel fibers used in concrete are (24):

- Smooth cold-drawn wire;
- Deformed cold-drawn wire;
- Smooth or deformed cut sheet;
- Melt-extracted fibers;
- Mill-cut or modified cold-drawn wire.

The most important steel fiber production countries around the world are Belgium, Italy, Germany and USA. The tensile strengths of steel fibers are in the range of 345÷2100 MPa and the ultimate elongations of 0.5÷35%. The main disadvantage of high strength fibers is that it causes severe spalling around the fiber ends. Straight and smooth fibers have poor bond with the matrix. Thus the surfaces of fibers were modified in the recent years to increase it. These include hooked, crimped, deformed and enlarged end fibers (24).

Fig. 2.7. *Hooked end fibers*

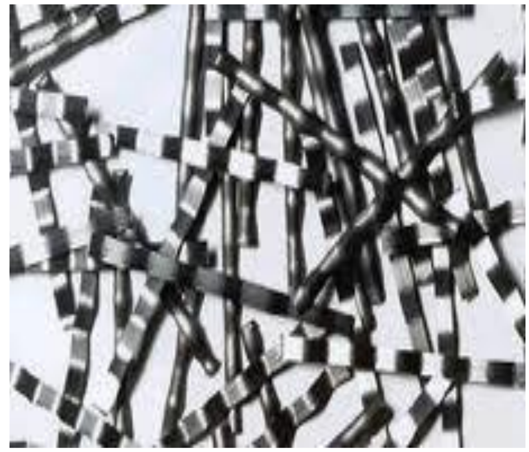

Fig. 2.8. *Crimped steel fibers*

Round fibers are produced by cutting or chopping wires, with diameters typically in the range of 0.25÷1 mm and flat fibers are produced by shearing sheets or flattening wire. The dimensions of flat fibers are in the range of 0.15÷0.4 mm thick and 0.25÷0.9 mm wide. Fibers are also produced by the hot melt extraction process (24).

2.9. Polypropylene FRC in Compression

According to Balaguru (1988), the uniaxial compression test is normally used to evaluate the behavior of concrete in compression. This produces a combination of shear failure near the ends of the specimen with lateral swelling of the unconfined central section accompanied by cracking parallel to the loading axis when the lateral strain exceeds the matrix cracking strain in tension. Fibers can affect these facets of uniaxial compressive behavior that involve shear stress and tensile strain. This can be seen from the increased strain capacity and toughness (area under the curve) in the post-crack portion of the stress-strain curve (24).

The addition of fibers up to a volume fraction of 0.1% does not affect the compressive strength. When tested under compression, failure occurs at or immediately after the peak load providing very little toughness. In some instances, if more water is added to fiber concrete to improve its workability, a reduction in compressive strength can occur. This reduction should be attributed to additional water or an increase in entrapped air (24).

2.9.1. Literature on ASTM C1550

The need for a reliable and economical estimation for the post-crack performance of fiber-reinforced concrete material has led to the development of a determinate panel test. Post-crack performance in fiber reinforced concrete was assessed using beams. In the past years, ASTM C1018 beam test was used to assess the post crack performance. In Australia, a similar beam test method called EFNARC was used for the measurement of post crack performance. EFNARC beam test is a third-point loaded test used for the assessment of Fiber Reinforced Shotcrete (FRS) performance. The EFNARC specification does not clearly mention how to test the beam in order to obtain central deflections excluding the extraneous deformation. But these methods often caused problems for designers and contractors as the results obtained from the beam tests had high with-in batch variability (25).

The area of the concrete beam that experiences failure is very small compared to the volume of the concrete contained within an FRS structure. The performance of the beam is not representative of the majority of concrete, because the performance is strongly dependent on the number of fibers involved in the crack (25).

2.10. Concrete with high stifness

The concrete with higher stifness can tolerate many deformation without fail. The purposes of utilization of fibers in concrete increases tensile strength, cracks control, etc. In the fabrication of tunnels, the fiber concrete is used by spraying on the tunnel wall without armature to remove the crack in tuneel coverage.

In a new kind of fiber concrete can be reached high fineness with pouring slurries on the fibers. In this way the fibers are first shed then the spaces among them are filled with slurry mortar. The amount of fiber in this concrete is about 10%, which is about ten times the amount in conventional fiber concretes (26). This type of material can create protective layers without crack. The compressive strength of this type of concrete is 85÷110 Pascal and the bending strength is 35÷45 N/m. These components can be used not only as small protective layers but also in the runways of airports, where it shows good performance against blows (26).

In order to improve the concrete technology standards, the fibers can be made with conventional reinforced or prestressed concrete. These are as follows:

- Foundations of engines and large industrial machinery;

- Protective walls;
- Shelters and aircraft hangars;
- Atomic reactor building;
- Refractory parts with steel fibers.

2.11. Effects of SFRC for Concrete Pavement Slab Replacement in Transport

2.11.1. Concrete pavement slab replacement standards

The Florida Department of Transportation (FDOT) Design Standards, require a full depth replacement of concrete slab with severe distresses. The construction standards and requirements of the replacement slab are provided in Section 353 of the Standard Specifications for Road and Bridge Constructions. Two of the most important acceptance criteria for the replacement slab are the plastic property, specifically the 6-hour compressive strength of 2,200 psi, and the 24-hour compressive strength of 3,000 psi. The 6-hour compressive strength is also used as the determination point to open the slab to traffic and, therefore, it is highly emphasized in the standard specifications. In fact, if the replacement slab does not meet the plastic property requirements and this will severely impact the replacement slab service life, the contractor would have to replace the slab at no cost to the FDOT. Thus, to ensure the replacement slab meets the plastic property requirements, low water/cement ratio concrete and concrete accelerators are used. As a consequence, the FDOT also specified a limit on the concrete temperature not to exceed 100°F and requires the contractor to cure the slab with curing compound and cover the surface with white burlap-polyethylene curing blanket immediately after the slab hardens. Furthermore, if uncontrolled cracks appear on the replacement slab, the contractor will have to replace the slab free of charge (27).

2.11.2. Project objectives

The main purpose of this project is to explore the potential use of FRC for concrete pavement slab replacement. Accordingly, this project has four objectives (27):

- To develop FRC replacement slab mixtures;
- To evaluate the performance of FRC mixtures particularly on early-age cracking;
- To evaluate the performance of FRC slab using demonstration slabs;

- To develop guidelines for proportioning, mixing, placing, finishing and curing of FRC
- To replace slab.

2.11.3. Construction practices

Mixing

There are some important differences in mixing FRC compared to conventional concrete. One of these is the effect of fiber balling that prevents good dispersion of the fiber in concrete. There are two methods that have been effectively used in the past to prevent fiber balling of steel fiber:

1. to add fibers to transit mix truck after all ingredients have been added and mixed;
2. to add fiber to aggregate on a conveyor belt.

Using vibration is necessary for consolidating the concrete and, therefore, traditional slump cone test cannot be used for quality control. Although increasing the fiber amount could potentially improve the concrete properties (28).

Placing and finishing

According to literature, there are few differences between the methods for placing and finishing conventional concrete and FRC. A difference for slab construction is that vibration is needed for the FRC since the material tends to hang together. Additionally, high-range water-reducing admixtures should be added to FRC to increase the workability of the mixture and for easy placement (29).

Curing and protection

There is no special treatment when fibers are added to concrete. Like conventional concrete, FRC needs appropriate protection when placing during hot and cold weather (29).

2.11.4. Shrinkage and cracking properties

There are four main types of shrinkage cracks in concrete:

1. Autogenous;
2. Plastic;
3. Drying;
4. Carbonation.

Autogenous shrinkage is associated with the loss of water due to the hydration process of concrete at early age and is considered relatively small compared to drying shrinkage. However, for high-early strength concrete, as a result of high heat of hydration, autogenous shrinkage contributes quite significantly and in some cases it could be as high as drying shrinkage (30).

Plastic shrinkage occurs when the rate of evaporation exceeds the bleeding rate or, in other words, the concrete dries too fast due to the combination of heat and wind of the surrounding area. For typical concrete pavement, the plastic shrinkage could be controlled by applying appropriate moist curing practices. However, for replacement slab, traditional moist curing for 7 days could not be achieved because the road will need to be reopened to traffic within 24 hours. Thus, both autogenous and plastic shrinkages are a big problem for concrete pavement slab replacement that could potentially lead the slab to crack. The other two types of shrinkage cracks are not a potential problem for concrete pavement slab (30).

Wecharatana and *Shah* (1983) and *Göteborg* (2005) suggested that three distinct regions exist and can be identified as:

- Traction free zone, which occurs for relatively large crack openings (figure 9);
- Fiber bridge zone, where stress transfers result by frictional slip of fiber (figure 10);
- Macro and Micro crack growth zones, where aggregates interlock and transfer stress (figures 2.11 and 2.12).

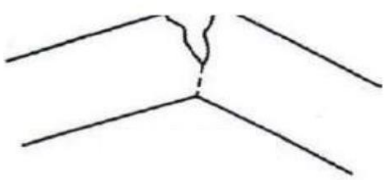

Fig. 2.9. *Crack without Fiber*

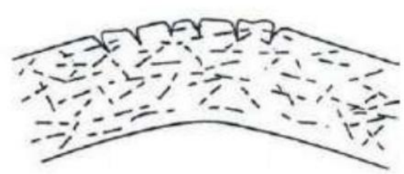

Fig. 2.10. *Crack with Fibers*

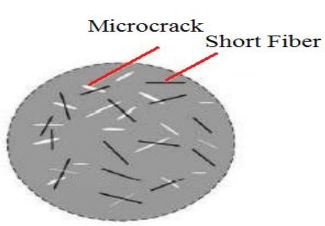

Fig. 2.11. *Effect of short fibers on microcracking*

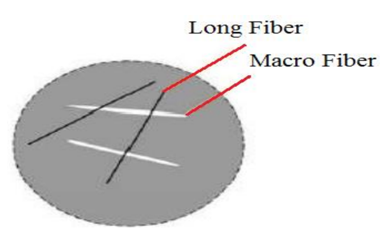

Fig. 2.12. *Effect of long fibers on macrocracking*

2.12. Executive notes on the manufacture of fiber concrete

The fibers can be added to the concrete mixture before, after or during mixing, but for easy broadcasting it must be mixed dry. It should be noted that in the process of manufacturing of fiber concrete it has to avoid the balling phenomenon occurring for high and incorrect use of fibers. Because, in this case, the clogging phenomenon occurs in concrete and the effect of the fiber virtually disappears.

2.12.1. Utilization of fiber concrete

Because of this reason, the amount of fiber used in concrete to prevent the balling phenomenon is low (approximately 0.1%), the compressive strength does not increase much, because the fiber was not a macroscopic mechanical element and it is only an auxiliary element. To compare the cost of building fiber with reinforced concrete we should consider the advantages of fiber concrete including higher impact resistance, shrinkage and less crack width, more durable and reduced maintenance costs, control of local defects, creation and expansion of cracks, longer technical life and more permeation control. In the implementation of concrete, we should consider longer internal vibration because it leads to separate the fibers in concrete, therefore external vibration is always recommended. Nonetheless, operation and maintenance of fiber concrete is similar to ordinary concrete.

Increase the apparent aspect ratio (I/d) causes the accumulation and conflict of fibers. For a uniform mixture, the maximm aspect ratio is 100. As recommended by ACI 211 the required steps in the mixing plan are as follows:

- Smooth slump with type of work and required resistance (25÷50 mm for massive concrete, about 100 mm for arrows and columns;
- Increased slump without reducing resistance by using super lubricant;
- Determination of the amount of water, grain size and air bubbles;
- Amount of air bubbles depending on the weather condition, particularly for frost areas, though it decreases resistance;
- Fiber concrete including more fines;
- Recommended grain size of 9.5÷19, anyway not exceeding 37 mm.

2.12.2. Example of the use of fiber concrete in the construction of slab railways

Utilization of steel fiber in a high speed railway project in North America (figure 2.13) to decrease the amount of rebar in concrete up to 50% with constant amount of cracks. The objective is to increase the efficiency and the quality of materials to save time and money.

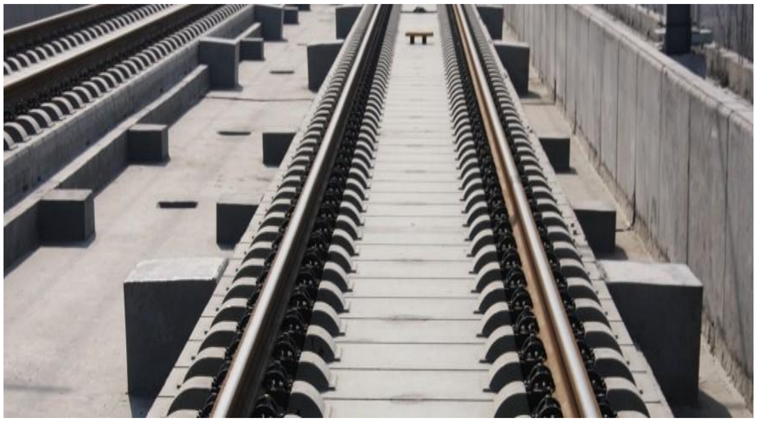

Fig. 2.13. *High speed slab railway project in North of America (Bekaert Company, 2002)*

Reconstruction of junctions in Newmarket City in Auckland, New Zealand, as a part of DART railroad Project (figure 2.14). The limitation of the traffic interruption has been a key element in favour of the use of fiber of RC-80/60-BN Dramix Company typology with a consumption volume of 40 kg/m^3.

Fig. 2.14. *Reconstruction of junctions in railroad project in Auckland (DART project)*

2.13. A summary of papers and research in field of fiber concrete

Due to the growing requirement of industry foor fiber concrete, scientists around the world found out the importance of using this technology. Therefore, due to the newness of this technology and the arising implementation problems, extensive researches, both theoretical and experimental, are focusing on better understanding concrete fiber. A summary of the published articles on this topic is presented in the table below.

Row	***Research Title***	***Research Year***	***Researcher Name***	***Abstract***	***Result Summary***
1	*Fatigue Behavior of Steel Fiber Reinforced Concrete*	*1990*	*Antonio Nanni*	*Study of fatigue and residual strength of reinforced concrete to steel fibers. Bending test, sample cylinder gap and cubes reinforced.*	• *Fatigue response SFRC is better than simple concrete.* • *The same effect Cut Sheet Fibers with Hooked fiber with same dimention.*
2	*Compressive stress±strain relationship of steel fibre-reinforced concrete at early age .*	*1999*	*Yining Ding*	*Effect of steel fibers on compressive strength, maximum load time, Absorption of energy under uniaxial compressive loading.*	• *The mechanical properties of concrete/shotcrete can be improved by the addition of steel fibres.* • *The compressive load increase continued after visible crack-opening on the specimen surface.* • *After achieving the maximum strength, the load of SFRC was sustained over some minutes, while the load of other concrete samples without fibres fell down quickly from the maximum value.*
3	*Fatigue behavior of fiber-reinforced concrete in compression*	*2000*	*Paulo B. Cachim* *Joaquim A. Figueiras*	*Evaluation of the performance of plain and fiber-reinforced concrete under compressive fatigue loading. Two types of hooked-end steel fibers (30 mm*	• *Experimental program pointed out some of the most relevant characteristics of the behavior of plain and steel fiber concrete under compressive fatigue loading.* • *The addition of fibers to concrete provides an*

			Paulo A.A. Pereira	length and 60 mm length) have been tested and their performance compared.	increase in the deformation at failure. • The key to the success of improving the fatigue life of concrete with the addition of fibers seems to be related with the distribution of the fibers in concrete.
4	Uniaxial tension test for steel fibre reinforced concrete—a parametric study	2002	Bryan E. Barragaan. Ravindra Gettu . Miguel A. Martıın . Ra uul L. Zerbino	A RILEM Draft Recommendation was proposed in 2001 for obtaining the stress versus crack opening (σ–w) response of steel fibre reinforced concrete through a uniaxial tension test.	• The ranges of the used parameters and the limited number of specimens tested here, the uniaxial tensile test for SFRC, using a notched moulded cylinder, proposed recently as a RILEM Draft Recommendation. • The post-peak stresses and toughness parameters obtained from the tests exhibit coefficients of variation of up to 30%. • The test methodology has also been employed for the characterisation of the tensile response of cores extracted from cast SFRC elements. • Toughness measures based on the post-peak response have been proposed for representing the tensile behaviour of SFRC, and for possible use in structural analysis and design.
5	Flexural behaviour of small steel fibre reinforced concrete slabs	2002	AliR. Khaloo.	Influence of length and volumetric percentage of steel fibres on energy absorption of	• Addition of fibres does not significantly increase the ultimate flexural strength of SFRC slabs. • In slabs with low fibre volume (0.5%) the

			Majid Afshari.	*concrete slabs with various concrete strengths is investigated by testing 28 small steel fibre reinforced concrete (SFRC) slabs under flexure.*	*resisting load after cracking was relatively small. The rate of improvement in energy absorption reduced with increase in fibre content.* • *According to comparison between experimental load–deflection curves and a theoretical prediction method, based on allowable deflection is developed for SFRC slabs. The method covers volumetric percentages of steel fibres in the range of 0.75÷1.75.*
6	*Effect of steel fiber on the deicer-scaling resistance of concrete*	*2005*	*Yang Quanbing.* *Zhu Beirong*	*The deicer-scaling resistance of concrete is reduced by the addition of steel fibers at the same air content, especially for the air-entrained concrete, even though the flexural strength of concrete is significantly improved by the addition of fibers*	• *Based on the above results, the addition of steel fibers has the following effects on concrete: (1) reducing the slump; (2) increasing the flexural strength; (3) reducing the deicer-scaling resistance.*
7	*Behavior of high strength concrete with and without steel fiber reinforcement in triaxial compression*	*2005*	*Xiaobin Lu.* *Cheng-Tzu Thomas Hsu*	*Based on an extensive experimental program, this paper studies the behavior of high strength concrete and steel fiber reinforced high strength concrete under uniaxial and*	• *Under the uniaxial compression, the steel fiber reinforcement only slightly increased the uniaxial compressive strength and the peak axial and lateral strains of HSC, but notably improved its capability of resisting post peak deformation on the*

				triaxial compression.	*descending branch of the stress–strain curve.* • *Under the triaxial compression, the steel fiber reinforcement has an insignificant effect on the nonlinear stress–strain relation of HSC.* • *In the triaxial compression, the HSC and SFHSC essentially fall within the same ultimate strength envelops in terms of the Mohr-Coulomb and Willam-Warnke failure criteria.* • *Under the triaxial compression, a uniform relationship between the octahedral shear stress and the engineering octahedral shear strain at peak stress can be adopted for both HSC and SFHSC.*
8	*Effect of aspect ratio and volume fraction of steel fiber on the mechanical properties of SFRC*	*2005*	*Semsi Yazıcı* *Go¨zde*	*Effects of aspect ratio (l/d) and volume fraction (V_f) of steel fiber on the compressive strength, split tensile strength, flexural strength and ultrasonic pulse velocity of steel fiber reinforced concrete (SFRC) were investigated. Three different fiber volumes were added to concrete mixes at 0.5%, 1.0% and 1.5% by*	• Significant improvement in flexural strength SFRC with increase of I/d ratio and Vf. • Improve the flexural strength of the concrete compared to the compressive strength and tensile strength of the gap.

				volume of concrete	
9	*Properties of steel fiber reinforced fly ash concrete*	*2007*	*Cengiz Duran Atis* *Okan Karahan*	*Properties studied include unit weight and workability of fresh concrete, and compressive strength, flexural tensile strength, splitting tensile strength, elasticity modulus, sorptivity coefficient, drying shrinkage and freeze–thaw resistance of hardened concrete. Fly ash content used was 0%, 15% and 30% in mass basis, and fiber volume fraction was 0%, 0.25%, 0.5%, 1.0% and 1.5% in volume basis.*	• *Increase the specific gravity of the concrete uniformly by increasing the amount of fiber.* • *Reduces specific concrete weight by increasing the amount of ash dust.* • *Reduced concrete performance by increasing the amount of fiber.*
10	*Torsional behavior of steel fiber reinforced concrete beams*	*2011*	*Fuad Okay* *Serkan Engin*	*Torsion of structural members and the behavior of steel fiber reinforced concrete became the area of interest of many researchers in the past and it is still newsworthy. The volumetric steel fiber content, fiber*	• *Improve the torsion capacity of the beam by adding steel fibers.* • *Improve energy absorption capacity by adding fibers.* • *Decrease in width and avoid increase of cracks with increase of steel fiber in concrete.*

				aspect ratio, and the longitudinal reinforcement were the variables of the investigation.	
11	*Effect of steel and carbon fiber additions on the dynamic properties of concrete containing silica fume*	*2011*	*V.T. Giner,* *F.J. B aeza,* *S. Ivorra ,* *E. Zornoza,* *Ó. Galao*	*Fiber reinforced concretes (FRC) are technologically important due to their combination of good structural properties, durability and multifunctional properties.* *The behavior of a structure under dynamic actions is determined by its dynamic mechanical properties and its total overall damping*	• *Slight increase in resonant frequency with increase of Carbon fiber.* • *Decrease in resonant frequency with increase of steel fiber.*

2.14. Experimental Program by Khaloo

Fourteen concrete mixtures with four different fiber contents, two different fibre lengths and two concrete strengths were designed. The slabs were square with dimensions of 820 x 820 mm and thickness of 80 mm. Four corners of slabs were seated on roller points which provided clear span length of 680 mm. Point load was applied by stroke mode of an actuator on 80 x 80 x 10 mm steel plate placed at slab center. The displacement at the loading point was increased at rate of 1.5 mm/min. Sensitive linear voltage differential transducers were used to measure the deflection at slab center (13). The compressive strengths of 152.4 x 304.8 mm cylindrical plain specimens were 30 and 45 MPa at the age of 28 days. The volumetric percentages of steel fibres, i.e., the ratios of the volume of fibres to the volume of matrix were 0.5, 1.0 and 1.5, which correspond to 25, 50 and 75 kg of steel fibres for mix proportions used in the tests. Cement type I along with river aggregates was used. Sand had a fineness modulus of 2.7 and coarse aggregates had a maximum aggregate size of 19 mm. The superplasticiser corresponded with ASTM C494 Type F. The crimped shape steel fibres had a rectangular cross-section (13) (Fig. 2.15).

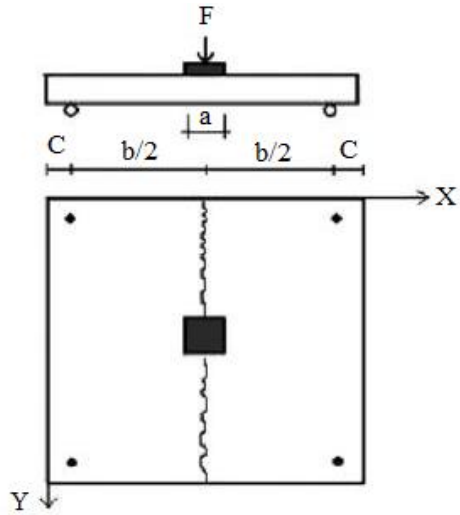

Fig. 2.15. *Slabs in the four corners of the square on the roller supports and load on the center of the slab*

The description of the experimental program is in Table 2.2.

The quantity of concrete and fibers are in Table 2.3 and 2.4.

2.14.1 Experimental results and discussion

The average test results for each pair of slabs are presented in Table 2.5. Also flexural test results of slabs are shown as load-deflection and absorbed energy-deflection curves in Fig. 2.16.

Concrete strength (f'_c, MPa)	Fibre type	Fibre volumetric percentage	Specimen number	Number of cylindrical specimens	Number of slabs
30	–	0	1	3	2
	jc25	0.5	2	3	2
		1.0	3	3	2
		1.5	4	3	2
	jc35	0.5	5	3	2
		1.0	6	3	2
		1.5	7	3	2
45	–	0	8	3	2
	jc25	0.5	9	3	2
		1.0	10	3	2
		1.5	11	3	2
	jc35	0.5	12	3	2
		1.0	13	3	2
		1.5	14	3	2
Total number of specimens				42	28

Table 2.2. *Experimental Program*

Concrete strength (MPa)	Cement (kg)	Fine aggregates (kg)	Coarse aggregates (kg)	Water (kg)	Superplasticiser	Water–cement ratio
30	400	800	1000	192	0.5% = 2 kg	0.48
45	450	750	1000	166.5	1.5% = 6.75 kg	0.37

Table 2.3. *Mix Proportion of Concrete* (m^{-3})

Fibre type	Length (L, mm)	Width (W, mm)	Thickness (T, mm)	Equivalent diameter (d_f, mm)	Aspect ratio (L/d_f)
jc25	25	0.8	0.35	0.597	41.9
jc35	35	1.0	0.35	0.668	52.4

Table 2.4. *Shape Properties of steel fibers*

2.14.2 Ultimate strength of slabs and energy absorption characteristics

The presence of steel fibres in concrete did not significantly influence the ultimate strength of slabs. Small variation in the ultimate strength was due to changes in compressive strength of concrete caused by addition of fibres. Essentially, ultimate strength corresponds to initiation of major cracks. The fibres did not considerably influence flexural characteristics of slabs prior to cracking (13). The main effect of fibres is on energy absorption capacity that is dealt with in this study. Steel fibres increased energy absorption capacity as measured by the area under load-deflection curve. Also, increase in fibre content decreased the growth rate of total energy absorption (Table 2.5) (13).

Specimen number	Concrete strength (f'_c, MPa)	Ultimate load (F_{max}, KN)	Deflection at F_{max} (mm)	Energy absorption at F_{max} (J)	Ultimate deflection (mm)	Total energy absorption (J)
1	30.0	22.1	0.52	6.1	0.52	6.1
2	32.2	21.3	0.40	6.0	12.50	78.5
3	31.6	20.2	1.50	21.0	21.00	129.0
4	30.4	22.4	0.70	8.8	23.00	192.4
5	32.4	18.4	0.22	2.2	18.50	73.0
6	33.1	23.2	0.52	8.1	33.00	172.0
7	33.0	22.4	0.95	12.2	28.00	170.5
8	44.9	26.9	0.37	6.2	0.37	6.2
9	47.6	28.0	0.42	7.0	2.75	24.1
10	45.7	34.6	0.40	7.4	23.00	166.6
11	43.7	32.4	1.25	28.1	30.50	335.2
12	45.5	25.0	0.46	7.1	17.50	94.5
13	48.3	27.2	0.78	11.7	20.50	169.8
14	45.9	33.8	0.85	17.8	36.05	372.0

Table 2.5. *Test Result*

As is shown in Fig. 2.16.b, for jc35 fibres with concrete strength of 30 MPa, increase in fibre volume from 1% to 1.5% did not influence energy absorption of the SFRC slab. In specimens with 0.5% fibre volume, a sudden dropin load-deflection curve is observed which is more pronounced for higher strength concrete (Fig.2.16.c). Steel fibres of 0.5% did not enhance the behaviour of concrete slabs significantly (13).

Generally longer fibres (or fibres with larger aspect ratio) provided slightly higher energy absorption capacity (Fig. 2.16). In average, the total energy absorption of slabs with jc35 fibres was about 1.2 times that of slabs with jc25 fibres (Table 2.5). Increase in concrete strength increased the energy absorption capacity of the SFRC slabs (13).

2.14.3 Mode of Failure

The slabs did not show any visible cracks prior to ultimate strength. The plain slabs failed suddenly at cracking load without any appreciable deflection warning. The deflection for plain slabs was in the neighbourhood of 0.35÷0.55 mm with small energy absorption that was about 6 J. The SFRC slabs experienced appreciable deflection after ultimate load and withstood deflections in the range of 12.5÷36 mm, except the slab no. 9 which contained low quantity of short fibres and high strength concrete (deflection of this slab was as low as 2.75 mm at failure). This deflection range corresponds to deflection /span ratio from 1.8% to 5.3%. The SFRC slabs with fibre content of 1.0% and 1.5% failed gradually while the fibres were pulled out of concrete. The plain slabs broke in two pieces at ultimate strength, while SFRC slabs maintained their integrity to relatively high deflection after ultimate strength (13).

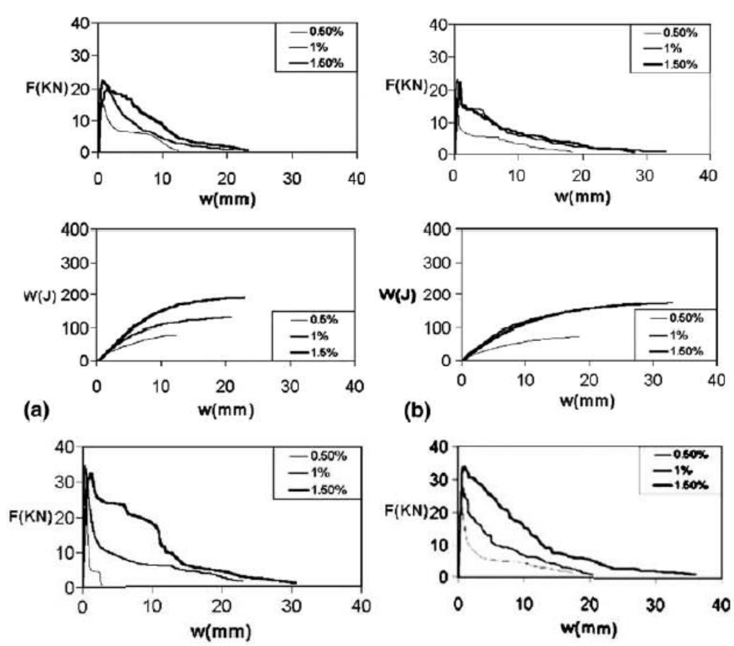

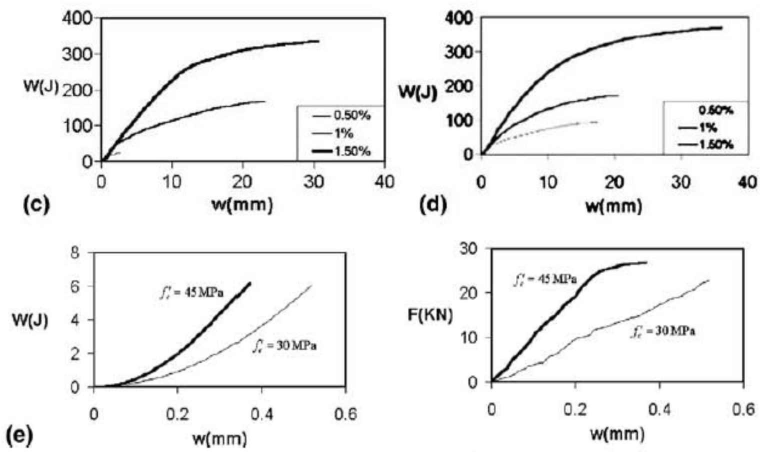

Fig. 2.16. *Load-deflection and absorbed energy-deflection curves for slabs. Concrete strength of (a) 30 MPa and jc25 fibres, (b) 30 MPa and jc35 fibres, (c) 45 MPa and jc25 fibres, (d) 45 MPa and jc35 fibres; and (e) plain concrete slabs.*

2.15 Conclusions

The reached conclusions are as follows.

- Addition of fibres does not significantly increase the ultimate flexural strength of SFRC slabs. However, it improves the energy absorption capacity of slabs. The energy absorption of slabs with fibre volume of 0.5% was about 12 times that of plain concrete slabs. The slabs with fibre volume of 1.0% experienced energy absorption of about 2 times that of slabs with 0.5% fibres. In 1.5% SFRC slabs, the energy absorption was about 1.5 times that of slabs with fibre volume of 1.0% (13).
- In slabs with low fibre volume (0.5%) the resisting load after cracking was relatively small. The rate of improvement in energy absorption reduced with increase in fibre content. It is recommended to use fibre volumetric percentages in the range of 0.75÷1.75. Longer fibres (i.e. fibres with higher aspect ratio) provided higher energy absorption. The energy absorption of jc35 fibres was about 1.2 times that of jc25 fibres. Increase in strength of fibre reinforced concrete enhances the energy absorption capacity. Moreover, fibres have similar effects on behaviour of slabs with different concrete strengths (13).
- According to comparison between experimental load-deflection curves and a theoretical prediction method, a design method based on allowable deflection is developed for SFRC slabs. The method covers volumetric percentages of steel fibres in the range of 0.75÷1.75 (13).

Chapter 3

Overview on fiber concrete design criteria: shear, bending, and crack width

3.1 Inroduction

To ensure adequate safety and economy are the design purposes of a structure or a structure's component. Adequate safety means to have a sufficient stability. This chapter explained a short summary about structural design methods and the choice of the state mode for design of reinforced slab lines with fibers and armature.

3.2 Design methods

3.2.1 Allowable stress design

Allowable stress design, which is known as exploitation method, is one of the old method of structural design. Although the design process based on allowed tension method is simple and mostly obtaining a safety plan, it does not represent a realistic estimate from consumption capacity and, in many cases, it is possible that the coefficient of confidence is higher than considered.

3.2.2 Resistance design method

Resistance design method, known as ultimate strength design of a component at each level should be equal or more than necessary the resistance, which is calculated by coefficients under load combinations (U):

$$(U) Resistance\ Required \leq Design\ Resistance \tag{3-1}$$

In this equation, the design resistance is calculated by multiplying resistance coefficient (φ) and nominal resistance.

$$Design\ Resistance = Resistance\ Coefficient\ \varphi * Nomial\ Resistance \tag{3-2}$$

In equation (3-2), the resistance coefficient is lower than 1 that is considered for the compensation of the following issues:

- Probability of less resistance of a component based on possible variations used in the strength of materials and their dimensions;
- Inaccuracy in design equations;
- Importance of the component in the structures.

3.2.3 Design at limit state

Limit state design (LSD), also known as load and resistance factor design (LRFD), refers to a design method used in structural engineering. A limit state is a condition of a structure beyond which it no longer fulfills the relevant design criteria. The condition may refer to a degree of loading or other actions on the structure, while the criteria refer to structural integrity, fitness for use, durability or other design requirements. A structure designed by LSD is proportioned to sustain all actions likely to occur during its design life and to remain fit for use, with an appropriate level of reliability for each limit state. Design at limit state is a design approach basing on the concept of probabilities. The probability of a structural failure can be reduced by estimate of load effects higher than the assurance that $R \geq S$. This concept can be show by this equation:

$$\varphi R_n \geq \alpha S_n \tag{3-3}$$

Where:

- R_n: nominal resistance;
- φ: resistance coefficient;
- S_n: nominal load effect based on specified loads;
- α: load factor, usually <1.

This equation expresses the behavior of the scheme in a simplified way. In operation, the right side of equation is divided into different load factors like (dead load, live load, wind load, etc.) showed by (3-4) equation:

$$\alpha S_n = \alpha_D S_{Dn} + \alpha_L S_{Ln} + \alpha_W S_{Wn} \tag{3-4}$$

Where:

- S_{Dn}: nominal dead factor effect;
- S_{Ln}: nominal live factor effect;
- S_{Wn}: nominal wind factor effect;
- α_D: dead factor coefficient;
- α_L: live factor coefficient;
- α_W: wind factor coefficient;

Basically, the dead load is more predictable rather than live factor coefficient (31).

3.3 Fiber concrete design

This part is considered a review of the criteria and available regulations concerning analysis and design of fiber concrete. In this way the RILEM, FIB, and ACI regulations are investigated. The FIB and RILEM regulations are explained about flexural design discussion, shearing, and crack control in fiber concrete beams with and without armature, whereas from these two regulations FIB explains about the fiber concrete slab without armature only and it did not about component of fiber concrete and armature (32).

3.4 Design of fiber reinforced concrete beams in RILEM regulation

RILEM is an international committee that is created by purposes of structural development and materials used in structures. In this regulation for fiber concrete design used to TC-162-TDF RILEM. This regulation is used these equations to get concrete tensile stress and modulus of elasticity (33).

$$f_{ctm} = 0.3 f_{ck}^{\frac{2}{3}} \tag{3-5}$$

$$f_{ctk} = 0.7 f_{ctm} \tag{3-6}$$

$$f_{ct} = 0.6 f_{ct,fl} \tag{3-7}$$

$$f_{ct,fl} = 0.7 f_{ctm,fl} \tag{3-8}$$

Where:

f_{ctm}: medium tensile strength of concrete;

f_{ck}: cylindrical compressive strength of concrete;

f_{ctk}: specification of concrete tensile strength;

$f_{ct,fl}$: flexural strength of concrete;

$f_{ctm,fl}$: medium concrete flexural strength.

3.4.1. Determination of flexural tensile strength

In this regulation, one of the important element in fiber concrete design is the flexural tensile strength ($f_{R,j}$). It should be used for displacement rate of crack opening experiment (CMOD), to determine this parameter according to the results of this trial, where f_{R1} and f_{R2} are calculated by this equation with substitution of $CMOD_1$ and $CMOD_4$ (33) (fig. 3.1):

$$f_{R,j} = 3\,\frac{F_j l}{2bh_{sp}^2} \tag{3-9}$$

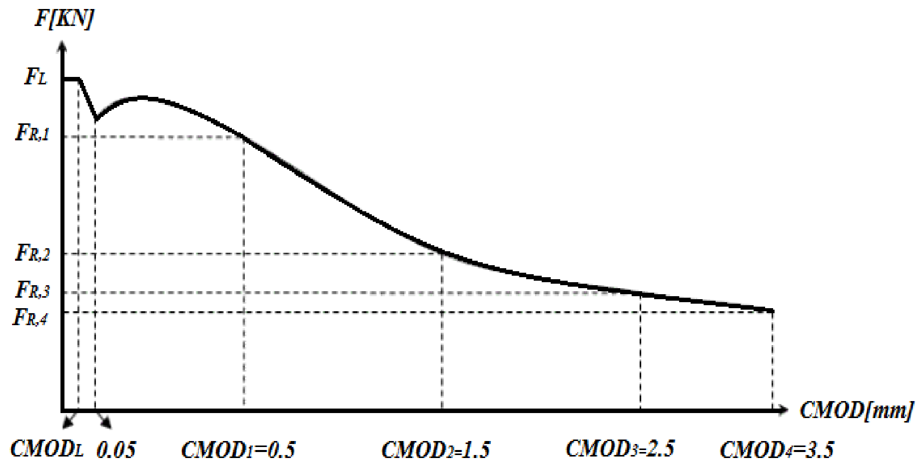

Fig. 3.1. *F-CMOD graph in TC-162-TDF RILEM regulation to determine flexural tensile strength*

Where:

l: sample crater;

b: sample width;

h_{sp}: distance between gap top up to the sample tested;

f_j: Corresponding load with $CMOD_j$;

$f_{R,j}$: flexural tensile strength corresponding with $CMOD_j$ *[j=1,2,3,4]*.

3.4.2 Flexural capacity calculation in RILEM

In the following forms, strain-stress relationship in fiber concrete and also strain-stress distribution method are indicated according to the RILEM TC-162-TDF2003 regulation (33).

Parameters in Fig.3.2, starting from the fiber concrete flexural strength, are calculated by this equation (33).

$$\sigma_1 = 0.7 f_{ctm,fl}(1.6 - d) \tag{3-10}$$

Where d: Effective depth in meter

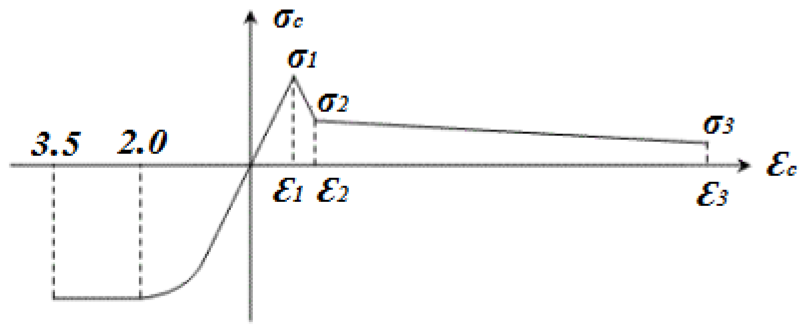

Fig. 3.2. *Fiber Concrete Strain-Stress graph in RILEM TC-162-TDF 2003*

$$\sigma_2 = 0.450 f_{R1} K_h (1.6 - d) \tag{3-11}$$

K_n: Size Factor

f_{R1}: Tensile − flexural strength corresponding to CMOD_1

$$\sigma_3 = 0.37 f_{R4} K_h \tag{3-12}$$

f_{R4}: Tensile − flexural strength corresponding to CMOD_4

$$E_{cm} = 9500(f_{cm})^{\frac{1}{3}} \tag{3-13}$$

$$\varepsilon_1 = \frac{\sigma_1}{E_c} \tag{3-14}$$

$$\varepsilon_2 = \varepsilon_1 + 0.1\ \% \tag{3-15}$$

$$\varepsilon_3 = 25\ \% \tag{3-16}$$

$$K_h = 1.0 - 0.6\ \frac{h[cm] - 12.5}{47.5}\ [12.5 \leq h \leq 60(cm)] \tag{3-17}$$

Where:

h: *Height of beam in (cm)*

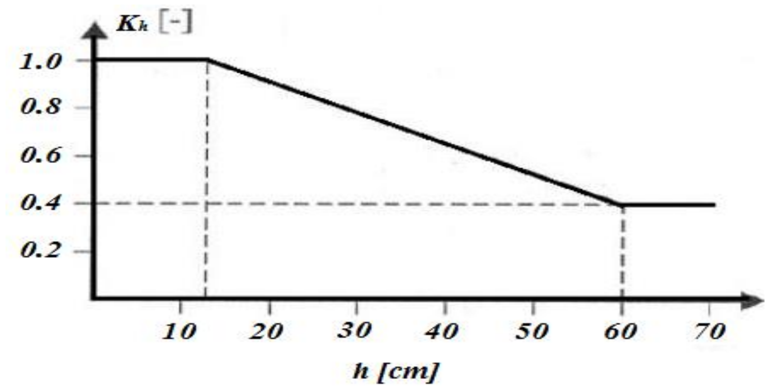

Fig. 3.3. *K_h Size factor range in RILEM TC-162-TDF 2003*

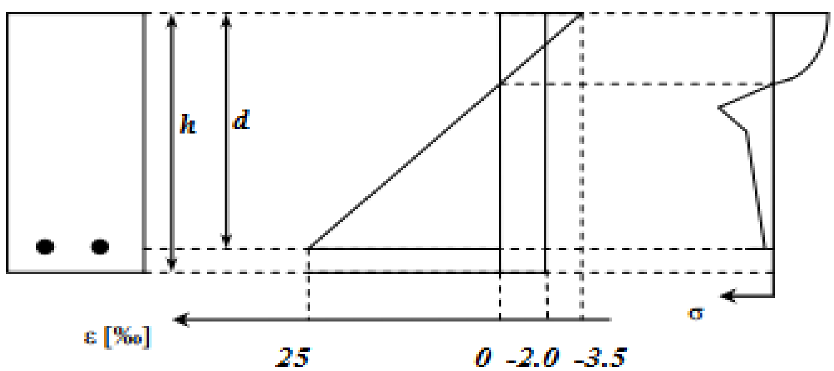

Fig. 3.4. *Fiber concrete stress-strain diagram in RILEM TC-162-TDF 200*

3.4.3 Anchor Cracking

For anchor cracking calculation it is used to (3-18) equation (33).

$$M_{cr} = W_1 \sigma_1 \qquad (3\text{-}18)$$

$$W_1 = \frac{bh^2}{6} \qquad (3\text{-}19)$$

3.4.4 Surrender Moment Calculation

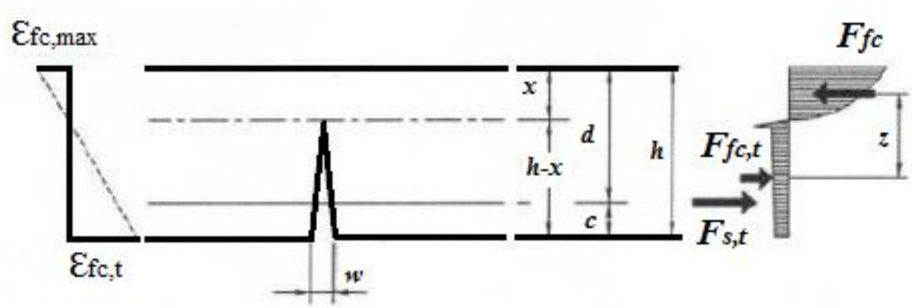

Fig. 3.5 *Fiber concrete stress-strain diagram with Armature in RILEM TC-162-TDF*

$$M_{Rd} = f_{sy}A_s\left(d - \frac{x}{2}\right) + F_{fc,t}(h-x)\,b\,[\,\beta x + x_{tot}(h-x)\,] \qquad \textit{(3-20)}$$

Where:

f_{sy}: armature surrender resistance;

$F_{fc,t}$: fiber strength of the tensile stress;

A_s: armature area;

d: effective depth;

h: beam height.

βx: Distance to the highest point of the beam from the center of the compressive area of the concrete.

x_{tot}: Center of gravity of the tensile fiber block,Percentage of total height;

y: Tensile stress block height

3.4.5 Calculatio of the final moment

$$M_{uRd} = f_{sy}A_s\left(d - \frac{x}{2}\right) + F_{fc,t}(h-x)b\,[\,\beta x + x_{tot}(h-x)\,] \qquad \textit{(3-21)}$$

3.4.6 Fiber concrete beams design without ordinary Armature

Design of fiber concrete beams without armature is simillar to design of fiber concrete with armature with this difference that armature has been deleted (33).

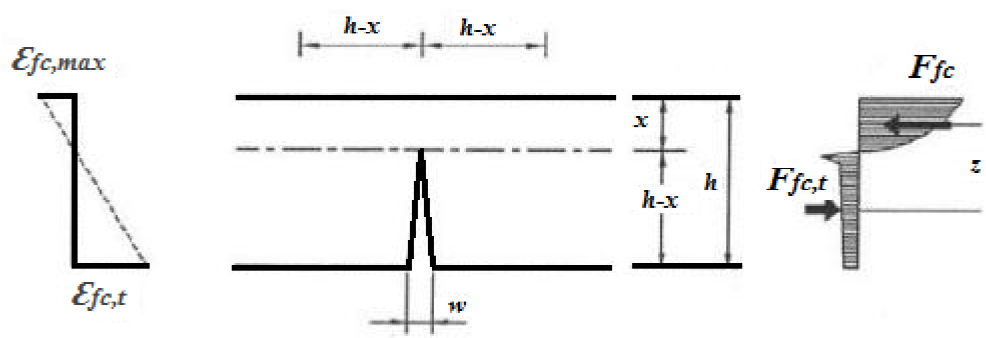

Fig. 3.6. *Fiber concrete stress-strain diagram without armature in RILEM TC-162-TDF*

3.4.7 Shear Capacity in RILEM Requlation

The shear capacity in RILEM is calculated by the sum of concrete shear strength, shear reinforcement of the armature, and fiber shear strength (33).

$$V_{Rd} = V_{cd} + V_{fd} + V_{wd}V_{Rd} \quad (3\text{-}22)$$

$$V_{Rd} = \left[0.12k(100\rho_1 f_{ck})^{\frac{1}{3}} + 0.15\sigma_{cp}\right] bd \quad (3\text{-}23)$$

Where:

- σ_{cp}: average stress on concrete due to loading;
- ρ_1: armature percentage.

$$k = 1 + \sqrt{\frac{200}{d}} \ , (k \leq 2) \quad (3\text{-}24)$$

$$\rho_1 = \frac{A_s}{bd} \leq 2\% \quad (3\text{-}25)$$

$$\sigma_{cp} = \frac{N_{sd}}{A_c} \quad (3\text{-}26)$$

Where:

$N_{sd}: Axial\ force\ in\ the\ form\ of\ pre-stress$

$\sigma_{cp} = 0,\ In\ the\ absence\ of\ axial\ force\ in\ the\ section$

$$V_{fd} = 0.7k_f k \tau_{fd} bd \quad (3\text{-}27)$$

$$k_f = 1 + n\left(\frac{h_f}{b_w}\right)\left(\frac{h_f}{d}\right) , k_f \leq 1.5 \quad (3\text{-}28)$$

$$\tau_{fd} = 0.12 f_{Rk,4} \quad (3\text{-}29)$$

$$n = \frac{b_f - b_w}{h_f} \leq 3 \ , \ n \leq \frac{3b_w}{h_f} \quad (3\text{-}30)$$

$$V_{wd} = \frac{A_{sw}}{s} 0.9 d f_{ywd}(1 + \cot\alpha)\sin\alpha \quad (3\text{-}31)$$

Where:

S: distance between shear armature;

α: *shear armature angle*:

f_{ywd}: $Surrender\ Resistance\ of\ armature\ shear\ reinforcement$

A_{sw}: $Shear\ armature\ area$

3.4.8 Calculation of crack width

$$w_k = \beta s_{rm} \varepsilon_{sm} \tag{3-32}$$

$$\varepsilon_{sm} = \frac{\sigma_s}{E_s}\left[1 - \beta_1 \beta_2 \left(\frac{\sigma_{sr}}{\sigma_s}\right)^2\right] \tag{3-33}$$

For considering fiber effect in calculation of crack width, the RILEM regulation changed the S_{rm} data in formula and with multiplying by $(\frac{50d_f}{l_f})$, this regulation changed this formula with the maximum amount:

$$S_{rm} = \left(50 + 0.25 k_1 k_2 \frac{\emptyset_b}{\rho_r}\right)\left(\frac{50}{L/_{\emptyset}}\right) \tag{3-34}$$

The important note in the above equation is that the amount of fiber is not indicated and the effect of fiber changing on crack width, is too less. The main weakness of this model to predict the average cracks is that the amount of fiber is not considered. Crack distance modified model is recommended by *Moffatt (2001)* and has been developed in *Eurocode 2* (33):

$$S_m = \left(50 + 0.25 k_1 k_2 \frac{d_b}{\rho_{eff}}\right)\left(1 - \frac{f_{res}}{f_{cr}}\right) \tag{3-35}$$

3.4.9 Fiber crack width calculation without armature in RILEM

$$W = \varepsilon_{fc,t}(h - x) \tag{3-36}$$

$$\varepsilon_{fc,t} = \varepsilon_{fc,max} \frac{(h-x)}{x} \tag{3-37}$$

Where:

$\varepsilon_{fc,max}$: $Concrete\ pressure\ strain$

$\varepsilon_{fc,t}$: $Concrete\ tensile\ strain$

Crack width calculation without armature indicated that in the final, the crack width is more than allowed amount. So, it requires a high percentage of fibers (33).

3.5 Design of fiber reinforced concrete beams in FIB Requlation

FIB is an international institute created by merging two CEB and FIP Committees. In this regulation all conventional RC assumptions are considered, except concrete tensile strength. This regulation used the following formula to calculate concrete tensile stress and elasticity modulus (34).

$$f_{cm} = f_{ck} + 8 \quad \text{(3-38)}$$

$$f_{ctm} = 0.3 f_{ck}^{\frac{2}{3}} \quad \text{(3-39)}$$

$$E_{cm} = (\frac{f_{cm}}{10})^{0.3} \quad \text{(3-40)}$$

$$\varepsilon_{cu} = 3.5 * 10^{-3} \quad \text{(3-41)}$$

It should be noted that E_{cm} is defective because elasticity modulus can no be less than compressive resistance. So, equation (3-42) is used in RILEM TC-162-TDF 2003 (34).

$$E_{cm} = 9500(f_{cm})^{\frac{1}{3}} \quad \text{(3-42)}$$

3.5.1 Determination of tensile-flexural strength

According to this regulation, the fiber concrete design is one of the important parameter in tensile-felxural strength, $f_{R,j}$. It should use displacement rate test of crack opening (CMOD) for determination of this parameter. CMOD is a loading test that is controlled by deformation and determine the amount of crack opening. The FIB regulation has recommended detail of EN14651 regulation (34).

$$f_{R,j} = 3\frac{F_j l}{2bh_{sp}^2} \quad \text{(3-43)}$$

Where are:

l: sample craters;

b: Sample width;

$h_{sp:}$ space between gap to top;

$F_{j:}$ coressponding load with $CMOD_j$;

$f_{R,j}$: tensile-flexural strength corresponding with $CMOD_j$ with [j=1,2,3,4];

f_{R1} : correspond to CMOD1, f_{R3} correspond to CMOD3: (Fig. 3.7)

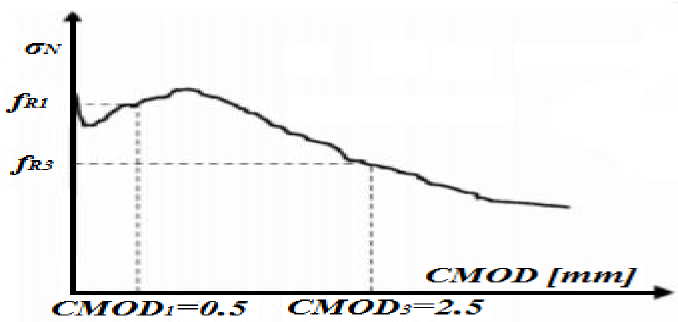

Fig. 3.7 *Beam flexural test with soft handling in FIB regulation*

The FIB regulation shows the actual response in stretching like (Fig.3.7) and simplifies in form of tension combination and crack opening (Fig. 3.8).

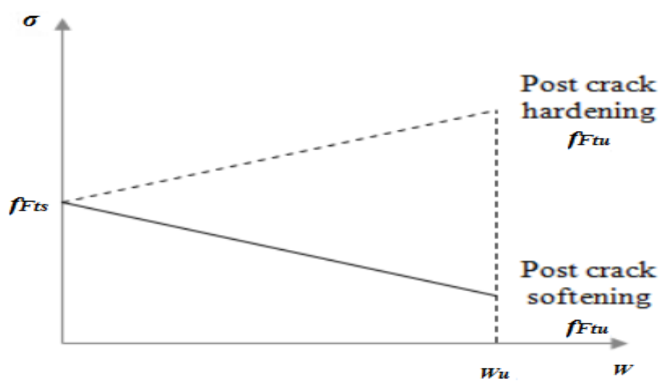

Fig. 3.8 *Softening and hardening behavior after fiber concrete crack in FIB*

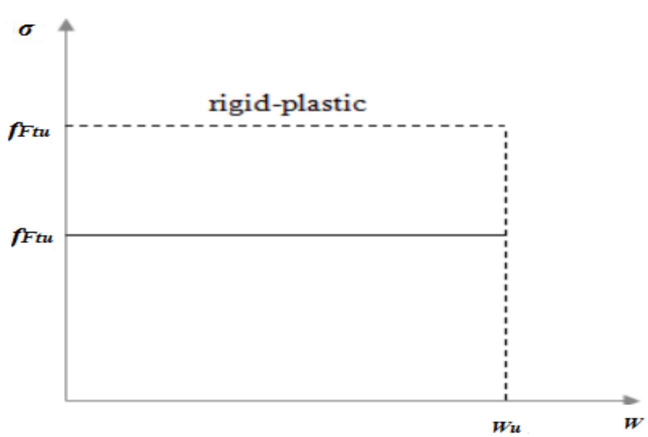

Fig. 3.9 *Rigid plastic behavior of concrete fiber anche in FIB*

There are two important parameter in this part that include f_{Fts} as mode operation resistance and f_{Ftu} as final mode resistance (34).

$$f_{Fts} = 0.45 f_{R1} \tag{3-43}$$

Where:

f_{Fts}: $m$ode operation resistance

f_{R1}: Flexural tensile strength correspond with CMOD1

$$f_{Ftu} = f_{Fts} - \frac{W_u}{CMOD_3}(f_{Fts} - 0.5 f_{R3} + 0.2 f_{R1}) \geq 0 \tag{3-44}$$

Where:

f_{Ftu}: $final\ mode\ resistance$

$CMOD_1$: the amount of openning crack scater $= 0.5$ mm

$CMOD_3$: the amount oppening crack scater $= 2.5$ mm

3.5.2 Bending Strength

The well known design model for steel reinforced concrete with the design at the cross section will be extended with an additional tension force for the calculation of the load carrying capacity of flexural strengthened slabs (Fig. 3.10) (35).

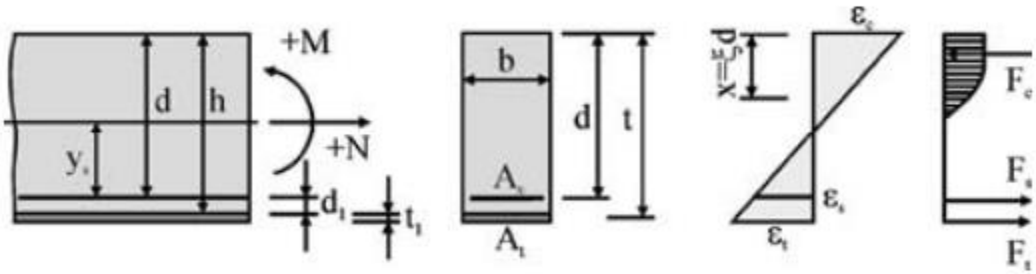

Fig. 3.10 *Internal forces and strains on the cross section*

During the test, the deformation on the web side of the RC-member was measured by a displacement transducer at several points. At each measuring point the deformations in three directions were documented: those towards the textile reinforcement, those towards the steel stirrups and also those towards the concrete struts. In addition the deflection of the specimen and the crack pattern on the web side were recorded (35).

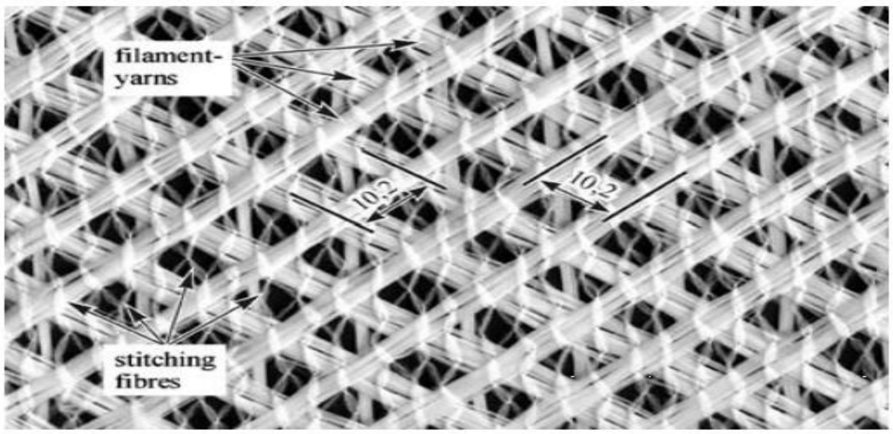

Fig. 3.11 *Textile structure for shear strengthening*

The fiber concrete bending strength resistance added as a stress block. In FIB regulation bending anchor and axial force are simplified and are indicated. In Fig. 3.12, softening and hardening behavior are indicated on the left and distribution of plastic rigidity is indicated on the right. Compressive resistance is less than 50 Pascal, η=1, λ=0.8 for the concrete (34).

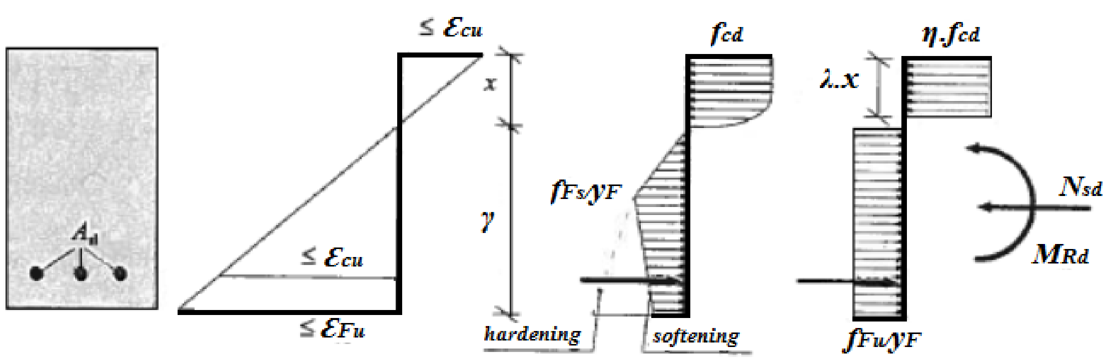

Fig. 3.12 *Simplified Strain-Stress Relation in FIB requlation*

3.5.3 Anchor Cracking

For anchor cracking calculations use to equation 3-45.

$$M_{cr} = W_1 f_{ctm} \tag{3-45}$$

$$W_1 = \frac{bh^2}{6} \tag{3-46}$$

Where:

W_1: Intermediate module

b: Width

h: Heigth

3.6 Fiber concrete beams design without armature

This design is simillar to that with armature (34):

$$M_{Rdy} = f_{Ft}(h - x)\ b\ [\beta x + x_{tot} y] \tag{3-47}$$

3.6.1 Flexibility

Design at limit state requires flexibility. In FIB regulation, flexibility condition is estimated with minimum armature. The minimum amount of armature in reinforced concrete beam is calculated by (34):

$$A_{s,min} = k_c k (f_{ctm} - f_{Ftsm}) \frac{A_{ct}}{\sigma_s} \tag{3-48}$$

Where:

- A_{ct}: area of concrete tensile section;
- σ_s: maximum tensile stress of armature while fraction;
- k_c: stress distribution coefficient before fraction;
- k: Coefficient of non − uniform tensions.

In reinforced concrete beams with fiber, it is possible to decrease the amount of armature. According to the FIB regulation, the flexibility condition in fiber concrete structure is performing one of the following equation (34).

$$\delta_u \geq 20\delta_{SLS} \tag{3-49}$$

$$\delta_{peak} \geq 5\delta_{SLS} \tag{3-50}$$

Where:

- δ_u: Final displacement;
- δ_{peak}: Displacement in maximum force;
- δ_{SLS}: Displacement in service load.

3.6.2 Shear Capacity

The shear capacity in FIB regolation is calculated by the sum of shear strength and armature (34):

$$V_{Rd} = V_{Rdc} + V_{Rd,s} \tag{3-51}$$

The concrete beam shear strength with fiber is calculated by this equation:

$$V_{Rd,c} = k_v \frac{\sqrt{f_{ck,cyl}}}{\gamma_c} Zb; \tag{3-52}$$

γ_c: Concrete safety factor

Z = 0.9 d

3.6.3 Concrete shear capacity with different precentage of Fiber and armature

$$V_{Rd} = \left[\left(\frac{0.18}{\gamma_c} \right) k \ \left[100 \rho_1 \left(1 + 7.5 \frac{f_{Ftu}}{f_{ct0}} \right) f_{ck,cyl} \right]^{\frac{1}{3}} + 0.15 \sigma_{cp} \right] bd \tag{3-53}$$

Where is:

σ_{cp}: average stress on concrete in effect of loading:

ρ_1: percentage of conventional armature;

f_{Ftu}: final mode resistance.

3.6.4 Crack width calcultion in FIB regulation

FIB regulation, use to following equation for all cracking steps from combination of fiber concrete beams and armature. In this equation, steel fiber bending resistance (f_{Fts}) is nonzero because of fiber (34).

$$w_d = \frac{1}{2} \frac{\varphi_s}{\rho_{s,ef}} \frac{(f_{ctm} - f_{Fts})}{\tau_{bm}} (\sigma_s - \beta \sigma_{sr}) \frac{1}{E_s} \tag{3-54}$$

$$\sigma_{sr} = \frac{f_{ctm}}{\rho_{s,ef}} (1 + \alpha_e \rho_s) \tag{3-55}$$

$$\rho_{s,ef} = \frac{A_s}{A_{s,ef}} \tag{3-56}$$

Where is:

A_s: $armature\ area$

$A_{s,ef}$: $concrete\ effective\ area$

α_e: $steel\ to\ Concrete\ elastisity\ module\ ratio$

3.7 Fiber Concrete Beams design in ACI544 regulation

3.7.1 Bending analysis of the beam containing fibers and reins

This method is for predicting armed beams with fibers and armature that is simillar to final resistance design in ACI. The reinforced concrete nominal resistance with fiber and armature is calculated by (3-57) equation (36).

$$M_n = A_s f_y \left(d - \frac{a}{2}\right) + \sigma_t b(h-e)(\frac{h}{2} + \frac{e}{2}\frac{a}{2}) \qquad (3\text{-}57)$$

$$\sigma_t = 0.00772\rho_f F_{be}\frac{l}{d_f} \qquad (3\text{-}58)$$

$$e = \frac{[\in_s(fibers)+0.003]c}{0.003} \qquad (3\text{-}59)$$

Where:

$\in_s$: $Tensile\ strain\ of\ fibers$;

ρ_f: % $Vol. Of\ steel\ fibers.$

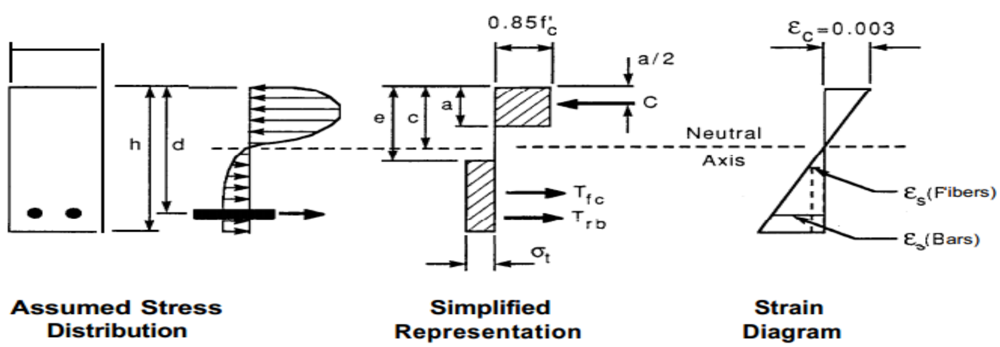

Fig. 3.13 *Basic assumptions for reinforced concrete design with fiber and armature*

3.7.2 Bending strength of fiber concrete beams in the first crack

$$\sigma_{cf} = 0.843 f_r V_m + 425 V_f \frac{l}{d_f} \quad (3\text{-}60)$$

3.7.3 Final bending resistance of fiber concrete beams

$$\sigma_{cu} = 0.97 f_r V_m + 494 V_f \frac{l}{d_f} \quad (3\text{-}61)$$

Where:

$\frac{l}{d_f}$: Length to fiber diameter ratio;

f_r: Concrete rupture modulus;

V_m: % Volume of concrete mortar;

V_f: Volume of fiber.

3.7.4 Fiber concrete slabs design in FIB regulation

In this part, concrete slab design has been posted on the simple support for ultimate state mode with fiber according to the FIB regulation. It used the rigid plastic scheme for slab design with fiber concrete without armature, which assumes that the compressive force is concentrated on the upper section of the cavity (34).

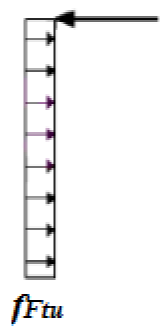

Fig. 3.14 *Simplified mode for determination of Ultimate Tensile Strength in FIB*

3.7.5 Ultimate Bending Strength of Fiber Concrete Slabs (KNm/m)

$$f_{Ftu} = \frac{f_{R3}}{3} \quad (3\text{-}61)$$

Bending strength (m_{Rd}), for fiber concrete slab without armature, is calculated by the following equation (34).

$$m_{Rd} = f_{ftu} h^2/2 \tag{3-62}$$

Where:

h: Slab Height;

f_{Ftu}: Residual flexural strength.

The above result shows that in fiber concrete mode should use to high volumes of fibers for provide flexural strength (34).

3.8 Conclusion

This chapter used FIB regulation to design fiber concrete slab without armature. Due to lack of design criteria in FIB regulation concerning the fiber concrete slab design with armature, it used to fiber concrete beams design criteria without armature.

Chapter 4

Development of Numerical Model for Analysis of Fiber Concrete Slabs

4.1 Introduction

The behavior of concrete is nonlinear and complex. Increasing use of computer based methods for designing and simulation have also increased the urge for the exact solution of the problems. This leads to difficulties in simulation and modeling of concrete structures. A good approach is to use general purpose finite element softwares like e.g. *ABAQUS*. In this paper a *3D* model of a concrete cube is prepared using smeared crack model and concrete damage plasticity approach. The validation of the model to the desired behavior under monotonic loading is then discussed. This thesis used the *ABAQUS* software for development of numerical model. The limitations of this software for fiber concrete modeling was randomly. To solve this problem it was used *MATLAB* to create the required number of fibers. Then enter the program that is written by *MATLAB* in *ABAQUS* software. Eventually, the desired fibers will made (37).

Since 1970, analyses of reinforced concrete structures using finite element method, have witnessed a remarkable advancement. Many researchers have made valuable contributions in understanding the behavior of concrete and have developed sophisticated methods of analysis (37). The past decade with the advancement in computing techniques and the computational capabilities of the high end computers has led to a better study of the behavior of concrete. However the complex behavior of concrete sets some limitations in implementing *FEM*. The complexity is mainly due to non-linear stress-strain relation of the concrete under multi-axial stress conditions, strain softening and anisotropic stiffness reduction, progressive cracking caused by tensile stresses and strains, bond between concrete and reinforcement, aggregation interlocks and dowel action of reinforcement, time dependant behaviors as creep and shrinkage (38).

The concrete used in common engineering structures, basically is a composite material, produced using cement, aggregate and water. Sometime some chemicals and mineral admixtures are also added. Experimental tests show that concrete behaves in a highly nonlinear manner in uniaxial compression. *Fig 4.1* shows a typical stressstrain relationship subjected to uniaxial compression. This stress-strain curve is linearly elastic up to *30%* of the maximum compressive strength. Above this point tie curve increases gradually up to about *70÷90%* of the maximum compressive strength (39).

Eventually it reaches the pick value, which is the maximum compressive strength σ_{cu}. Immediately after the pick value, this stress-strain curve descends. This part of the curve is termed as softening. After the curve descends, crushing failure occurs at an ultimate strain ε_{cu}. A numerical expression has been developed by *Hognestad*, which treats the ascending part as parabola and descending part as a straight line (40). This numerical expression is given as:

$$For \;\; 0 < \varepsilon < \varepsilon'_0, \qquad \frac{\sigma}{\sigma_{cu}} = 2\frac{\varepsilon}{\varepsilon'_0}(1 - \frac{\varepsilon}{\varepsilon'_0}) \tag{4-1}$$

$$For \;\; \varepsilon'_0 < \varepsilon < \varepsilon_{cu}, \qquad \frac{\sigma}{\sigma_{cu}} = 1 - 0.15(\frac{\varepsilon - \varepsilon'_0}{\varepsilon_{cu} - \varepsilon'_0}) \tag{4-2}$$

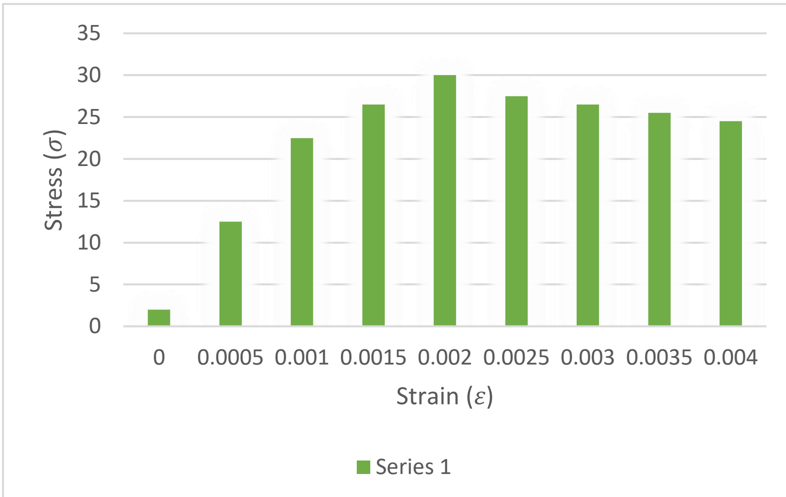

Fig. 4.1 *Stress-Strain curve for concrete*

4.2 Concrete Behavior Model

Determination of nonlinear concrete behavior is the most important step in numerical modeling of reinforced concrete structure. Nonlinear behavior of crude materials can be divided into three methods that include (1) Smeared crack concrete model, (2) Brittle crack concrete model, and (3) Concrete damaged plasticity model. Each of these models has advantages that can use s required (37).

4.2.1 ABAQUS damaged plasticity model

Out of the three concrete crack models, the concrete damaged plasticity model is selected in the present study as this technique has the potential to represent complete inelastic behaviour of concrete, both in tension and compression, including damage characteristics. Further, this is the only model, which can be used both in ABAQUS/Standard and ABAQUS/Explicit and thus enable the transfer of results between the two. Therefore, the development of a proper damage simulation model using the concrete damaged plasticity model will be useful for the analysis of reinforced concrete structures under any loading combinations including both static and dynamic loading (41). The concrete damaged plasticity model assumes that the two main failure mechanisms in concrete are the tensile cracking and the compressive crushing. In this model, the uniaxial tensile and compressive behaviour is characterized by damaged plasticity. This chapter is explained about the calculation method of concrete plastic damage parameters and to ensure it used to numerical modeling.

4.3 Strength hypothesis and its parameters

One of the strength hypotheses most often applied to concrete is the Drucker-Prager hypothesis (1952). According to it, failure is determined by non-dilatational strain energy and the boundary surface itself in the stress space assumes the shape of a cone (Fig.4.2). The advantage of the use of this criterion is surface smoothness and thereby no complications in numerical applications. The drawback is that it is not fully consistent with the actual behaviour of concrete (2).

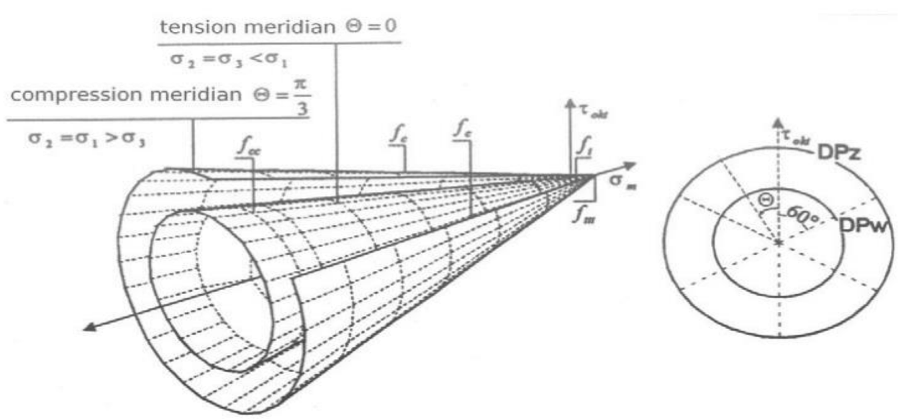

Fig.4.2 *Drucker–Prager boundary surface 0: a) view, b) deviatoric cross section*

The *Concrete Damaged Plasticity* (CDP) model used in the ABAQUS software is a modification of the Drucker-Prager strength hypothesis. In recent years the latter has been further modified by *Lubliner*, *Lee* and *Fenves*. According to the modifications, the failure surface in the deviatoric cross section needs not to be a circle and it is governed by parameter k_c (2) (Fig. 4.3).

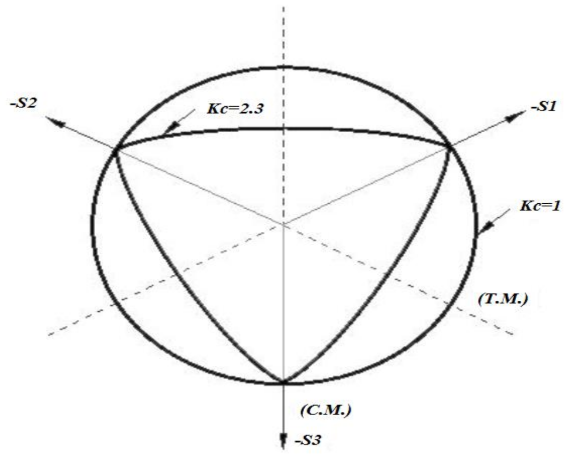

Fig.4.3 *Deviatoric cross section of failure surface in CDP model*

Physically, parameter *Kc* is interpreted as a ratio of the distances between the hydrostatic axis and, respectively, the compression meridian and the tension meridian in the deviatoric cross section. This ratio is always higher than 0.5 and when it assumes the value of 1, the deviatoric cross section of the failure surface becomes a circle (as in the classic Drucker-Prager strength hypothesis). *Majewski* reports that according to experimental results this value for mean normal stress equal to zero amounts to 0.6 and slowly increases with decreasing mean stress. The CDP model recommends to assume *Kc = 2/3*. This shape is similar to the strength criterion (a combination of three mutually tangent ellipses) formulated by *William* and *Warnke* in 1975. It is a theoretical-experimental criterion based on triaxial stress test results (2).

Similarly, the shape of the plane's meridians in the stress space changes: experimental results indicate that the meridians are curves. In the CDP model the plastic potential surface in the meridional plane assumes the form of a hyperbole (fig. 4.4). The shape is adjusted through eccentricity (plastic potential eccentricity). It is a small positive value which expresses the rate of approach of the plastic potential hyperbola to its asymptote. In other words, it is the length (measured along the hydrostatic axis) of the segment between the vertex of the hyperbole and the intersection of the asymptotes of this hyperbole (the centre of the hyperbole). Parameter eccentricity can be calculated as a ratio of tensile strength to compressive strength (42).

The CDP mode recommends to assume $\epsilon = 0.1$ when $\epsilon = 0$, the surface in the meridional plane becomes a straight line (the classic Drucker-Prager hypothesis) (2).

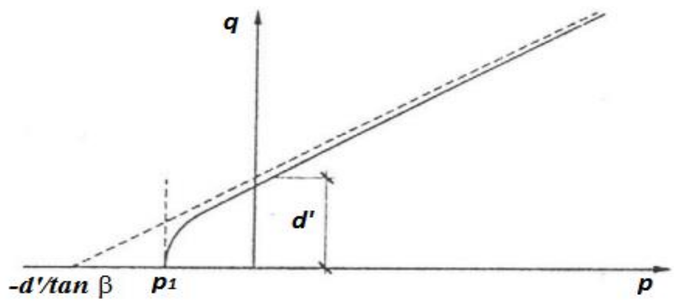

Fig. 4.4 *Hyperbolic surface of plastic potential in meridional plane*

Another parameter describing the state of the material is the point in which the concrete undergoes failure under biaxial compression. σ_{b0}/σ_{c0} (f_{b0}/f_{c0}) is a ratio between the strength in the biaxial and the uniaxial state (Fig. 4.5). The most reliable in this regard are the experimental results reported by *Kupler* in 1969. After their approximation with the elliptic equation, uniform biaxial compression strength f_{cc} is equal to $1.16248\, f_c$. The ABAQUS user's manual specifies default $\sigma_{b0}/\sigma_{c0} = 1.16.$ The last parameter characterizing the performance of concrete under compound stress is the angle of inclination of the failure surface towards the hydrostatic axis, measured in the meridional plane (*dilation angle*). Physically, dilation angle Ψ is interpreted as a concrete internal friction angle.

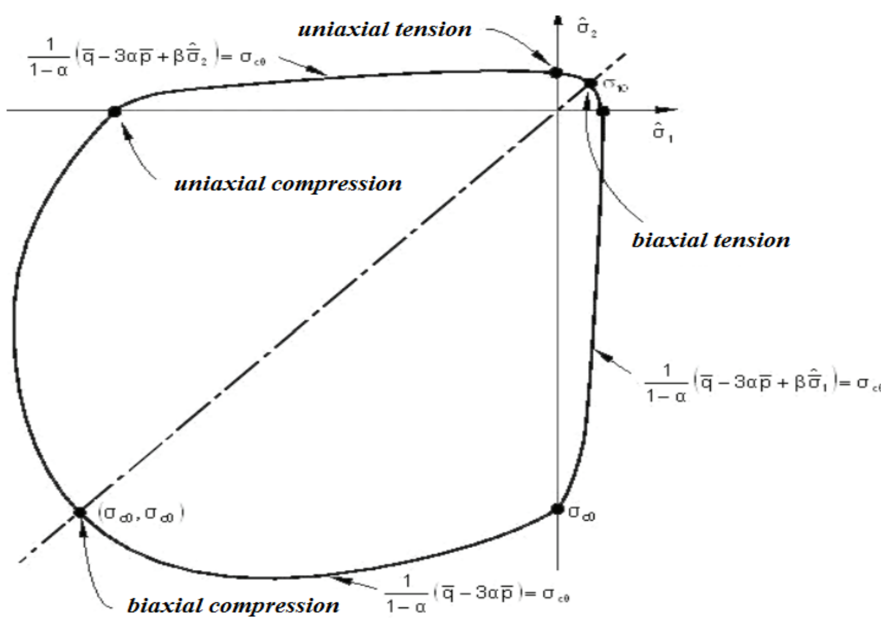

Fig. 4.5 *Strength of concrete under biaxial stress in CDP model*

4.4 Stress-strain curve for uniaxial compression

The stress-strain relation for a given concrete can be most accurately described on the basis of uniaxial compression tests carried out on it. Having obtained a graph from laboratory tests one should transform the variables. Inelastic strains $\varepsilon_c^{\sim in}$ are used in the CDP model. In order to determine them one should deduct the elastic part (corresponding to the undamaged material) from the total strains registered in the uniaxial compression test:

$$\varepsilon_c^{\sim in} = \varepsilon_c - \varepsilon_{0c}^{el} \tag{4-3}$$

$$\varepsilon_{0c}^{el} = \frac{\sigma_c}{E_0} \tag{4-4}$$

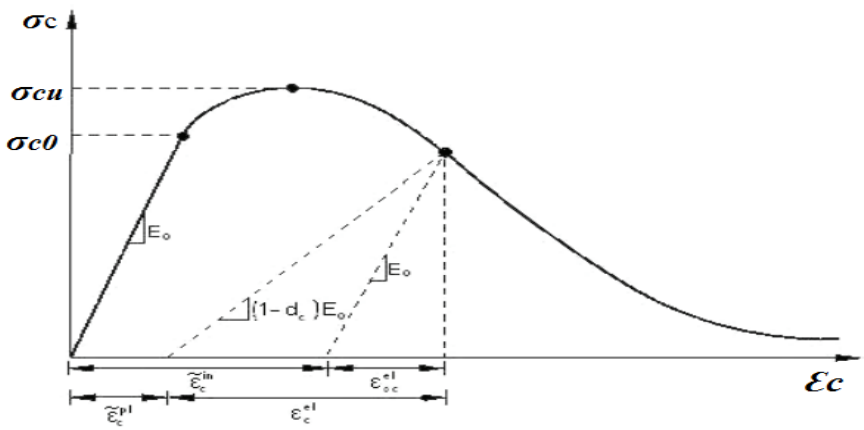

Fig. 4.6 *Definition of inelastic strains*

When transforming strains, one should consider from what moment the material should be defined as nonlinearly elastic. Although uniaxial tests show that such behaviour occurs almost from the beginning of the compression process, for most numerical analyses it can be neglected in the initial stage. According to *Majewski*, a linear elasticity limit should increase with concrete strength and it should be rather assumed than experimentally determined. He calculated it as a percentage of stress to concrete strength from this formula:

$$e_{lim} = 1 - \exp(\frac{-f_c}{80}) \tag{4-5}$$

This ceiling can be simply arbitrarily assumed as 0.4 f_{cm}. Eurocode 2 specifies the modulus of elasticity for concrete to be in a range of 0÷0.4 f_{cm}. In most numerical analyses it is rather not the initial behaviour of the material, but the stage in which it reaches its yield strength which is investigated. Thanks to the level of 0.4 f_{cm} there are fewer problems with solution convergence. Having defined the yield stress-inelastic strain pair of variables, one needs to define now degradation variable d_c. It ranges from zero for an undamaged material to one for the total loss of load-bearing capacity. These values can also be obtained from uniaxial compression tests, by calculating the ratio of the stress for the declining part of the curve to the compressive strength of the concrete. Thanks to the above definition the CDP model allows one to calculate plastic strain from the formula:

$$\varepsilon_c^{\sim pl} = \varepsilon_c^{\sim in} - \frac{d_c}{1-d_c}\frac{\sigma_c}{E_0} \tag{4-6}$$

where E_0 stands for the initial modulus of elasticity for the undamaged material. Knowing the plastic strain and having determined the flow and failure surface area one can calculate stress σ_c for uniaxial compression and its effective stress $\bar{\sigma}_c$.

$$\sigma_c = (1 - d_c)\, E_0\, (\varepsilon_c - \varepsilon_c^{\sim pl}) \tag{4-7}$$

$$\bar{\sigma}_c = \frac{\sigma_c}{(1-d_c)} = E_0(\varepsilon_c - \varepsilon_c^{\sim pl}) \tag{4-8}$$

4.4.1 Plotting stress-strain curve without detailed laboratory test results

On the basis of uniaxial compression test results one can accurately determine the way in which the material behaved. However, a problem arises when the person running such a numerical simulation has no such test results or when the analysis is performed for a new structure. Then often the only available quantity is the average compressive strength (f_{cm}) of the concrete. Another quantity which must be known in order to begin an analysis of the stress-strain curve is the longitudinal modulus of elasticity (E_{cm}) of the concrete. Its value can be calculated using the relations available in the literature (2):

$$E_{cm} = 22(0.1 f_{cm})^{0.3} \tag{4-9}$$

Where:

$E_{cm}[GPa]$

$f_{cm}[MPa]$

Other values defining the location of characteristic points on the graph are strain ε_{c1} at average compressive strength and ultimate strain ε_{cu} (2):

$$\varepsilon_{c1} = 0.7\ (f_{cm})^{0.31} \tag{4-10}$$

$$\varepsilon_{cu} = 3.5\ ‰ \tag{4-11}$$

On the basis of experimental results, *Majewski* proposed the following (quite accurate) approximating formulas:

$$\varepsilon_{c1} = 0.0014\,[2 - \exp(-0.024 f_{cm}) - \exp(-0.140 f_{cm})] \qquad (4\text{-}12)$$

$$\varepsilon_{cu} = 0.004 - 0.0011[1 - \exp(-0.0215 f_{cm})] \qquad (4\text{-}13)$$

Knowing the values of the above one can determine the points which the graph should intersect (2).

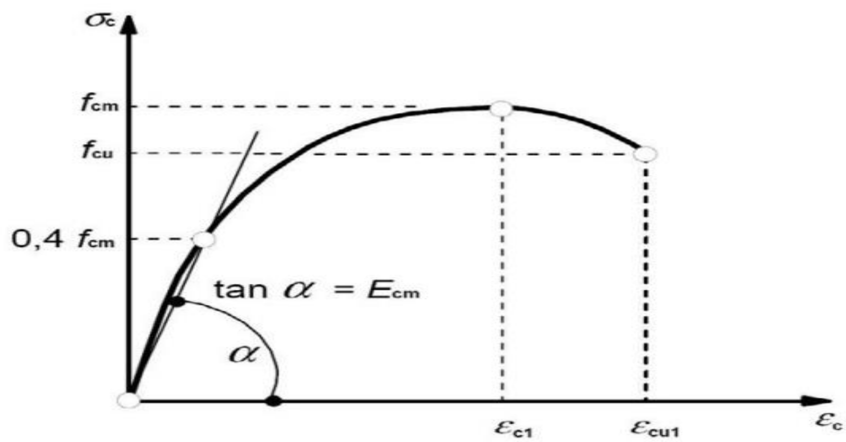

Fig.4.7 *Stress-strain diagram for analysis of structures, according to Eurocode 2*

Choosing a proper formula form to describe relation $\sigma_c - \varepsilon_c$ one should note whether the longitudinal modulus of elasticity represents initial value E_c ($at\ stress\ \sigma_c = 0$), or that of secant modulus E_{cm}. Most of the formulas use initial modulus E_c which is neither experimentally determined nor taken from the standards. Another important factor is the functional dependence itself. Even though the Madrid parabola has been recognized as a good relation by CEB *(Comité Euro-International du Béton)*, this function is not flexible enough to correctly describe the performance of concrete (2).

Madrid parabola

$$\sigma_c = E_c \varepsilon_c \left[1 - \frac{1}{2}\left(\frac{\varepsilon_c}{\varepsilon_{c1}}\right)\right], \quad \sigma_c = f(E_c, \varepsilon_{c1}) \qquad (4\text{-}14)$$

Desay & Krishnan formula

$$\sigma_c = \frac{E_c \varepsilon_c}{1+\left(\frac{\varepsilon_c}{\varepsilon_{c1}}\right)^2} \quad , \quad \sigma_c = f(E_c, \varepsilon_{c1}) \tag{4-15}$$

EN 1992-1-1

$$\sigma_c = f_{cm} \frac{k\eta - \eta^2}{1+(k-2)} \, , \quad k = 1.05 E_{cm} \frac{\varepsilon_{c1}}{f_{cm}} \, , \; \eta = \frac{\varepsilon_c}{\varepsilon_{c1}} \quad , \quad \sigma_c = f(E_{cm}, f_{cm}, \varepsilon_{c1}) \tag{4-16}$$

Majewski formula

$$\sigma_c = E_c \varepsilon_c \;\; if \; \sigma_c \le e_{lim} f_{cm}$$

$$\sigma_c = f_{cm} \frac{(e_{lim}-2)^2}{4(e_{lim}-1)} \left(\frac{\varepsilon_c}{\varepsilon_{c1}}\right)^2 + f_{cm} \frac{(e_{lim}-2)^2}{2(e_{lim}-1)} \left(\frac{\varepsilon_c}{\varepsilon_{c1}}\right) + f_{cm} \frac{{e_{lim}}^2}{4(e_{lim}-1)} \} \; E_c = \frac{f_{cm}}{\varepsilon_c}(2 - e_{lim}) \quad , \; \sigma_c = f(E_c, f_{cm}, \varepsilon_{c1}) \tag{4-17}$$

Sáenz formula

$$\sigma_c = \frac{\varepsilon_c}{A + B\varepsilon_c + C{\varepsilon_c}^2 + D{\varepsilon_c}^3} \; , \sigma_c = f(E_c, f_{cm}, f_{cu}, \varepsilon_{c1}, \varepsilon_{cu1}) \tag{4-18}$$

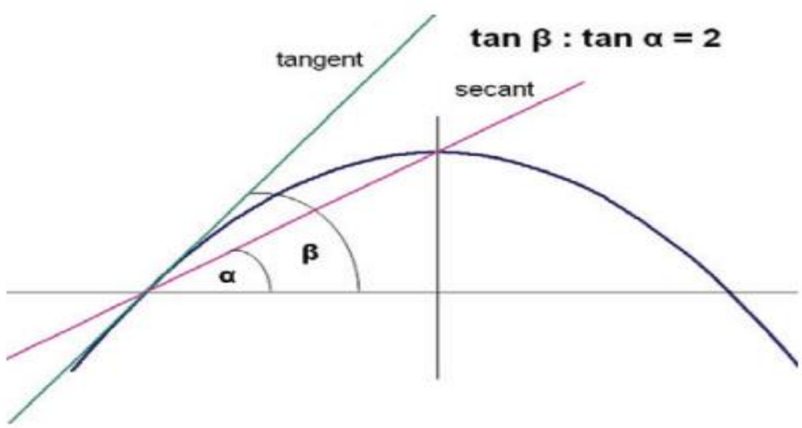

Fig.4.8 *Property of 2nd order parabola*

The 2nd order parabola has this property that the tangent of the angle of a tangent passing through a point on its branch, measured relative to the horizontal axis passing through this point, is always double that of the angle measured as the inclination of the secant passing through the same point and the extremum of the parabola, relative to the same horizontal axis (2).

4.5 Stress-Strain curve for uniaxial tension

The tensile strength of concrete under uniaxial stress is seldom determined through a direct tension test because of the difficulties involved in its execution and the large scatter of the results. Indirect methods, such as sample splitting or beam bending, tend to be used (43).

$$f_{ctm} = 0.30 f_{ck}^{(\frac{2}{3})}$$

(4-19)

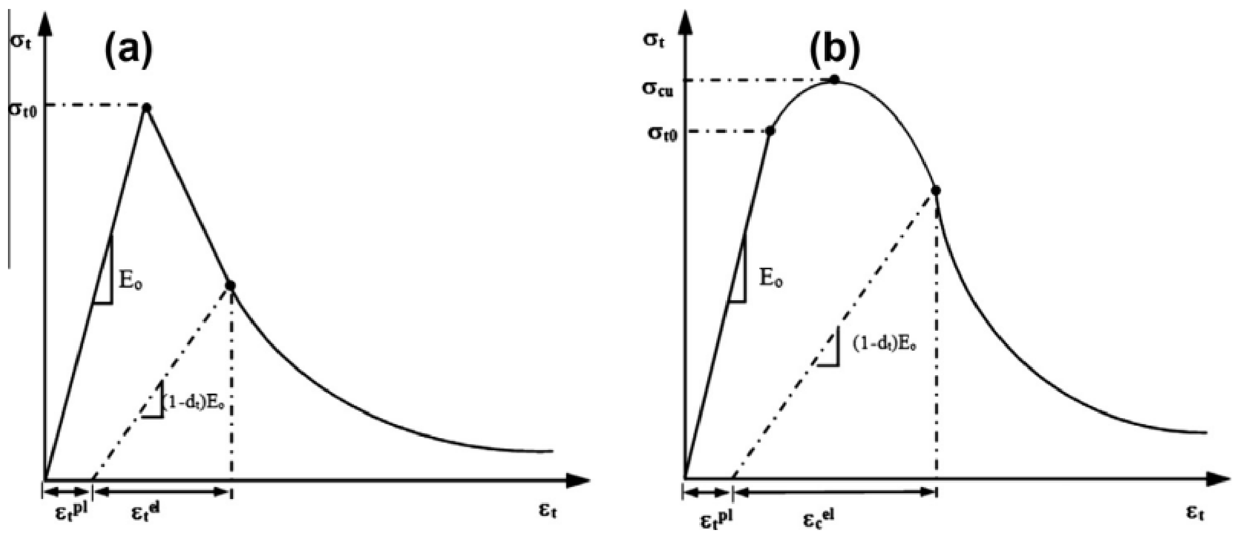

Fig.4.9 *Uniaxial stress–strain curve with damage in tension (a) and compression (b)*

According to the ABAQUS user's manual, stress can be linearly reduced to zero, starting from the moment of reaching the tensile strength for the total strain ten times higher than at the moment of reaching f_{ctm}. But to accurately describe this function the model needs to be calibrated with the results predicted for a specific analyzed case. The proper relation was proposed by, among others, *Wang* and *Hsu* (44).

$$\sigma_c = E_c \varepsilon_t \;\; if \;\; \varepsilon_t \leq \varepsilon_{cr} \qquad (4\text{-}20)$$

$$\sigma_t = f_{cm} (\frac{\varepsilon_{cr}}{\varepsilon_t})^{0.4} \;\; if \;\; \varepsilon_t > \varepsilon_{cr} \qquad (4\text{-}21)$$

Where ε_{cr} stands for strain at concrete cracking. Since tension stiffening may considerably affect the results of the analysis and the relation needs calibrating for a given simulation, it is proposed to use the modified *Wang & Hsu* formula for the weakening function.

$$\sigma_t = f_{cm} (\frac{\varepsilon_{cr}}{\varepsilon_t})^{n} \quad if \quad \varepsilon_t > \varepsilon_{cr} \qquad (4\text{-}22)$$

Where *n* represents the rate of weakening.

Here used to *Nayal* and *Rasheed* model to determine Stress-Strain diagram form. In this model, to avoid runtime error in ABAQUS software, there is a decrease in resistance to 0.8 σ_t. To get the maximum tensile stress, if laboratory results are not available (cylinder fissure testing or direct stretching), it is possible to use (4-23) equation (45).

$$\sigma_t = 0.3\sigma_c^{\frac{2}{3}} \qquad (4\text{-}23)$$

Failure parameter (d_t) is equal to the ratio between Strain failure (ε_t^{ck}) and General strain (ε_t): 0, for healthy materials and 1 for unhealthy materials. According to (Fig 4.10), the accuracy of results increase with strain during loading (45).

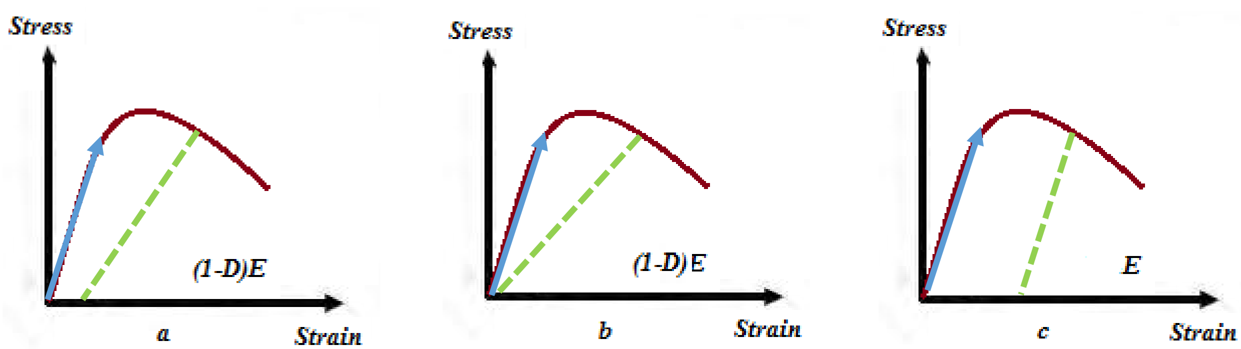

Fig 4.10 *Loading behavior - Concrete handling a) Experimental, b) Plastic damage model regardless of failure parameter, c) Plastic damage model in terms of failure parameter*

4.6 Development of numerical model of finite element for analysis of fiber concrete

In this project, to validate the numerical model of fiber concrete in ABAQUS software, is used laboratory research done by *Khaloo*. This project studied the impact of concrete strength, percentage and ratio of steel fibers on fiber concrete. The slabs were square with dimensions of *820x820 mm* and thickness of *80 mm*. Four corners of slabs were seated on roller points which provided clear span length of *680 mm*. Point load was applied by stroke mode of an actuator on *80x80x10 mm* steel plate placed at slab centre. The displacement at the loading point was increased at rate of *1.5 mm/min*. Sensitive linear voltage differential transducers were used to measure the deflection at slab centre (13).

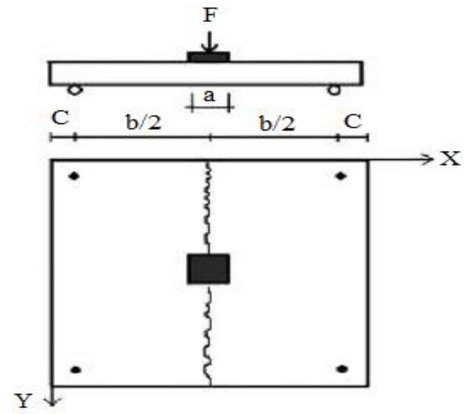

Fig. 4.11 *Four corners of slabs are seated on roller points which provided clear span*

This laboratory has used percentages in volume of *0.5,1.0,* and *1.5* in combination with concrete as specified in table 4.1.

Type of Fiber	*Length (L)*	*Width (W)*	*Thickness (T)*	*Equivalent Diameter* (d_f)	*Aspect Ratio* L/d_f
Jc25	*25*	*0.8*	*0.35*	*0.597*	*41.9*

Table 4.1 *Specifications of the fiber used in concrete slabs*

For fibers with *Jc25* the ratios are:

$$d_f{}^2 = \frac{T*W}{\pi/4} \quad (4\text{-}23)$$

$$d_f = \sqrt{\frac{4*T*W}{\pi}} \quad (4\text{-}24)$$

The values are expressed as a percentage of the mortar volume, i.e. the mean the concrete volume minus coarse grain or gravel. The fiber calculation method is presented below.

Steel specific weigth = $7850\ kg/m^3$.

Sand grain specific weigth = $2760\ kg/m^3$.

Gravel volume of concrete in a cubuc meter = $\frac{1000}{2760} = 0.362$.

Concrete mortar volume in a cubic meter = $1 - 0.362 = 0.638\ m^3$.

Fibers half percent equivalent weigth = $\frac{0.5*7850*0.638}{100} = 25\ kg.$

Required number of fiber in a cubic meter = $\frac{25}{\frac{25*\pi*(0.597)^2}{4}*10^{-9}*7850} = 455084.$

*Slab required number of fiber with 82*82*8 cm dimension* = $455084 * 0.82 * 0.82 * 0.08 = 24479.$

4.6.1 Limited component model of Laboratory Work

For concrete modeling, it used homogeneous materials *(Solid 3D Deformable)* and for modeling of medium slab rigid plate, it used homogeneous rigid material *(Solid 3D Descrete Rigid)*. Overview of the slab is indicated in Fig 4.12.

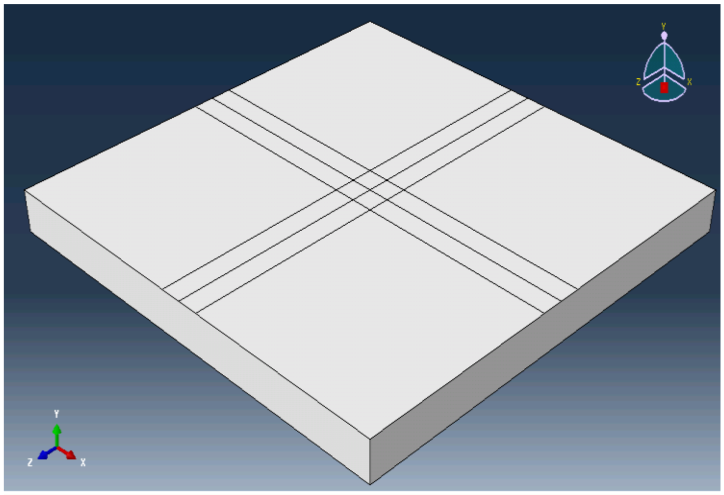

Fig. 4.12 *Overview of the concrete slab in ABAQUS software*

This work used *ABAQUS* software program for the development of the numerical model. The limitations of this software for fiber concrete modeling was random. To solve this problem, *MATLAB* was used to create the required number of fibers. Then enter the program that is written by *MATLAB* in *ABAQUS* software. Eventually, the desired fibers will made (37).

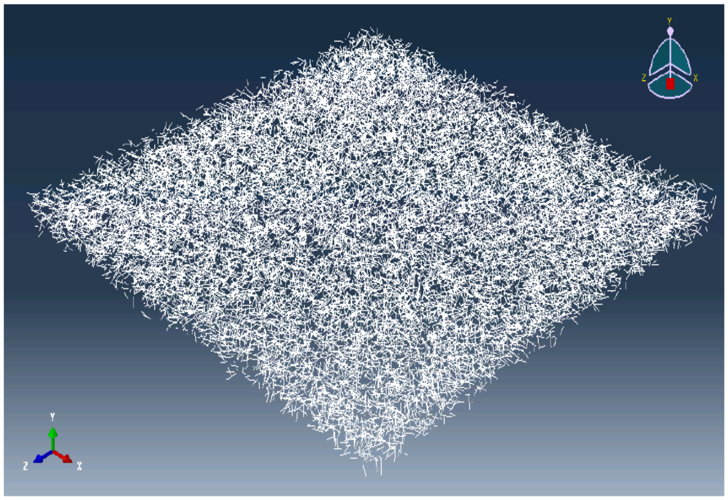

Fig. 4.13 *Random Distribution of Steel Fibers in ABAQUS software*

4.6.2 Concrete Behavior Model

According to descriptions and relations in concrete behavior model, the parameters of concrete plastic damage, stress-strain pressure and concrete tensile stress-strain values are indicated in Tables 4.2, 4.3 and 4.4.

Stress σ_c (MPa)	ε_c	Inelastic Strain ε_c^{in}	Damage d_t
15.58	0.0011	0.000487	0.49
17.25	0.00121	0.000544	0.49
18.90	0.00132	0.0006	0.50
20.51	0.00143	0.000658	0.50
22.09	0.00154	0.000717	0.50
23.63	0.00165	0.000778	0.51
25.10	0.00176	0.00084	0.51
26.48	0.00187	0.000906	0.51
27.75	0.00198	0.000975	0.52
28.84	0.00209	0.00105	0.53
29.66	0.0022	0.001133	0.54
30.00	0.00231	0.001232	0.56
29.45	0.00242	0.00136	0.59
26.81	0.00253	0.001555	0.64
17.25	0.00286	0.001974	0.78
12.55	0.00323	0.00297	0.92

Table 4.2 *concrete tensile stress-strain*

Strees σ_c (MPa)	$\boldsymbol{\varepsilon_t}$	***Cracking Strain ε_t^{ck}***	***Damage d_t***
2.26	*0.000091*	*0*	*0*
1.27	*0.000365*	*0.00029*	*0.80*
0.10	*0.000900*	*0.00082*	*0.92*

Table 4.3 *Tensile stress-strain values*

Dilation Angle	***Eccentricity***	$\boldsymbol{f_{bo}/f_{co}}$	***K***	***Viscosity Parameter***
36	*0.1*	*1.16*	*0.666*	*0.0001*

Table 4.4 *Parameters used in plastic concrete damage model*

4.6.3 Steel Behavior Model

The steel has been introduced in term of elastic-plastic behavior, including elastic behavior before the submission point and plastic behavior after the submission point. Fiber elastic-plastic specifications are indicated in Tables 4.5 and 4.6.

Density	*7800* kg/m^3
Young's Module	*200 GPa*
Poisson's Ratio	*0.3*

Table 4.5 *Fiber elastic specifications*

Plastic Strain	***Yield Stress***
0	*280*
0.09	*370*

Table 4.6 *Fiber plastic specifications*

4.6.4 Mesh dependency

In continuum mechanics, the constitutive model is normally expressed in terms of stress-strain relations. When the material exhibits strain-softening behavior, leading to strain localization, this formulation results in a strong mesh dependency of the finite element results, where the energy dissipated decreases upon mesh refinement. To illustrate the problem let us consider a bar subjected to uniaxial tension (Fig. 4.14) (46).

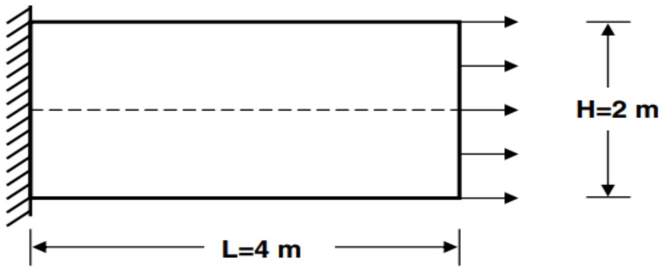

Fig. 4.14 *Bar subjected to axial load.*

The bar consists of a material that is linearly elastic until a peak value of stress is reached and softens linearly in the post-peak regime (Fig. 4.15) (46).

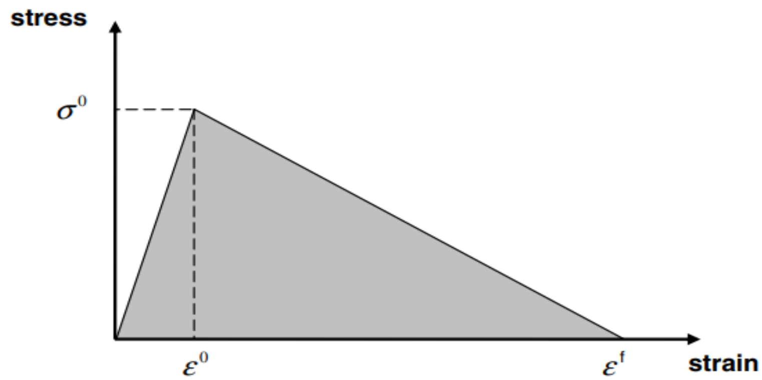

Fig 4.15 *Stress versus strain diagram for a linearly softening material.*

Further, let us assume that a narrow band of material perpendicular to the axis has strength slightly lower than the rest of the bar. The finite element solutions for the force-displacement response of the bar are strongly mesh dependent, clearly indicating a reductions in the external work for fracture as the element size decreases (Fig. 4.16 and 4.17). The strain localization is confined to a layer of one element thickness (in this example the element in the middle has been fully damaged). The energy dissipated is proportional to the volume of the failed element rather than the area of the fractured surface and, consequently, it tends to zero with the mesh refinement (46).

4.6.5 Meshing

For concrete modeling are used *8D-3C* elements, with approximately *30 mm* dimension like (Fig 4.18) and for steel fiber modeling *2D-3T* element with approximately *10 mm* dimensions. The fiber is bonded to concrete with *Embeded Regions* technique.

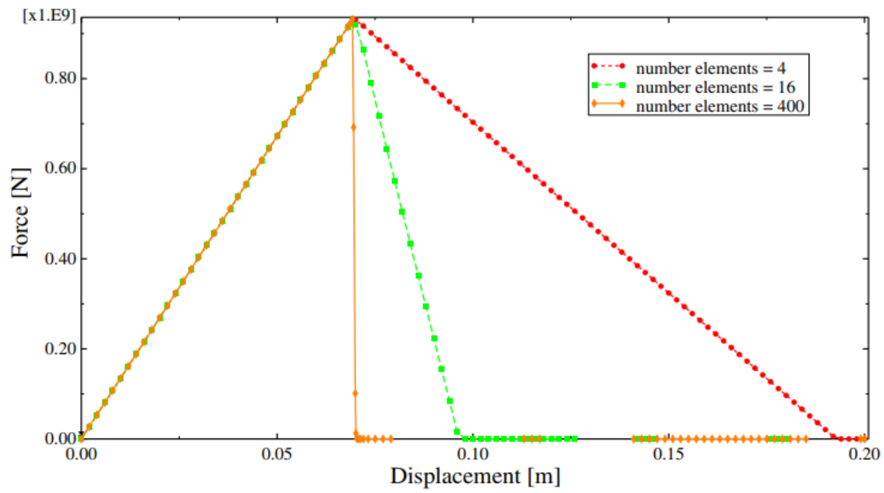

Fig. 4.16 *Force–displacement for different discretizations (results without using the crack band model).*

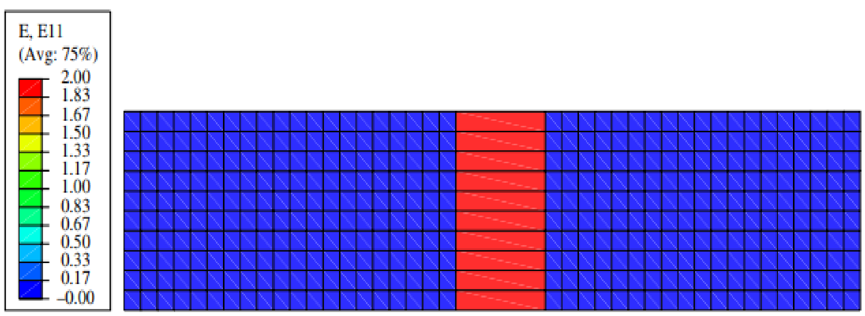

Fig. 4.17 *Localization of deformation*

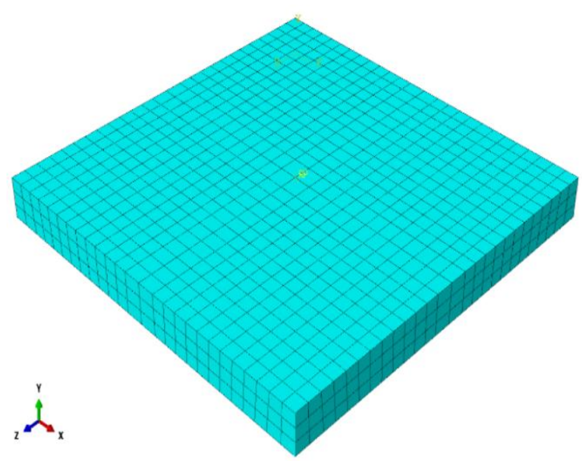

Fig. 4.18 *Fiber Concrete Slab Meshing in ABAQUS*

4.7 Examining and analyzing test results and comparison of laboratory results with numerical modeling results

4.7.1 Slab Failure Mode

According to Fig. 4.19 and 4.20, the laboratory failure mode is creating a rupture from the middle of the slab to both sides.

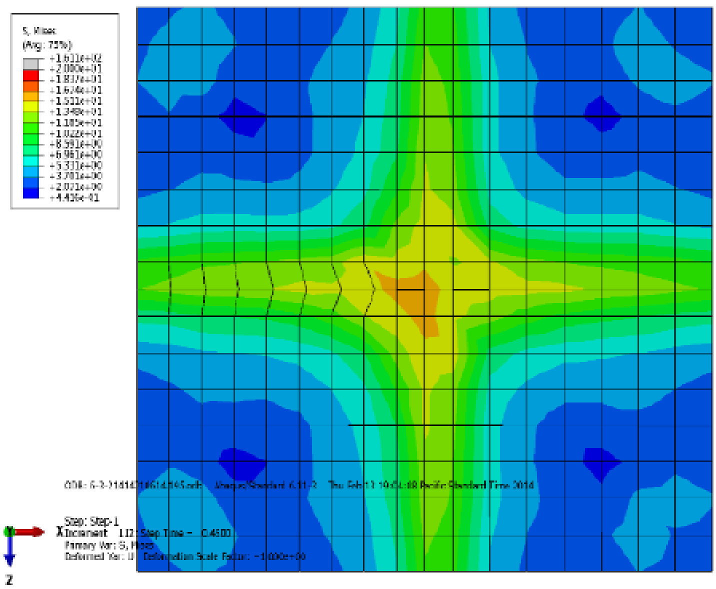

Fig. 4.19 *Concrete Tension Distribution of Fiber Concrete Slab*

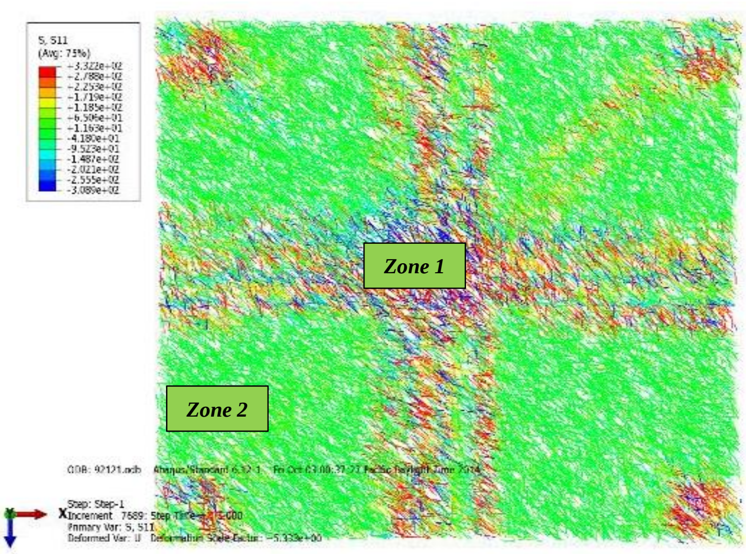

Fig. 4.20 *Distribution of steel fiber tension in Fiber Concrete Slab*

4.7.2 Steel fiber stress-strain graph in fiber concrete slab

According to Fig. 4.20, the fibers that were in the direction of concrete failure, have more stresses rather than other fibers. As the Fig.4.21 shows, the fibers in the central zone of the slab have reached their elastic limits and entered to the plastic zone. As Fig. 4.22 shows, the fibers are in the plastic zone.

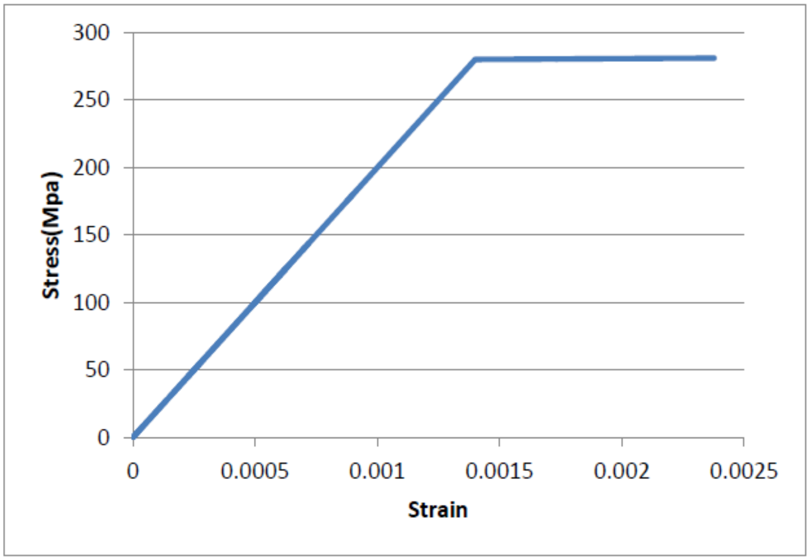

Fig.4.21 *Strain-Stress graph, A sample of steel fibers in zone 1*

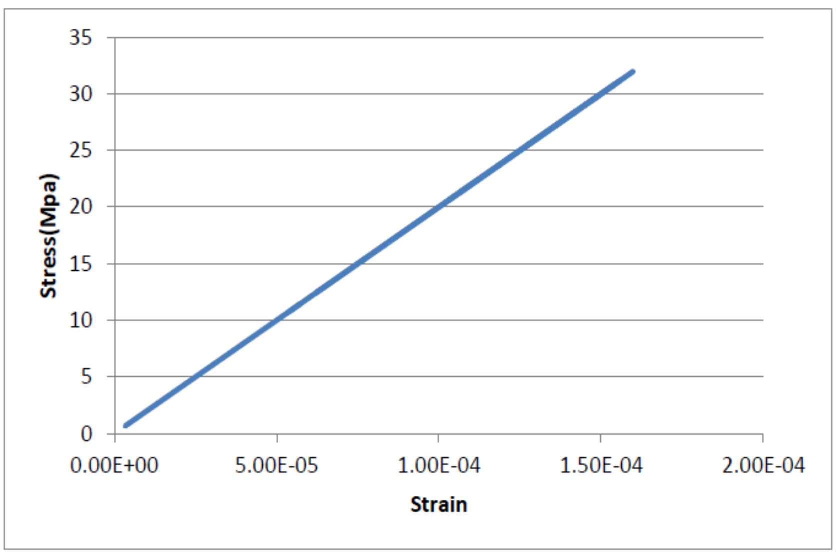

Fig. 4.22 *Strain-Stress graph, A sample of steel fiber in zone 2*

4.7.3 Comparison of laboratory results with numerical modeling results

According to Fig. 4.23 and 4.24, simple concrete load-displacement graph with 30 MPa as a characteristic resistance, there is a good match in numerical modeling and laboratory result. By adding a 0.5% volume of fibers in concrete slab, it is possible to see that in loading-displacement graph, there is difference in the level below the chart and the process after cracking. This difference can be caused by fiber modeling in concrete quite stick together. Percentage of fiber in concrete may get out of concrete and loses the necessary performance when slab cracking occurs.

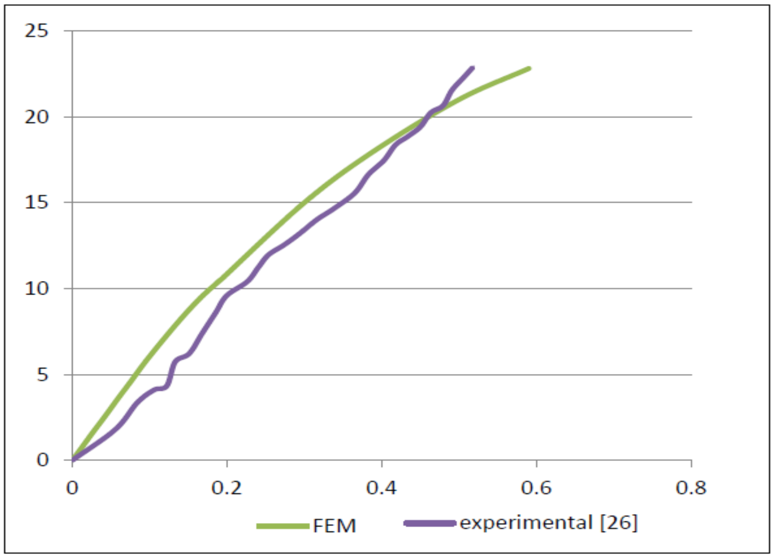

Fig. 4.23 *Load-displacement graph of concrete without fiber with characteristic resistance of 30 MPa*

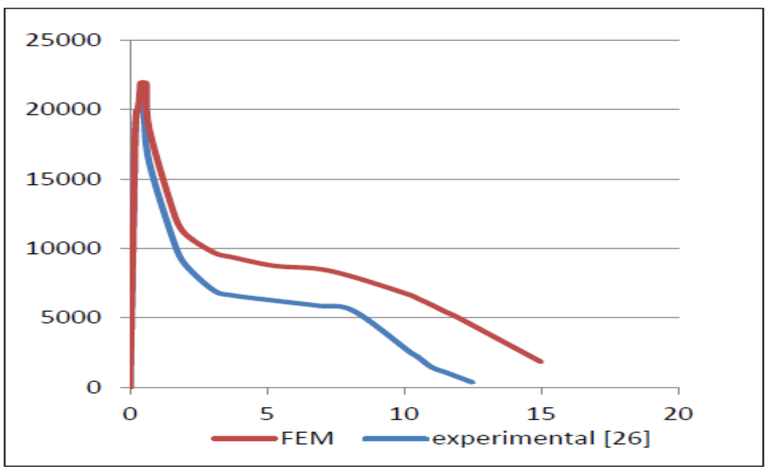

Fig. 4.24 *Fiber concrete load-displacement graph with characteristic resistance 30 MPa*

4.8 Conclusion

According to the results of numerical analysis of fiber concrete slab, available laboratory results and differences between these due to distension of fibers in laboratory work, the results of numerical analysis were globally satisfactory. They can be used as numerical model of the slab in railroad applications with behavioral models of concrete and fiber and in the validation model.

Chapter 5

Technical-economic review and the possibility of using fiber concrete in the slab line of railway lines

5.1 Introduction

This work presents a material model which can be used to simulate the non-linear behaviour of reinforced concrete elements. The material model needs only the maximum compressive strength of the concrete and utilise two numerical techniques to derive stresses train curves both at compression and tension including softening regimes. Necessary modifications are suggested to the above numerical techniques to be applicable with ABAQUS damaged plasticity model to simulate damage in RC structures. This material model is validated using experiment results available in the literature with different material and structural arrangements. Result section indicates that both displacement and crack patterns obtained from FEM are well matched with the experiment results. Therefore, the above material model minimise the number of tests needed to develop an accurate material model in FE simulation (41).

The numerical technique used to develop the stress-strain relationship for tensile region is acceptable for both reinforced and fibre reinforced concrete as reported by *Nayal* and *Rasheed* (45). Though the present study focus only on reinforced concrete elements, the similarity in the tension stiffening model may enable to adopt the present material model with fibre reinforced concrete as well with minor parametric changes. The stress-strain relation is capable of accurately representing the strain softening regime as proven by *Hsu*, enabling to accurately simulate damage caused by concrete crushing. Thus the material model presented can be applied for both reinforced and fibre reinforced concrete elements to simulate or assess the damage 2due to both tensile cracking and concrete crushing. This thesis verifies the accuracy of the proposed material model using experiment results for reinforced concrete elements subjected to flexural loading and tensile cracking (47).

The behavioral model of fiber and concrete with length of 6 meters, explained in the previous chapter require computer systems with high memory, therefore, it is decided to decrease the length of the slab line: by comparing the results of shear force and bending anchor, it is selected 3 meters for the modeling. Then it is possible to model fiber concrete and concrete without fiber slab lines in ABAQUS. In comparison of results between slabs with fibers, without fibers and lack of fiber effect on slab line incoming forces on service loads, continue working took place on the SAP software without fiber.

5.2 Appropriate length of slab-line model investigation

After ABAQUS numerical model validation with laboratory results and the proximity of experimental and numerical results, it should be modeled a piece of slab line Originally, slab line was modeled with $6*2.6*0.3\ m$ dimensions. The number of required fibers in this slab is calculated by the following equations:

$$\textit{Number of fibers required per concrete cubic meter} = \frac{25}{\frac{25*\pi*0.597^2}{4}*10^{-9}*7850} = 455084$$

$$\textit{Required number os fibers in slab with 6*2.6*0.3} = 455084 * 6 * 2.6 * 0.3 = 2129793$$

High number of fibers need high computing volume that needs more powerful computer systems. For this reason, the length of the slab line is decreased. In this context four slabs with different lengths are investigated from longitudinal and transversal anchors view in SAP2000 software.

5.2.1 Slab line modeling with various lengths

In this part, four slabs with lengths of *3, 3.6, 5.4, 6* m are modeled. Slab thickness is 30 cm, concrete slab width is 2.6 m and sleepers are spaced 60 cm apart. For the rail modeling, it is used UIC 60 rail specifications. According to SKL14, the pad under the rails is equal to 450 N/mm. The substrate hardness below the slab is $k = 35\,kg/m^3$ that is modeled in form of an area spring. Dead loads in this project are include slab, rail and sleepers. Consumable concrete specific weigth is 2500 kg/m^3 and rail weigth is 60 kg/m. The AREMA regulation recommended LM71 in terms of the traffic load modeling.

Graphs in Fig. 5.1 and 5.2 indicate that, by reducing the slab up to 3 meters, the longitudinal and transversal anchorages have minor variations. Therefore, it is possible to model the slab with 3 meters length.

5.2.2 Fiber concrete slab line modeling in ABAQUS

This modeling is simillar to that in the previous chapter. This part used beam element for modeling of the rail and a spring with hardness of 450 kN/mm for modeling the pad between rail and slab (Fig. 5.3). The slab bed is modeled for two modes:

- Soft bed with $0.5\,kg/m^3$ hardness;
- Hard bed with $35\,kg/m^3$ hardness.

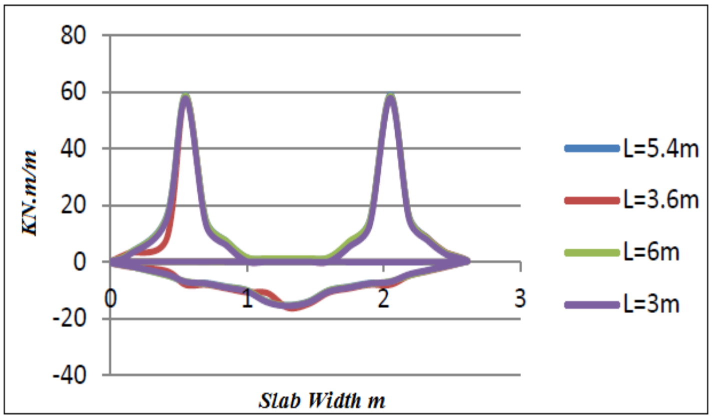

Fig. 5.1 *Slab transversal anchors with different lengths*

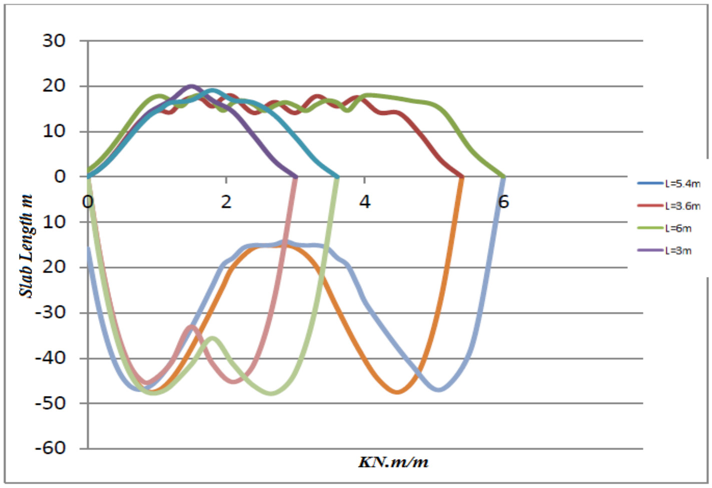

Fig.5.2 *Longitudinal anchor with different lengths*

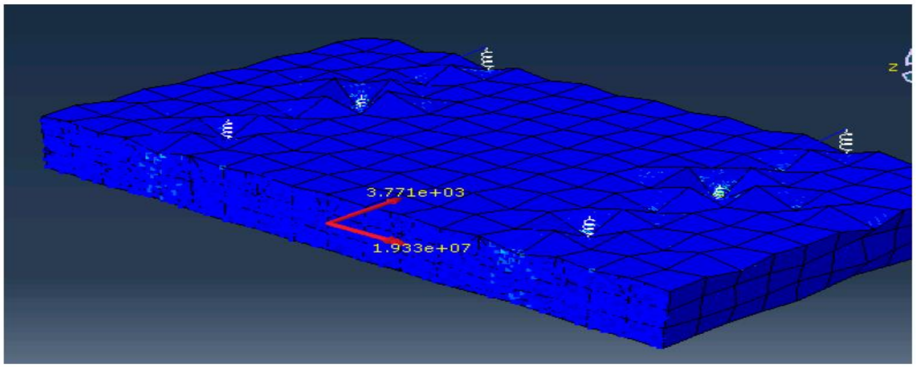

Fig. 5.3 *Fiber concrete slab line model in ABAQUS*

5.2.3 Results comparison of slab lines ABAQUS numerical modeling in concrete with and without fiber

The results are shown for fiber and no-fiber slab lines in two slab modes with K = 35 kg/m^3 *(Fig. 5.4, 5.5, 5.6 and 5.7)* and K = 0.5 kg/m^3 hardness *(Fig. 5.8, 5.9, 5.10 and 5.11).*

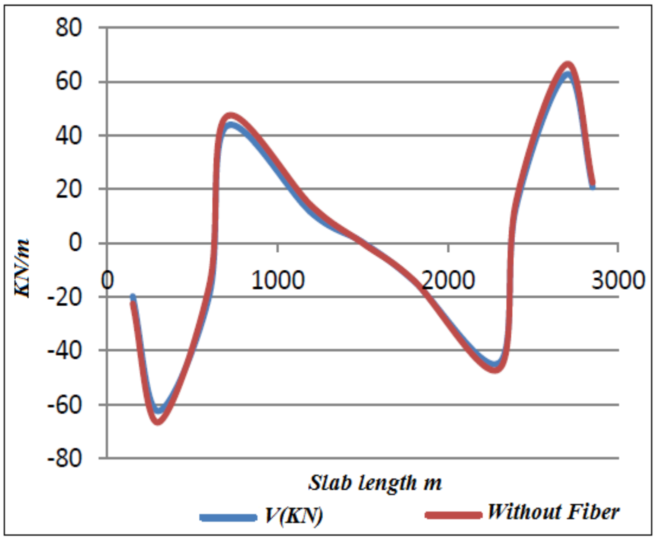

Fig. 5.4 *Longitudinal shear force of slab, with and without fiber - K = 35 kg/m^3*

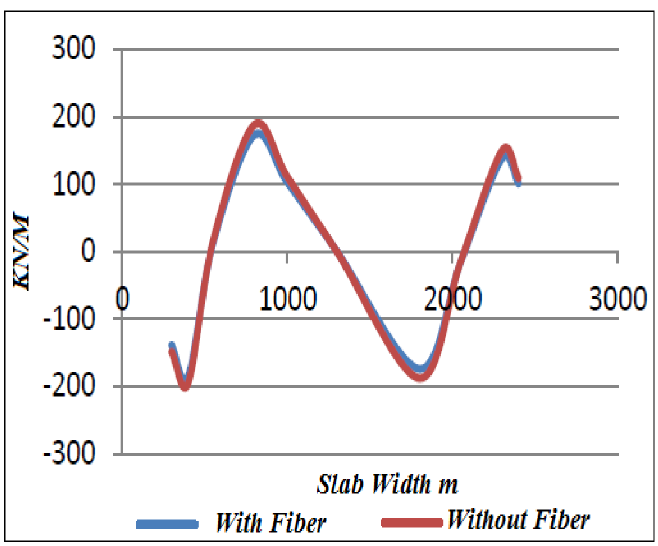

Fig. 5.5 *Transversal shear force of slab, with and without fiber - K = 35 kg/m^3*

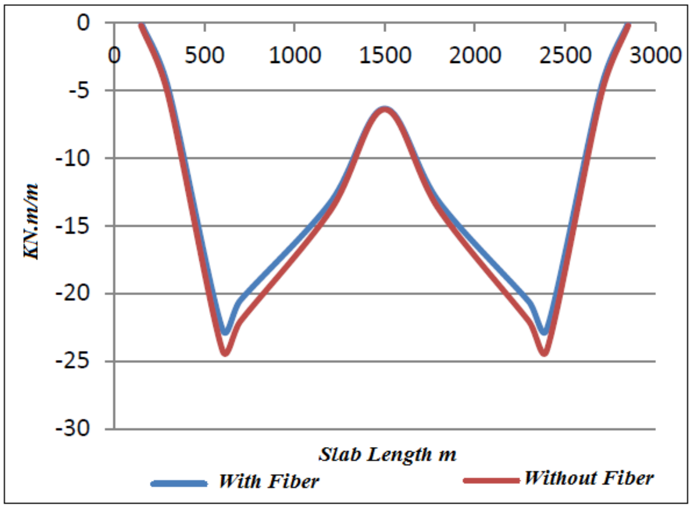

Fig. 5.6 *Longitudinal anchors of slab, with and without fiber - K = 35 kg/m³*

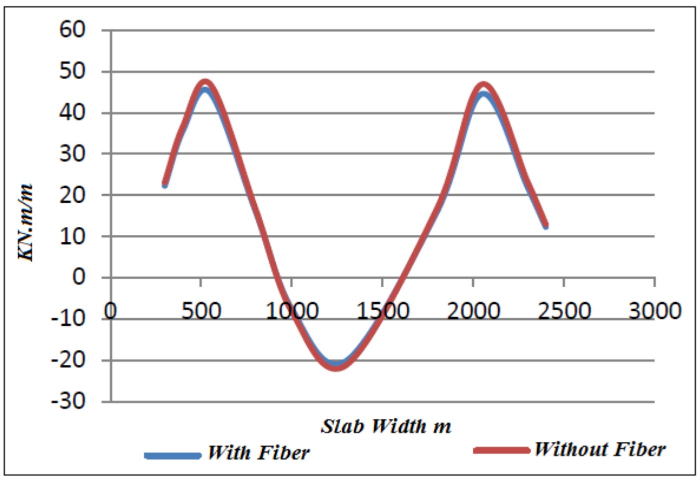

Fig. 5.7 *Transversal anchors of fiber slap, with and without fiber - K = 35 kg/m³*

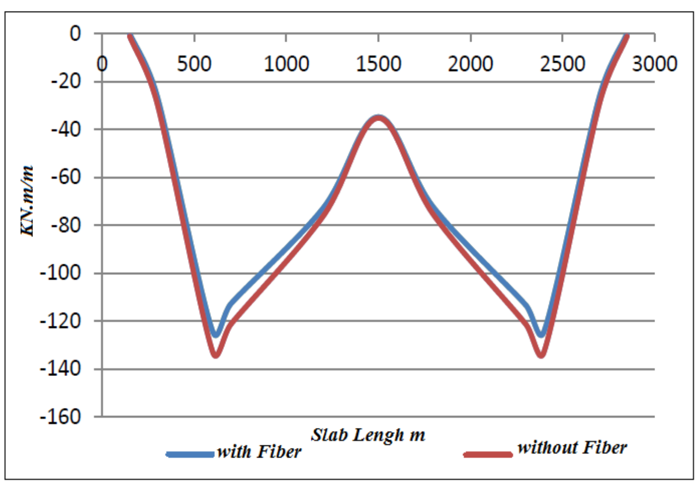

Fig. 5.8 *Longitudinal anchors of slab, with and without fiber - K = 0.5 kg/m³*

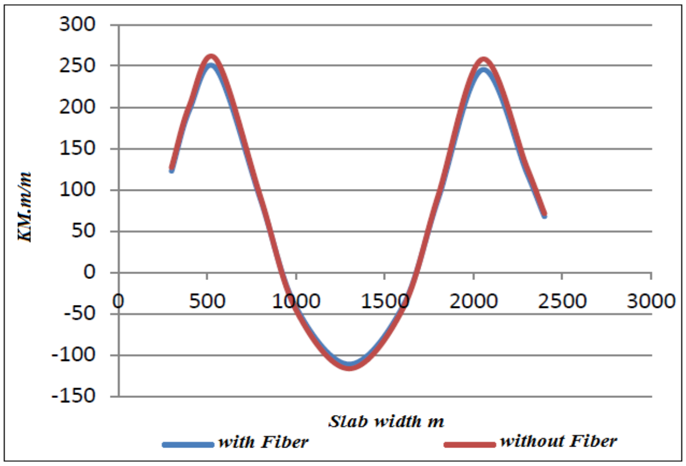

Fig. 5.9 *Transversal anchors of fiber slab, with and without fiber - K = 0.5 kg/m³*

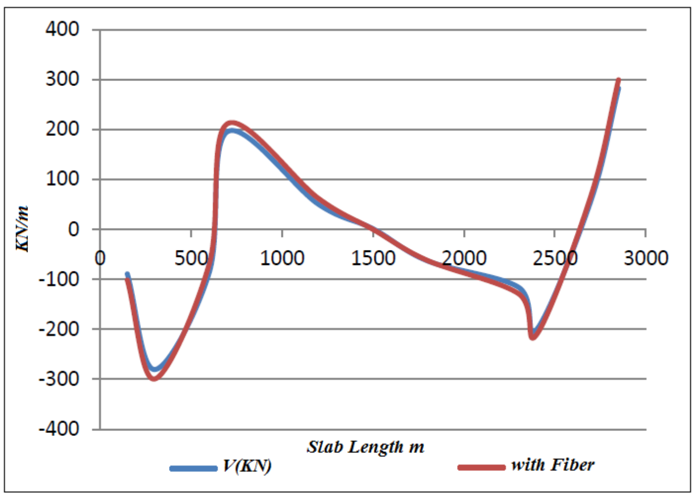

Fig. 5.10 *Longitudinal shear force of slab, with and without fiber - K = 0.5 kg/m³*

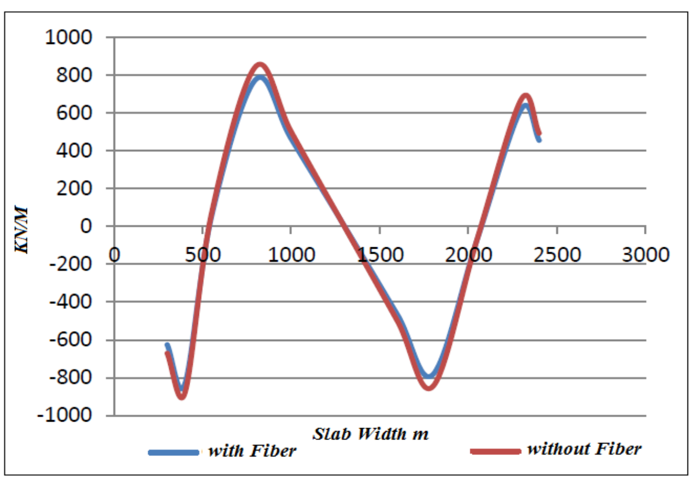

Fig. 5.11 *Transverse shear force of slab, with and without fiber - K = 0.5 kg/m³*

5.3 Conclusion

Service loading results in fiber concrete slabs and concrete slab without fibers show that increasing and adding fibers has no much impact in shear forces and bending anchors. As a result, it can be used concrete slab line without fiber for analyzing and designing fiber concrete slab.

5.4 Rail slab line analysis, flexural and shear forces

5.4.1 Characteristics of the slab line and introduction of applied loads

The scope is the investigation of a typical slab line on the soil bed. In order to provide proper operation conditions and high safety, it is necessary to consider criteria and assumptions of non-ballasted line system. Generally, the pavement system must meet the following requirements:

- Tolerate the operation loads in common operation and design speed;
- Resist to dynamic effects and inmpacts caused by train movement;
- Maintain its integrity without getting ruptures due to inner forces cretaed by differential loading.

Loading

Loads on the pavement include:

- Dead Load: it includes loads that are relatively constant over time, including the weight of the structure itself and fixtures such as walls, plasterboard or carpet. The roof is also a dead load. Dead loads are also known as permanent or static loads. Building materials are not dead loads until constructed in permanent position. The dead loads on the pavements include, bearing and non-load bearing components (48). Here the dead loads include slab, rail and sleepers. The consumable concrete specific weigth is 2500 kg/m^3 and rail unit weigth is 60 kg/m. It should be noted that the recommended amount in Eurocode regulation is 25 for reinforced concrete specific weigth.
- Live Load: it includes important components in each structural design combination. These information are determined based on available statistics, measurements, behavioral distributions, structural analysis and probability theory. Live Load pattern has an important role in the design of the slab line and different regulations have recommended patterns for it, depending on the type of operation: passing vehicles, traffic volume, speed, maintenance

conditions, different in various countries. In rail transport there are similarities in the loading pattern due to a smaller variety of vehicles and machinery. AREMA regulation recommended LM71 for traffic load modeling (49) (Fig. 5.12).

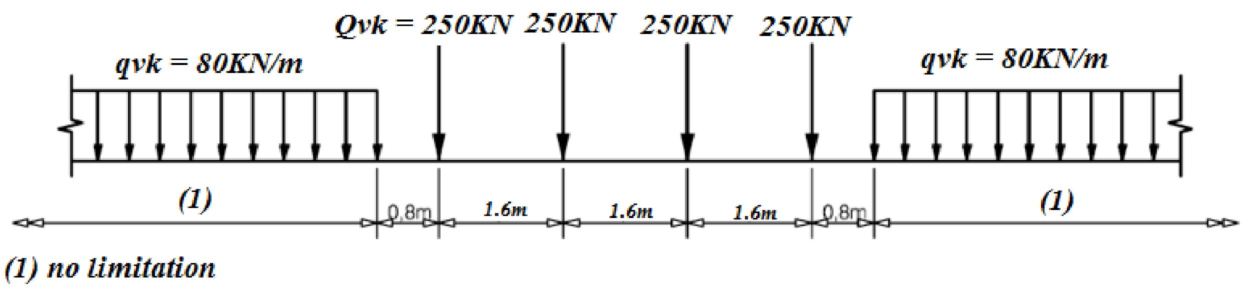

Fig. 5.12 *LM71 Loading Model*

5.4.2 Impact coefficient

Basically, the nature of the forces on the railways are dynamic and two main sources are effective in the emergence of these dynamic forces: passing property of the rail vehicles wheels and impacts due to wheels movements on the rippling level of worn and damaged rails. These dynamic effects are relevant fo the design of railway lines but dynamic forces prediction on railway lines is complex. Therefore, static forces from the wheel, is multiplied to the dynamic coefficient, and use a pseudo-static force in railway line design:

$$p_d = \varphi p_s \qquad (5\text{-}1)$$

Moreover, AREMA regulation formula are used for calculation of impact coefficient.

$$\emptyset = 1 + 5.21\frac{V}{D} \qquad (5\text{-}2)$$

Where is:

- *V*: Load passing speed [km/h];
- *D*: Wheel diameter [mm].

The present anlyisis uses loads of *15, 25 and 30 t* and *80, 120, 200 km/h* passing speeds. The coefficients in table 5.1 are used in equation (5-2) for calculation of dynamic impacts at various speeds.

D (mm)	*V (km/h)*	*∅*
1000	*80*	*1.4168*
	120	*1.6252*
	200	*2.042*

Table 5.1 *Dynamic impact coefficient for various speeds*

According to table 5-1 and following equations, it is possible to calculate the amount of centralized force of each wheel and wide force on each side of the rails:

$$p_{s_{wheel}} = \frac{p_{axle}}{2} \tag{5-3}$$

$$p_{dyn_{wheel}} = \emptyset . p_{s_{wheel}} \tag{5-4}$$

$p_{axle}\ (\frac{kN}{m})$	$q_{axle}\ (kN)$	$V(\frac{km}{h})$	$p_{dyn_{wheel}}\ (kN)$	$p_{dyn_{wheel}}\ (\frac{km}{h})$
150	*48*	*80*	*34.0032*	*106.26*
		120	*39.0048*	*121.89*
		200	*49.008*	*153.15*
250	*80*	*80*	*56.672*	*177.1*
		120	*65.008*	*190.775*
		200	*81.68*	*255.25*
300	*96*	*80*	*68.0064*	*212.52*
		120	*78.0069*	*228.93*
		200	*98.016*	*306.3*

Table 5.2 *Amount of focused and extensive dynamic forces*

5.4.3 Load combination

The load combination is represented by the followimg equation in FIB regulation:

$$\gamma_G * G + \gamma_Q * Q_{IR} \tag{5-5}$$

Where is:

- G: frequent dead load;
- Q_{IR}: non-frequent live load;
- γ_G: dead load coefficient = 1.35;
- γ_Q: live load coefficient = 1.5.

5.4.4 Instruments specification and pavement materials

In this project the slab thickness is 30 cm, the concrete slab width is 2.6 m, slab length is 6 m and the sleepers are in a distance of 60 cm apart. The used rails are UIC 60 (table 5.3 and Fig. 5.13).

Section Type	Rail Heigth (mm)	Stern Width (mm)	Warhead Width (mm)	Web Thickness (mm)	Warhead Heigth (mm)	Neutral Axis Heigth (mm)	Cross sectional Area (mm^2)	Momet of Inertia (cm^4)	Section Module (cm^3)
UIC-60	172	150	74.3	16.5	51	80.9	7587	3055	335.5

Table 5.3 *Geometric characteristics of rails UIC60*

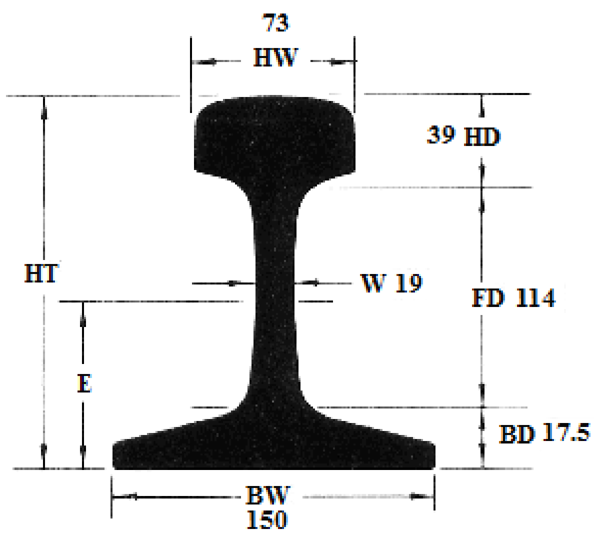

Fig. 5.13 *Rail balanced section introduced to the software*

Moreover, they where assumed:

- Steel elastic model = $2.1 * 10^5$ MPa;
- Tensile strength of steel = 900 MPa;
- Offset yield strength = 580 MPa.

The most effective bed's specification for the slab line design, is the soil reaction module. *Bowles* in *Foundation Analysis & Design* book, calculated the amount of bed reaction module, based on the amount of soil bearing capacity (50):

$$k_s = 40 * FOS * q_s \qquad (5\text{-}6)$$

Where:

- k_s: Soil Reaction Module;
- FOC: Coefficient of confidence = 2.5;
- q_s: Load capacity of the soil $\mathrm{kN/m^3}$.

5.4.5 Modeling

The concrete pavement modeling has done in 3D and using SAP2000 software. In Fig. 5.14 the three-dimensional view is represented.

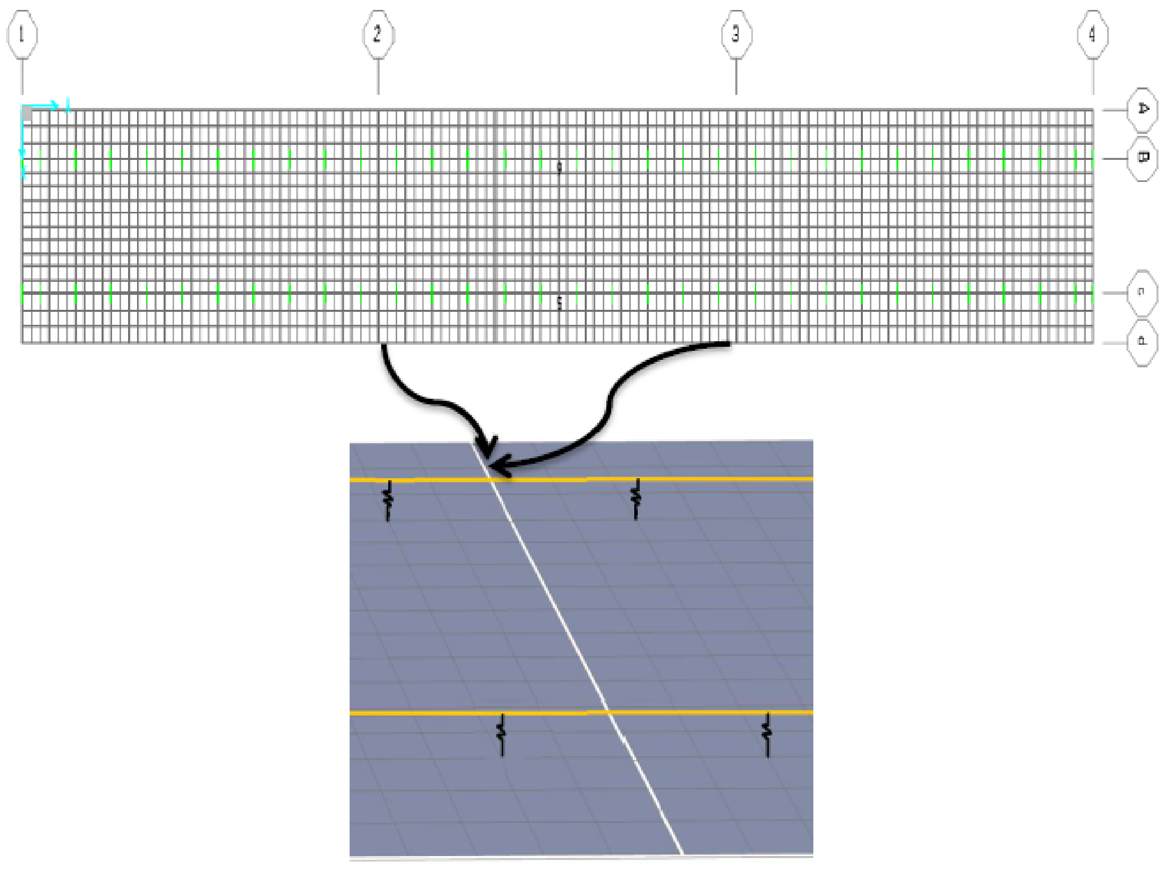

Fig. 5.14 *Concrete pavement modeling in 3D using SAP2000*

The original model simulated three slabs with *6 meter* length and *2 cm* as seam between the slabs. According to *(Fig 5.14)*, the line modeling of the rail to rail distance is *1.5* m that include concrete slab done by *Shell-Thick* element. It is considered *18 m* for the length and *260 cm* for the width. Axis to axis distance is considered *150 cm*. After applying the hit coefficients, the moving load, moves on the rails in two lanes. The rail connection to the concrete slab has done in *60 cm* distance with use of LINK element, a type of linear spring, which in the axial direction include *450 kN/mm* hardness. This hardness is equal to the pad hardness under the rail, and are free in the other directions (50).

The level under the slab is identified in the software, in terms of spring areas: *1) Soft = 5000, 2) Medium = 20000, 3) Hard = 100000.*

5.4.6 Analysis of results: determination of shear and bending forces on slab line

According to the results *(Fig. 5.15, 5.16, 5.17, 5.18 and 5.19)*, with increasing of bed reaction coefficient, the longitudinal, transversal and shear moments on slab lines will decrease a lot.

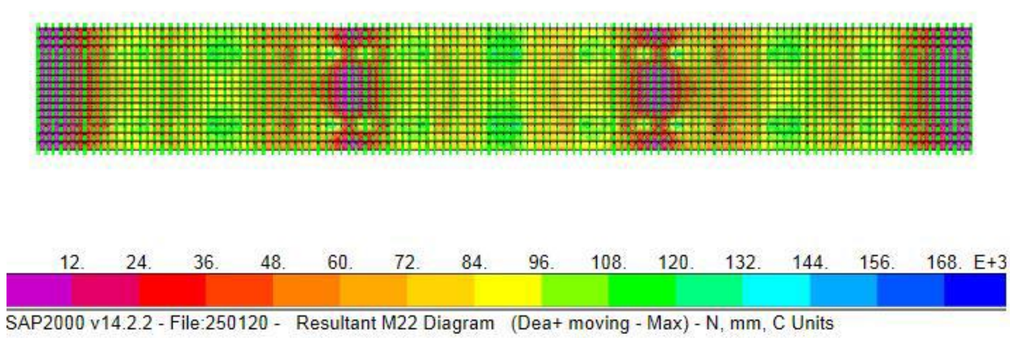

Fig. 5.15 *Max longitudinal moment in combination of 1.35DL+1.5LL loads*

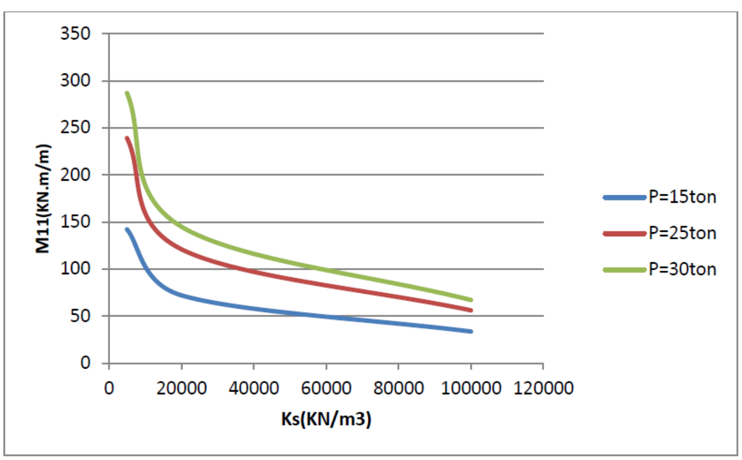

Fig. 5.16 *Results of transversal anchore, the axial load changing anf bed reaction coefficient in constant speed* $V = 120\ Km/h$

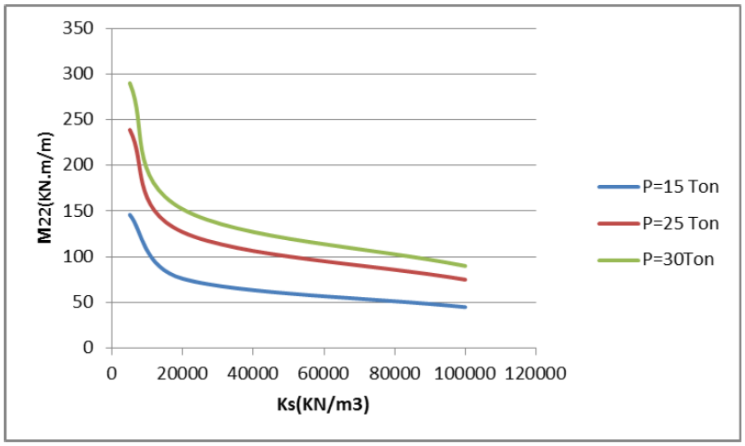

Fig. 5.17 *Results of longitudinal anchore, the axial load changing anf bed reaction coefficient in constant speed* $V = 120\ Km/h$

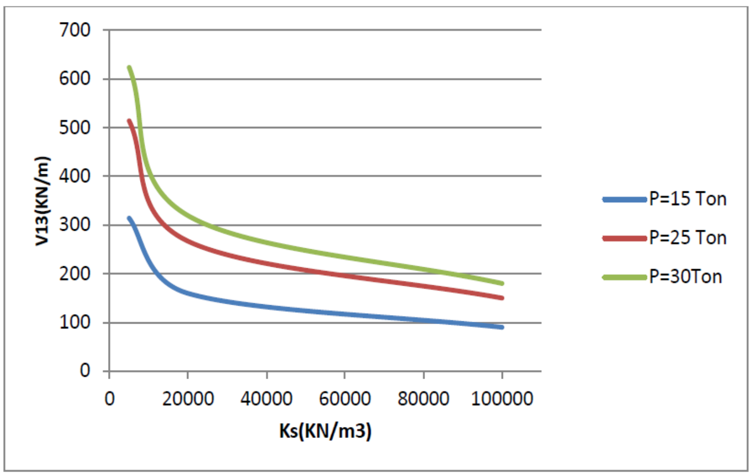

Fig 5.18 *Results of transversal cutting, the axial load changing anf bed reaction coefficient in constant speed* $V = 120\ Km/h$

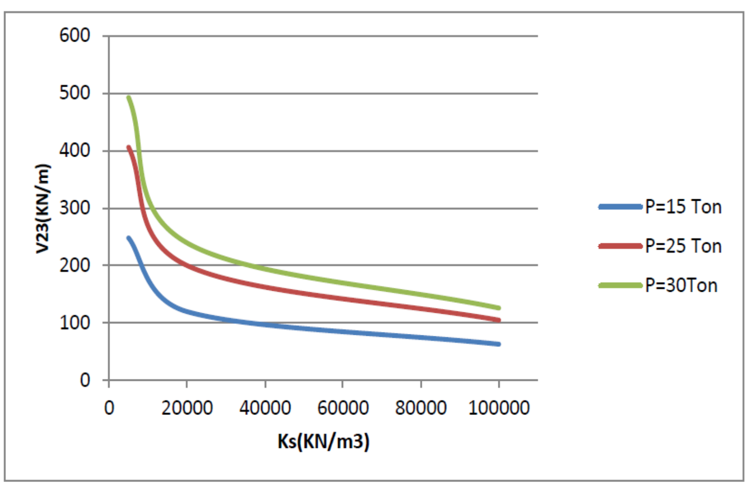

Fig 5.19 *Results of longitudinal cutting, the axial load changing anf bed reaction coefficient in constant speed* $V = 120\ Km/h$

After the analysis, results of shear forces and bending anchors are extracted and the design work can start.

5.5 Results representation and designed graphs for the use of fiber in slab lines

5.5.1 Investigation of using fiber concrete without armature in railway slab lines

According to the results in table 5.4, the utilization of fiber in concrete slabs, does not have required bending strength for tolerance of the incoming loads. On the other hand, in this condition the crack width has achieved manifold the maximum allowed value. So, it can be concluded that the slab lines need a high precentages of fiber that is not economically affordable.

V_f (%)	Slab's crack width (mm)	Slab's resistance moment per meter of length MRd (kN)
0.25	*285*	*6.79*
0.50	*207*	*10.21*
0.75	*156*	*14.48*

Table 5.4 *Results of using fiber alone in concrete slab lines*

5.5.2 Example of flexural design of fiber concrete slab with armature

According to table 5.5, there are axial load, bed's reaction coefficient and passing speed that are investigated in slab line.

Axle load (t)	V (km/h)	Ks (kN x m^3)
15	*80*	*5000*
25	*120*	*20000*
30	*200*	*100000*

Table 5.5 *Analysis parameters of fiber concrete slab design*

By adding fibers to concrete slabs, the amount of used armature is slightly reduced and also the crack width is greatly reduced. For example in axial load conditions with 25 t, load speed of 120 Km/h and hardness of 2000 KN/m^3, the amount of required fiber will decrease with volumetric percentage *(0.25, 0.5, 0.75)* and amount of consumable armature *(3.5, 4.9, 6.3)* and also the crack width decrease in amount of *26%, 30%* and *35%.*

Axle Load (t)	V (km/h)	Only	Armature	0.25 % of Amature	Combination fiber and	0.5 % of Armature	Combination fiber and	0.75% of Armature	Combination fiber and
		AS (mm^2)	W(mm)	AS (mm^2)	W(mm)	AS (mm^2)	W(mm)	AS (mm^2)	W(mm)
15	80	571	0.47	546	0.292	518	0.28	474	0.263
	120	678	0.444	637	0.29	606	0.278	562	0.262
	200	832	0.415	779	0.283	744	0.272	700	0.257
25	80	989	0.392	926	0.276	892	0.264	860	0.249
	120	1146	0.373	1080	0.267	1043	0.256	1002	0.242
	200	1467	0.343	1394	0.251	1363	0.24	1325	0.226
30	80	1193	0.368	1127	0.265	1093	0.253	1049	0.239
	120	1385	0.35	1316	0.255	1284	0.243	1240	0.23
	200	1762	0.323	1690	0.237	1661	0.226	1627	0.213

Table. 5.6 *amount of required armature and crack width in concrete slab with combination of fiber and armature*

Fig. 5.20 indicated that with increasing of axial load and passing speed, the amount of required armature in fiber concrete slab increase with different volumetric precentages. Therefore, by increasing the amount of required armature, the crack width will decrease. On the other hand, by increasing the bed reaction coefficient, the amount of required armature decrease and it causes the increase the crack width.

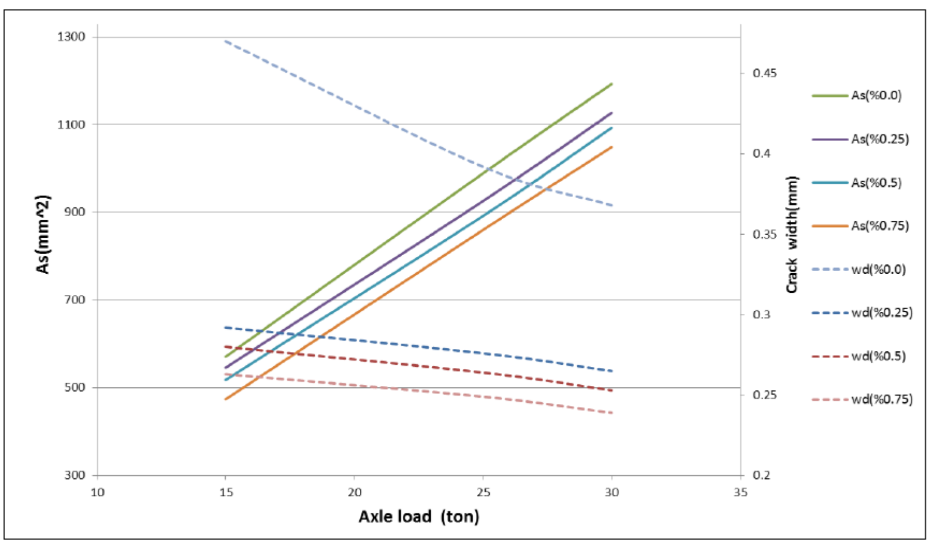

Fig 5.20 *Design of fiber concrete slab line by changing axial force and bed reaction coefficient Ks= 100000 kN/m^3 and passing speed V=80 Km/h*

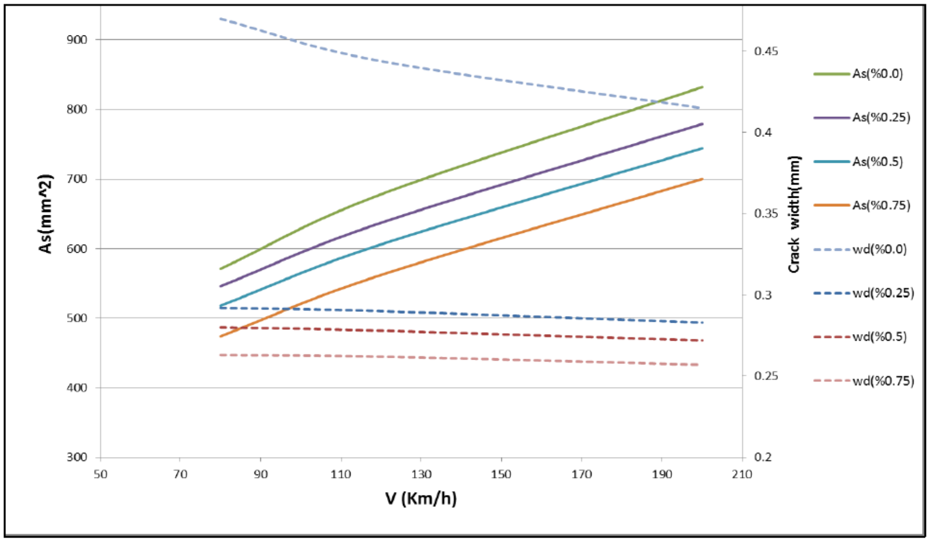

Fig. 5.21 *Design of fiber concrete slab line by changing axial force and bed reaction coefficient Ks= 100000 kN/m*^{3} *and axial load P= 15 t*

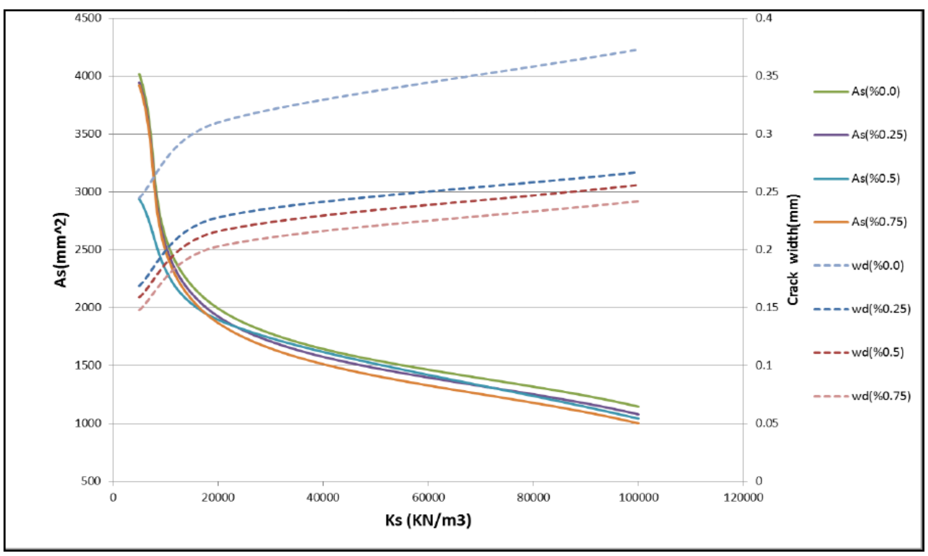

Fig. 5.22 *Design of fiber concrete slab by changing bed reaction coefficient under the slab line in passing speed V = 120 km/h and axial load P = 25 t*

5.5.3 Shear design of fiber concrete slab in combination with armature

According to the results from shear and bending design, it can be concluded that shear strength due to longitudinal armature and fibers is calculated by shear forces. Therefore, the bending armature is a good answer for incoming shear force and shear design.

Anchor Analysis	Shear Analysis	Axle Load (t)	V (km/h)	Armature only		Combination of fiber and 0.25 % armature		Combination of fiber and 0.25 % armature		Combination of fiber and 0.25 % armature	
				$AS\ (mm^{2})$	$W(mm)$	$AS\ (mm^{2})$	$W(mm)$	$AS\ (mm^{2})$	$W(mm)$	$AS\ (mm^{2})$	$W(mm)$
95	221	25	80	1712	265	1639	283	1611	288	1577	295
106	235		120	1994	278	1925	302	1897	307	1869	312
135	252		200	2544	290	2475	315	2456	320	2431	325

Table. 5.7 *Shear design of fiber concrete slab in combination with armature*

5.6 Technical and economic comparison of weights of armature and combination armature and fiber

In this part, design details for concrete slabs with 120 km/h speed, axial load 25 of t and bed reaction coefficient 20000 $\frac{KN}{m^3}$, are considered in table 5.8 by adding fibers to concrete slabs with a slightly reduced armature. The amount of cost will increase by combining fibers and armature in 6 m slab. This part investigated the advantages of utilization of fibers in slab line and also how long the slab line's life span will increase and the maintenance cost decrease. Then, it is possible to calculate the technical and economic comparison of weight of armature with the combination of armature and fiber.

Fiber Precentage [%]	Weigth of fiber in one cubic meter	Weigth of fiber with 6x2.6x0.3 dimensions	Cost of fiber	Weigth of armature	Cost of armature	Total cost	Increase of cost [%]
0	0	0	0	859.91256	2149781.4	2149781.4	0.0 %
0.25	12.5	58.5	292500	824.99040	2062476.0	2354976.0	9.5 %
0.50	25.0	117.0	585000	811.24056	2028101.4	2613101.4	21.6 %
0.75	37.5	175.5	877500	794.44872	1986121.8	2863621.8	33.2 %

Table. 5.8 *Technical and economic comparison of weigjts of armature and the combination of armature and fiber*

Chapter 6

Results & conclusion

6.1 Introduction

In this chapter we have a review from chapter 1 to chapter 5.

In developing countries, usage of steel fiber-reinforced cementitious composites is widely expanding in structures, due to their high mechanical performance and flexibility. The behavior of steel fiber-reinforced concrete exposed to corrosive environments has been investigated. Because of the properties of the material (concrete), computer simulations in the field of reinforced concrete structures is a challenge. As opposed to steel, concrete when subjected to compression exhibits nonlinearity right from the start. Moreover, it much quicker undergoes degradation under tension. All this poses difficulties for numerical analyses. Weak tensile strength combined with brittle behavior result in sudden tensile failure without warning. This is obviously not desirable for any construction material. Thus, concrete requires some form of tensile reinforcement to compensate its brittle behavior and improve its tensile strength and strain capacity to be used in structural applications. Historically, steel has been used as the material of choice for tensile reinforcement in concrete. Fibre Reinforced Concrete (FRC) is defined as a composite material essentially consisting of conventional concrete or mortar reinforced by the random dispersal of short, discontinious, and discrete fine fibres of specific geometry.

The elasto-plastic material model for concrete developed by considering the stress softening and degradation of the deformation modulus for the concrete was presented in the paper. A reduced plane stress state for the compression/tension range with shear was assumed. Steel fiber used in concrete is in the purpose of load increasing and crack control. In this project, the concrete is modeled directly with elasto-plastic behavior in concrete material. In the first step, the deformation behavior to the break is investigated in slab and the results are validated with laboratory work. In the following, it has shown that the fiber does not have much impact on shear and bending forces. According to these results, the design of bending, shearing and crack control in slab line has done for 15, 25, 30 t as axial loads, 80, 120, 200 km/h as speed and 5000, 20000, 100000 kN/m^3 as the bed hardness and the results are represented in form of graphs.

6.2 Conclusions

- With increasing of hardness under the concrete slab, the amount of incoming force to the slab will decrease. E.g. with 25 t axial load, 120 km/h speed, and change in hardness from 5000 to 20000 and 100000 kN/m^3, the amount of incoming longitudinal anchor, increased to 46% and 68%, while the amount of armature is reduced.

- Economically, the cost of utilization of fiber with armature is more than usage of armature in alone situation. E.g. with 25 t axial load, 120 km/h speed and 20000 kN/m^3 hardness, the amount of required fibers with 0.25, 0.5, 0.75 volumetric percentages the cost of building of the slab line increase respectively by 9.5%, 21% and 33%.

- By adding fiber to concrete slab, the amount of required armature reduced sligthly and the crack width greatly decreased. E.g. with 25 t axial load, 120 km/h speed, and 20000 kN/m^3 hardness, the amount of required fibers with 0.25, 0.5, 0.75 volumetric precentages cause the decrease of the amount of armature to 3.5%, 4.9% and 6.3% and the crack width decreased respectively to 26%, 30% and 35%.

- Utilization of fiber alone in concrete slab line, does not have required bending strength to tolerate the incoming loads. On the other hand, in this condition the crack width is several times larger than allowed cracks in regulation. According to the results, it can be concluded that a high precentage of fibers are required. Therefore, this work is not affordable.

- The service's loading results in concrete with and without fiber indicate that increasing fiber does not have much impacts in shear forces and bending anchors. As a result, it is possible to use a concrete slab without fiber for analyzing the fiber concrete slab and designing it.

- According to the results obtained from flexural and shear design, it can be concluded that the shear strength due to longitudinal armatures and fibers due to shear forces are from analysis of the slab line due to dynamic crossing loads that an increae of incoming bending forces and the shear design is not a criterion.

- Among all kinds of fibers which can be used as concrete reinforcement, steel fibers are the most popular ones. The performance of the Steel Fiber Reinforced Concrete (SFRC) has shown a significant improvement in flexural strength and overall toughness compared against conventional reinforced concrete.

- The behaviour of uncracked concrete and concrete between cracks was simulated under the elastoplasticity framework. The soil or other base material, supporting the concrete slab was simulated by distributed springs orthogonal to the concrete slab middle surface. An elasto-plastic model was used to modulate the non-linear behaviour of the springs. The loss of contact between the base and the slab was accounted for.

- Mechanical properties are improved by the incorporation of steel fibers in UHSC especially splitting tensile strength. Steel fibers increased the total charge passing and the electrical conductivity of the concrete and the increase depends on the volume fraction of the steel fibers.
- In slabs with low fibre volume (0.5%) the resisting load after cracking was relatively small. The rate of improvement in energy absorption reduced with the increase in fiber content.
- The compressive strength of highstrength, lightweight concrete was only slightly improved with the addition of steel fiber. The tensile/compressive strength ratio was obviously enhanced. These were attributed to the effect of the steel fiber arresting cracking.
- Use of fiber produces more closely spaced cracks and reduces crack width. Fibers bridge cracks to resist deformation. Fiber addition improves ductility of concrete and its post-cracking load-carrying capacity. The mechanical properties of FRC are much improved by the use of hooked fibers than straight fibers, the optimum volume content being 1.5%. While fibers addition does not increase the compressive strength, the use of 1.5% fiber increase the flexure strength by 67%, the splitting tensile strength by 57% and the impact strength 25 times.
- The properties like shear, torsion and bending is also improved due to addition of fibers in the concrete. This is obvious because the addition of fibers resists the development of internal micro crack in the concrete, which are responsible for the failure of the structure.

6.3 Advantages and disadvantages

6.3.1 How to save time and money

To eliminate completely steel fiber reinforcement, saving both materials and labour:

- Reduce slab thickness giving savings in concrete and placement costs;
- Make possible wider joint spacing, by saving joint forming costs and maintenance.

- Simplify the construction: simpler joints and no longer errors in steel fabric positioning.
- Increase speed of construction.

6.3.2 Technical and user benefits

- Significantly reduced risk of cracking.
- Reduced spalling joint edges.
- Stronger joints.
- High impact resistance.
- Greater fatigue endurance.
- Reduced maintenance costs.
- Longer useful working life.

6.3.3. Advantages

- Reinforcing concrete with steel fibres results in durable concrete with a high flexural and fatigue flexural strength, improved abrasion, spalling and impact resistance.
- The elimination of conventional reinforcement and, in some cases, the reduction in section thickness can contribute to some significant productivity improvements. Steel fibers can deliver significant cost savings, together with reduced material volume, more rapid construction and reduced labour costs.
- The random distribution of steel fibres in concrete ensures that crack free stress accommodation occurs throughout the concrete. Thus micro cracks are intercepted before they develop and impair the performance of the concrete.
- Steel fibres are a far more economical design alternative.

6.3.4. Disadvantages

- Steel fibers will not float on the surface of a properly finished slab, however, rain damaged slabs allow both aggregate and fibers to be exposed and will present as aesthetically poor whilst maintaining structural soundness.
- Fibers are capable to substitute reinforcement in all structural elements (including primary reinforcement), however, within each element, there will be a point where the fibers alternative's cost saving and design economies are diminished.
- Strict control of concrete wastage must be monitored in order to keep it at a minimum. Wasted concrete means wasted fibers.

6.4 Proposal

In this part there are some suggestions provided in the field of numerical, laboratory, and implementation.

6.4.1 Numerical Study

- Interaction investigation between fiber and concrete with different coefficients of continuity between steel and concrete in numerical model of finite element.
- Investigating the effect of various fiber lengths and diameters in the numerical analysis of fiber concrete finite element.
- Check how to create and expand the cracks in the slab line and numerical analysis of finite element.

6.4.2. Laboratory and executive studies

- Carrying out laboratory studies by panel manufacturing of fiber concrete slab line.
- Sensitivity analysis of fiber various geometric features, e.g. appearance ratio, and fiber lengths.
- Design and implementation of fiber concrete slab line in subways and railways and monitor their behavior along the years.

Reference

1. Alizade E, JANDAGHI AF, Zabihi S. Effect of steel fiber corrosión on mechanical properties of steel fiber reinforced concrete. 2016.

2. Kmiecik P, Kamiński M. Modelling of reinforced concrete structures and composite structures with concrete strength degradation taken into consideration. Archives of civil and mechanical engineering. 2011;11(3):623-36.

3. Behbahani H, Nematollahi B, Farasatpour M. Steel fiber reinforced concrete: A review. 2013.

4. Qian C, Stroeven P. Development of hybrid polypropylene-steel fibre-reinforced concrete. Cement and concrete research. 2000;30(1):63-9.

5. Szcześniak A, Stolarski A. A simplified model of concrete for analysis of reinforced concrete elements. Biuletyn Wojskowej Akademii Technicznej. 2016;65(4).

6. Esveld C. Recent developments in slab track application. Rail Tech Europe. 1999.

7. Michas G. Slab track systems for high-speed railways. 2012.

8. Nurchasanah Y, Masoud MA, Solikin M, editors. Steel Fiber Reinforced Concrete to Improve the Characteristics of Fire-Resistant Concrete. Applied Mechanics and Materials; 2016: Trans Tech Publ.

9. Wafa FF. Properties & applications of fiber reinforced concrete. Engineering Sciences. 1990;2(1).

10. Yongjiang X, Huajian L, Zhongwei F, Ilwha L. Concrete crack of ballastless track structure and its repair. International Journal of Railway. 2009;2(1):30-6.

11. Barros JA, Figueiras JA. Model for the analysis of steel fibre reinforced concrete slabs on grade. Computers & Structures. 2001;79(1):97-106.

12. Madhkhan M, Entezam M, Torki M. Mechanical properties of precast reinforced concrete slab tracks on non-ballasted foundations. Scientia Iranica. 2012;19(1):20-6.

13. Khaloo AR, Afshari M. Flexural behaviour of small steel fibre reinforced concrete slabs. Cement and concrete Composites. 2005;27(1):141-9.

14. Kershaw EE, Flier JS. Adipose tissue as an endocrine organ. The Journal of Clinical Endocrinology & Metabolism. 2004;89(6):2548-56.

15. Taucer F, Spacone E, Filippou FC. A fiber beam-column element for seismic response analysis of reinforced concrete structures: Earthquake Engineering Research Center, College of Engineering, University …; 1991.

16. Zollo RF. Fiber-reinforced concrete: an overview after 30 years of development. Cement and Concrete Composites. 1997;19(2):107-22.

17. Khaliq W, Kodur V. Thermal and mechanical properties of fiber reinforced high performance self-consolidating concrete at elevated temperatures. Cement and Concrete Research. 2011;41(11):1112-22.

18. Mertz DR. Application of fiber reinforced polymer composites to the highway infrastructure: Transportation Research Board; 2003.

19. Jaturapitakkul C, Roongreung B. Cementing material from calcium carbide residue-rice husk ash. Journal of Materials in Civil Engineering. 2003;15(5):470-5.

20. Altun F, Haktanir T, Ari K. Effects of steel fiber addition on mechanical properties of concrete and RC beams. Construction and Building Materials. 2007;21(3):654-61.

21. Song P, Hwang S. Mechanical properties of high-strength steel fiber-reinforced concrete. Construction and Building Materials. 2004;18(9):669-73.

22. Nanni A, Tanigaki M, Hasuo K. Bond anchorage of pretensioned FRP tendon at force release. Journal of Structural Engineering. 1992;118(10):2837-54.

23. Krishna PV, Rao NS. Durability Studies on Steel Fiber Reinforced Concrete. International Research Journal of Engineering and Technology (IRJET) Volume. 2016;3.

24. Neela S. Flexural Behavior of Basalt FRP Bar Reinforced Concrete Members With and Without Polypropylene Fiber: University of Akron; 2010.

25. Bernard E. Behaviour of round steel fibre reinforced concrete panels under point loads. Materials and Structures. 2000;33(3):181-8.

26. Shah SP, Batson GB, editors. Fiber reinforced concrete: properties and applications1987: American Concrete Institute.

27. Handbook M. Florida Department of Transportation. Tallahassee, FL. 1997.

28. Brandt AM. Cement-based composites: materials, mechanical properties and performance: CRC Press; 2005.

29. Folliard KJ, Sutfin D, Turner R, Whitney DP. Fiber in Continuously Reinforced Concrete Pavements. 2006.

30. Nassif H, Suksawang N, Mohammed M. Effect of curing methods on early-age and drying shrinkage of high-performance concrete. Transportation Research Record: Journal of the Transportation Research Board. 2003(1834):48-58.

31. Piryonesi SM, Tavakolan M. A mathematical programming model for solving cost-safety optimization (CSO) problems in the maintenance of structures. KSCE Journal of Civil Engineering. 2017;21(6):2226-34.

32. Bakis CE, Bank LC, Brown V, Cosenza E, Davalos J, Lesko J, et al. Fiber-reinforced polymer composites for construction—State-of-the-art review. Journal of composites for construction. 2002;6(2):73-87.

33. TC162-TDF R. Test and design methods for steel fiber reinforced concrete, σ ε-design method. Final Recommendation. Journal of Material and Structures. 2003;35:560-7.

34. Béton FID. Structural Concrete: Textbook on Behaviour, Design and Performance: Updated Knowledge of the CEB/FIP Model Code 1990: fib; 1999.

35. Brückner A, Ortlepp R, Curbach M. Textile reinforced concrete for strengthening in bending and shear. Materials and structures. 2006;39(8):741-8.

36. Shah AA, Ribakov Y. Recent trends in steel fibered high-strength concrete. Materials & Design. 2011;32(8-9):4122-51.

37. Chaudhari S, Chakrabarti M. Modeling of concrete for nonlinear analysis using finite element code ABAQUS. International Journal of Computer Applications. 2012;44(7):14-8.

38. Nazem M, Rahmani I, REZAEI PM. Nonlinear fe analysis of reinforced concrete structures using a tresca-type yield surface. 2009.

39. Hognestad E. Study of combined bending and axial load in reinforced concrete members. University of Illinois at Urbana Champaign, College of Engineering …; 1951.

40. Bangash M. Concrete and concrete structures: Numerical modelling and applications. 1989.

41. Wahalathantri BL, Thambiratnam D, Chan T, Fawzia S, editors. A material model for flexural crack simulation in reinforced concrete elements using ABAQUS. Proceedings of the first international *conference on engineering, designing and developing the built environment for sustainable wellbeing; 2011: Queensland University of Technology.*

42. *Jankowiak I, Kąkol W, Madaj A, editors. Identification of a continuous composite beam numerical model, based on experimental tests. 7th conference on composite structures, Zielona Góra; 2005.*

43. *De Normalisation CE. Eurocode 2: Design of concrete structures—Part 1-1: General rules and rules for buildings. Brussels, Belgium. 2004.*

44. *Wang T, Hsu TT. Nonlinear finite element analysis of concrete structures using new constitutive models. Computers & structures. 2001;79(32):2781-91.*

45. *Nayal R, Rasheed HA. Tension stiffening model for concrete beams reinforced with steel and FRP bars. Journal of Materials in Civil Engineering. 2006;18(6):831-41.*

46. *Lapczyk I, Hurtado JA. Progressive damage modeling in fiber-reinforced materials. Composites Part A: Applied Science and Manufacturing. 2007;38(11):2333-41.*

47. *Hsu L, Hsu C-T. Complete stress—strain behaviour of high-strength concrete under compression. Magazine of concrete research. 1994;46(169):301-12.*

48. *Zaccaria D, Bigoni D, Noselli G, Misseroni D, editors. Structures buckling under tensile dead load. Proceedings of the Royal Society of London A: Mathematical, Physical and Engineering Sciences; 2011: The Royal Society.*

49. *Esmaeili M, Naderi B, Neyestanaki HK, Khodaverdian A. Investigating the effect of geogrid on stabilization of high railway embankments. Soils and Foundations. 2018;58(2):319-32.*

50. *Costa DJRdS. Dynamic stiffness of the piled foundation of a onshore wind turbine 2014.*